CRUSTAL STRUCTURE STUDIES IN TASMANIA

B.D. JOHNSON, M.Sc. (Durham)

Submitted in partial fulfilment of the requirements

for the Degree of

Doctor of Philosophy

UNIVERSITY OF TASMANIA

HOBART

April, 1972

ABSTRACT

A regional gravity survey of Tasmania has revealed that the crust is of normal continental thickness (35 to 40 kms), increasing slightly under the Central Plateau region and thinning rapidly at the continental margin. The "regional" field, due to the variation in crustal thickness, has been obtained by approximating the observed data, using a terminated Fourier series; the trigonometric functions having been orthogonalised, with respect to the irregularly spaced data points, by the Gram-Schmidt method.

A time-term analysis of the Bass Strait crustal refraction data indicates near normal thicknesses in Tasmania and intermediate thicknesses in Bass Strait (23-28 kms).

Spectral analyses of high-level aeromagnetic data have indicated that, if the source layers of magnetic anomalies can be considered to give rise to a "white" spectrum, then the depth to the source layer is given by the gradient of the logarithm of the spectrum.

This thesis contains no material which has been accepted for the award of any other degree or diploma in any University and, to the best of my knowledge and belief, contains no copy or paraphrase of material previously published or written by another person, except where due reference is made in the text of this thesis.

B. David Johnson

April, 1972.

"Far over the misty mountains cold
To dungeons deep and caverns old
We must away, ere break of day,
To find our long-forgotten gold.

from The Dwarves Song, in
"The Hobbit", J.R.R. Tolkein

TABLE OF CONTENTS

LIST OF FIGURES

LIST OF TABLES

CHAPTER ONE

INTRODUCTION

1.1 OUTLINE OF PHYSIOGRAPHY AND GEOLOGY OF TASMANIA

Tasmania is the southern most portion of the continental land mass of Australia. Although it is an island, it is connected to the mainland by Bass Strait, which is of typical continental shelf depths (< 100 m).

To the east and west of Tasmania there is a narrow continental shelf with a steep continental slope. Normal oceanic depths (> 2000 m) are thus encountered within a distance of only 40-50 kms of the coastline. To the south there is a southward extension of the bathymetric contours. This feature consists of a deep ridge or rise, known as the South Tasmanian Rise with depths of the order of 1000 m. Very little is known about this structure.

Tasmania is therefore relatively unique in that it approaches being a continental land mass of very small aerial extent. In particular, an east-west profile taken across the island, consisting of an oceanic-continental-oceanic section, has a total length of only 5-600 kms.

The topography of Tasmania is dominated by the geological structure which often gives rise to spectacular land forms. In the north-eastern part of Tasmania, there is a high mountainous region with peaks at Ben Lomond (over 1600 m) and Mt. Barrow (1500 m). These peaks are situated on a granite mass which is exposed over a large part of the north eastern part of the state.

To the west, there is a low lying area dominated by the north-west trending Tamar valley. This is a graben feature of Tertiary age and is filled with Tertiary and more recent sediments.

To the south and west of the Tamar valley, there is a steep rise to the Central Plateau region. Near-vertical cliffs, or tiers, are formed at the edge of the plateau due to the exposure of sills of dolerite. The elevation of the Central Plateau region is around 1000 m reaching up to 1400 m at the north-eastern margin.

In the south-east, the dolerite forms a partial cover over a large portion of the area. The sediments and volcanic rocks in this region are relatively young being mainly Permian or younger. The topography is largely dominated by the local structure of the dolerite.

To the west and south of the Central Plateau, the terrain becomes much more rugged, partly due to the formation of deeply incised river valleys. The highest peaks in Tasmania are found in the area west of the Central Plateau (Mt. Ossa, 1700 m). Toward the south the mountains form distinct regions separated by deep river valleys. These mountains (Mt. Field West, Mt. Styx, Mt. Wellington, the Hartz mountains and Mt. La Perouse) form a chain of mountains extending to the south coast. The peaks are of the order of 1300 m rising from a plateau level of the order of 1000-1100 m.

In the remote south-western part of the state the mountains form long gently arcuate ridges, mainly composed of quartzite or metamorphosed sediments of Palaeozoic age or older. The regions between the ridges are flat low-lying swamps (one of the few regions of the state where the normally dense tree cover is not so marked).

The drainage pattern of Tasmania has been examined (e.g. Davis, 1959) and there are several interesting features. The drainage divide, between river systems, commonly occurs near the coast line. This is most clearly demonstrated on the east coast where the divide is within a few miles of the sea. The Derwent valley and its estuary has a typical drowned river valley appearance. This combined with the unusual drainage patterns indicate that the south-eastern part of the state has suffered subsidence during the Pleistocene (Jennings, 1959).

This very brief outline of Tasmania has been drawn from two major sources: the Atlas of Tasmania (Davis, 1965), and the Geology of Tasmania (Spry and Banks, 1962). Maps of the topography and geology of Tasmania are included as Figures 1.1 and 1.2, respectively. For the further background information the reader is referred to these two texts.

1.2 AIMS OF THIS STUDY

The primary aim of this study was to map the thickness of the crust in the Tasmanian region.

In order to properly fulfil this aim a number of secondary aims were detailed.

1. The establishment of a regional gravity survey over the whole state,

2. The development of techniques to separate the regional and residual components of the gravity field.

3. The choice of a suitable coefficient set such that the regional field could be evaluated in any part of the state.

4. The interpretation of the gravity data in terms of the crust-mantle interface and major upper crustal structures.

5. An independant estimate of the crustal thickness indicated by crustal seismic refraction data.

6. An examination of the spectral properties of high level aeromagnetic data to ascertain whether or not information on deep crustal structure could be found.

In brief, the problem, to obtain information on the crustal structure of Tasmania: the approach, to use suitable existing geophysical data and techniques and where necessary to develop new methods.

FIGURE 1.1

TOPOGRAPHY OF TASMANIA

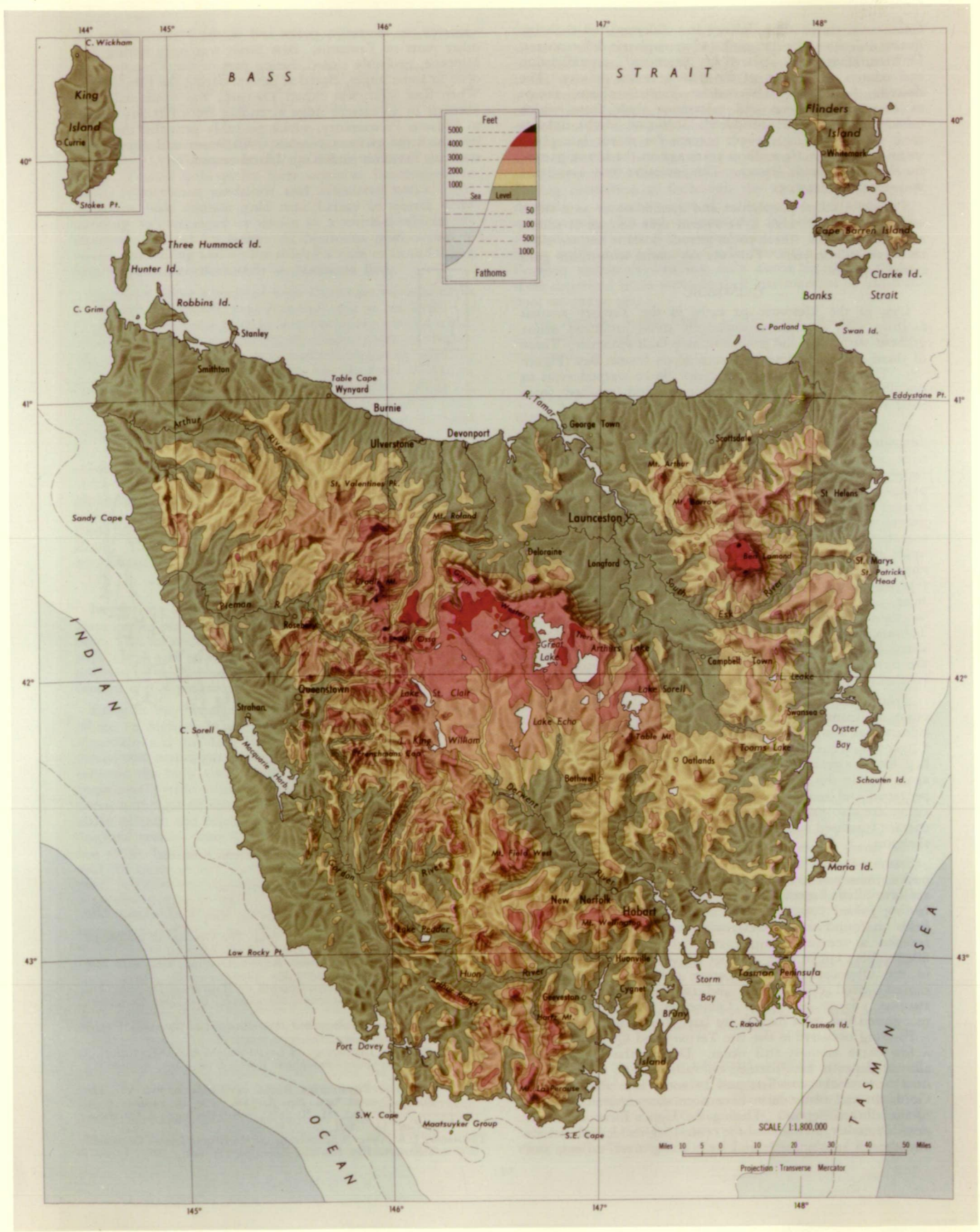
BASS
STRAIT
INDIAN
OCEAN
TASMAN
SEA
Feet
5000
4000
3000
2000
1000
Sea Level
50
100
500
1000
Fathoms
King Island
C. Wickham
Currie
Stokes Pt.
Flinders Island
Whitemark
Cape Barren Island
Clarke Id.
Banks Strait
Three Hummock Id.
Hunter Id.
Robbins Id.
C. Grim
Stanley
Smithton
Table Cape
Wynyard
Burnie
Arthur River
Ulverstone
Devonport
R. Tamar
George Town
C. Portland
Swan Id.
Eddystone Pt.
Scottsdale
Mt. Arthur
St. Helens
St. Valentines Pk.
Mt. Roland
Launceston
Sandy Cape
Deloraine
Longford
Ben Lomond
St. Marys
St. Patricks Head
South Esk River
Rosebery
Great Lake
Arthurs Lake
Campbell Town
L. Leake
Queenstown
Lake St. Clair
Lake Sorell
Strahan
Lake Echo
Swansea
Oyster Bay
C. Sorell
L. King William
Table Mt.
Oatlands
Tooms Lake
Macquarie Harbour
Bothwell
Derwent River
Schouten Id.
Mt. Field West
Gordon River
Maria Id.
New Norfolk
Hobart
Mt. Wellington
Lake Pedder
Low Rocky Pt.
Huonville
Huon River
Storm Bay
Tasman Peninsula
Cygnet
Geeveston
Bruny Island
C. Raoul
Tasman Id.
Port Davey
Mt. La Perouse
S.W. Cape
Maatsuyker Group
S.E. Cape
SCALE 1:1,800,000
Miles 10 5 0 10 20 30 40 50 Miles
Projection : Transverse Mercator
144°
145°
146°
147°
148°
40°
41°
42°
43°

FIGURE 1.2

GEOLOGY OF TASMANIA

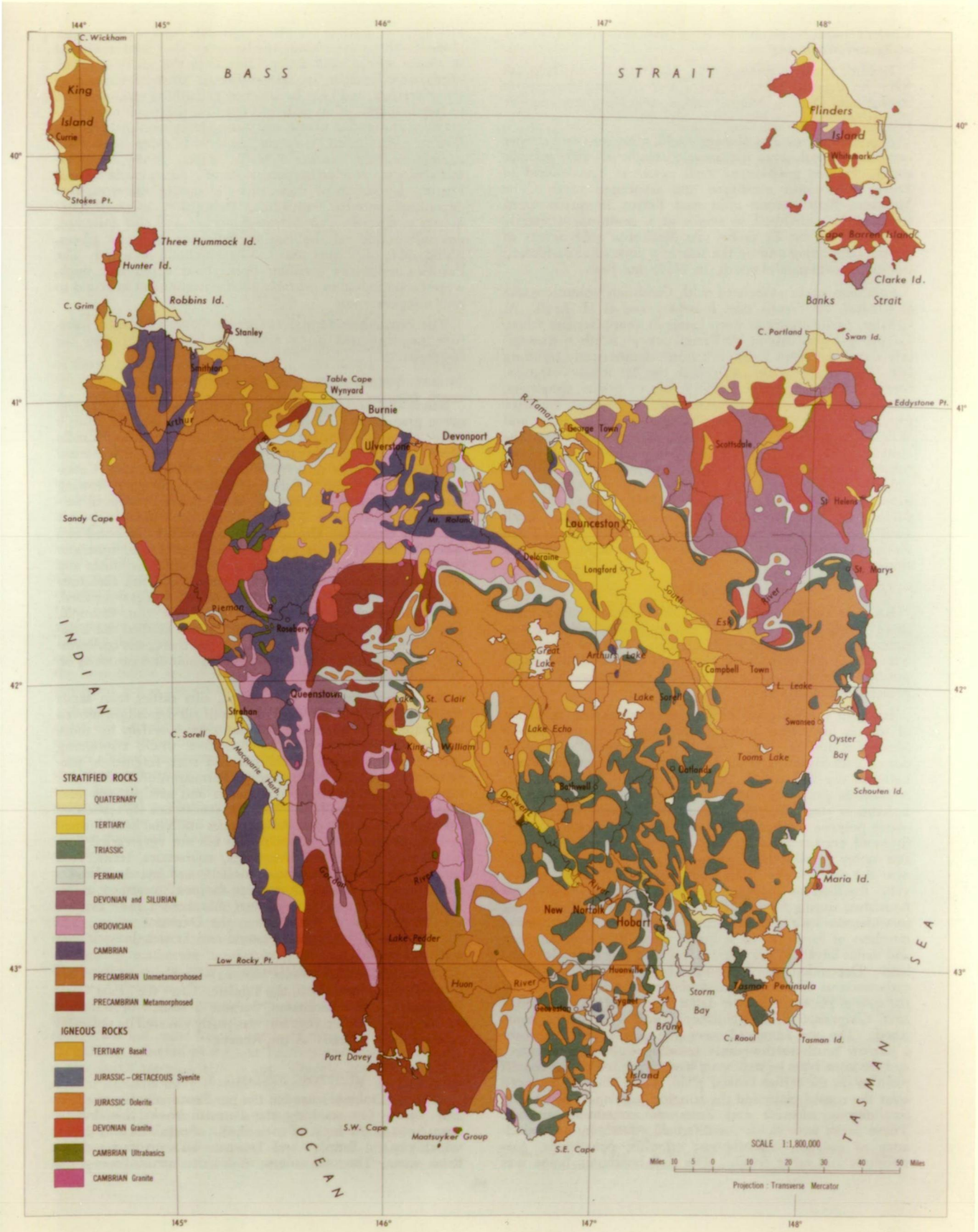
BASS STRAIT
INDIAN OCEAN
TASMAN SEA
King Island
C. Wickham
Currie
Stokes Pt.
Three Hummock Id.
Hunter Id.
Robbins Id.
C. Grim
Stanley
Smithton
Table Cape
Wynyard
Burnie
Arthur R.
Sandy Cape
Ulverstone
Devonport
R. Tamar
George Town
Launceston
Mt. Roland
Doloraine
Longford
Piemon
Rosebery
Queenstown
Lake St. Clair
Strahan
C. Sorell
Macquarie Harb.
King William
Great Lake
Arthurs Lake
Lake Sorell
Lake Echo
Tooms Lake
Campbell Town
L. Leake
Swansea
Oyster Bay
Schouten Id.
Orielton
Bothwell
Derwent River
New Norfolk
Hobart
Maria Id.
Lake Pedder
Low Rocky Pt.
Huon River
Port Davey
S.W. Cape
Maatsuyker Group
S.E. Cape
Huonville
Cygnet
Bruny Island
Storm Bay
Tasman Peninsula
C. Raoul
Tasman Id.
Flinders Island
Whitemark
Cape Barren Island
Clarke Id.
Banks Strait
C. Portland
Swan Id.
Eddystone Pt.
Scottsdale
St Helens
St Marys
Esk R.
144°
145°
146°
147°
148°
40°
41°
42°
43°
STRATIFIED ROCKS
QUATERNARY
TERTIARY
TRIASSIC
PERMIAN
DEVONIAN and SILURIAN
ORDOVICIAN
CAMBRIAN
PRECAMBRIAN Unmetamorphosed
PRECAMBRIAN Metamorphosed
IGNEOUS ROCKS
TERTIARY Basalt
JURASSIC–CRETACEOUS Syenite
JURASSIC Dolerite
DEVONIAN Granite
CAMBRIAN Ultrabasics
CAMBRIAN Granite
SCALE 1:1,800,000
Miles 10 5 0 10 20 30 40 50 Miles
Projection : Transverse Mercator

CHAPTER TWO

REGIONAL GRAVITY SURVEY OF TASMANIA

2.1 HISTORICAL DEVELOPMENT OF SURVEY

2.1.1 Initiation of survey

The regional gravity survey of Tasmania was initiated in 1960 by R. Green, then Senior Lecturer in geophysics at the University of Tasmania. In the initial phases of the gravity survey students carried out local exercises of very varying quality. Some of this work has been retained.

2.1.2 Early surveys (1960-1965)

A number of surveys of particular regions were carried out by Honours students in the period 1960-1965.

McDougall and Stott (1961) carried out an investigation of the Red Hill Dyke, near Margate. Shelley (1965) surveyed an area in the vicinity of Sorell and Leaman (1965) carried out a geological and geophysical investigation of the Cygnet Complex. These surveys were all of very restricted areas.

Larger scale surveys were carried out by Jones (1963); (Jones, Haigh and Green (1966)), who investigated the structural form of the Great Lake dolerite body, and by Hinch (1965), who surveyed the Cressy region near Launceston and interpreted the observed gravity low as a Tertiary sediment filled graben.

2.1.3 Isogal survey

In the period 1963 to 1965, the Bureau of Mineral Resources, Canberra carried out an "isogal" survey of

Australia. The purpose of that survey was to establish permanent gravity base stations along east-west lines across the Australian continent. The resulting measurements made by several independent gravity meters have been adjusted by least squares techniques and have achieved a national network of base stations that are considered accurate to ±0.1 mgals. (Barlow, B.C., in preparation).

The datum base for this survey is the Australian National Gravity Base Station in Melbourne, which is taken to have a value of 979.979 gals. (Barlow, B.C., 1970).

Some of the isogal stations have been used, in Tasmania, as a basis for adjustment of all the gravity surveys that have been carried out to date. These are Hobart (airport), Hobart, Launceston, St. Helens, Wynyard and Strahan. Each survey has therefore been made internally consistent and has also been adjusted so that the observed intervals correspond to those obtained during the isogal survey.

Figure 2.1 shows the locations and values obtained for the Tasmanian isogal stations.

2.1.4 Survey of Eastern Tasmania

During 1966, B.F. Cameron, carried out a compilation of existing surveys and completed the regional gravity survey of eastern Tasmania. (Cameron, 1967).

The first part of this project was to assemble all the gravity data that had been obtained to that date. This

BUREAU OF MINERAL RESOURCES
GRAVITY BASE STATIONS IN TASMANIA

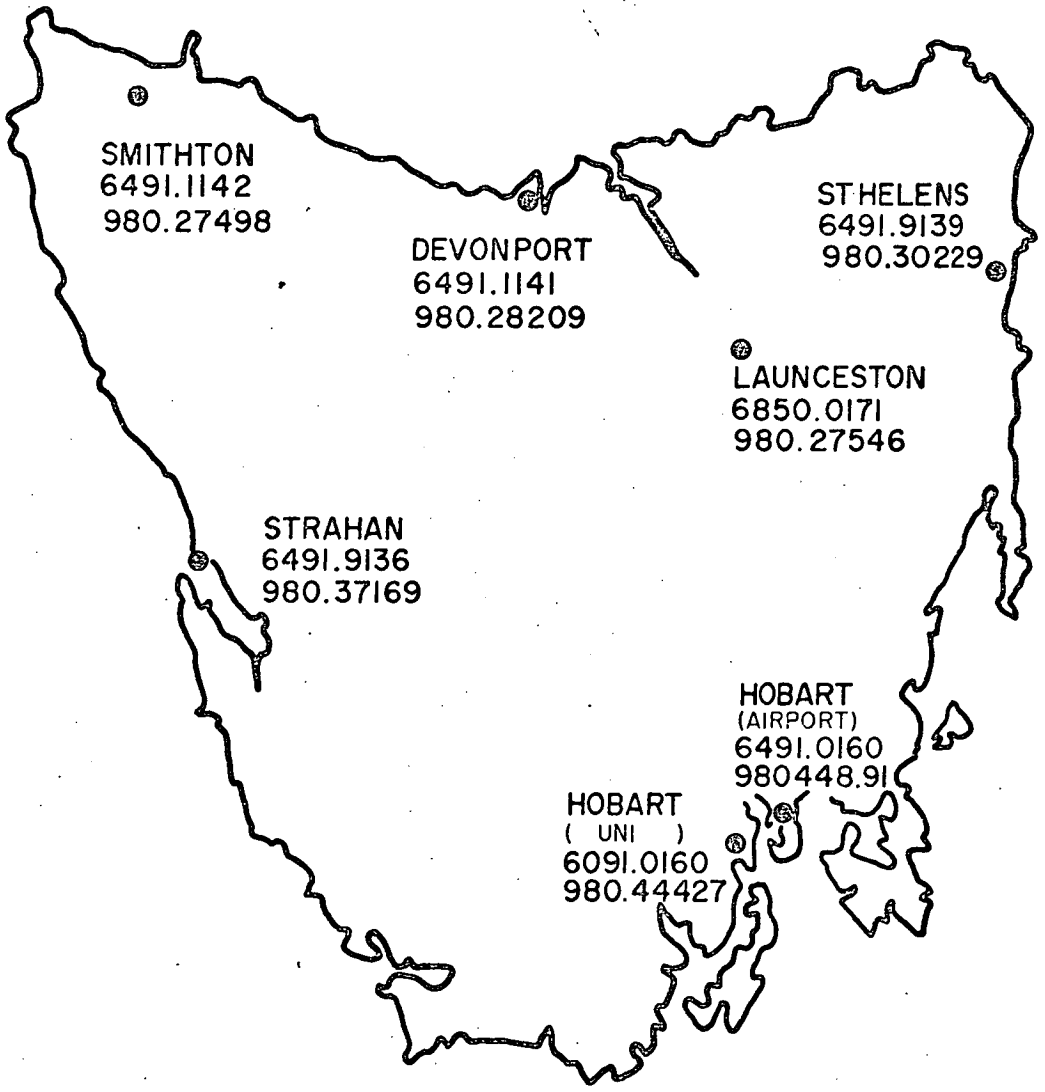

FIGURE 2·1

involved recomputation and adjustment of survey parameters. The original gravity reduction programme (U191, written by R. Green) was modified for this recomputation.

The second part of the project was to take gravity measurements in selected regions of eastern Tasmania. This was intended to provide a more complete coverage of the region and to tie together the previously unrelated surveys.

The result of this work was the establishment of a gravity survey, on a regional scale, which covered most of the eastern part of the state. The survey was confined to regions accessible by vehicular transport. Some interesting anomalies were identified and preliminary interpretations were carried out.

Cameron was able to define a regional gradient, in the Bouguer anomaly, which varies from +20 mgals at the east coast to -40 mgals in the Central Highlands area. This was interpreted as being due to crustal thickening towards the centre of Tasmania from 34 kms to about 39 kms.

The Great Lakes anomaly (Jones, 1963) and the Cressy anomaly (Hinch, 1965) were both reinterpreted by Cameron who did not markedly change the interpretations. The Great Lakes anomaly was interpreted as being due to a boss or neck of dolerite 1.2 kms deep and approximately 13 kms in diameter. The Cressy structure was interpreted as a sediment filled graben 11 kms wide and having a depth of the order of 1 km.

A large negative feature was identified on the northern margin of the area, near Avoca, which was interpreted as being due to either a granite body or a sedimentary feature. The remaining features of the gravity field were interpreted in terms of dolerite structures.

The thesis was completed by a useful list of recommendations for future surveys. This list was referred to in planning the subsequent stages of the regional gravity survey of Tasmania.

2.1.5 Survey of North-eastern Tasmania

Following the work of Cameron (1967) several additional surveys were undertaken in order to extend the coverage of the regional survey. A survey of the north-eastern part of the state was carried out by Cameron in order to establish the extent of the Avoca gravity low. The survey was restricted to road traverses as the terrain is very rugged.

The survey was able to delineate the shape of the gravity feature. The gravity low observed on the Avoca traverse is seen to extend northwards and coincides approximately with the outcrop of granite in the north-east. The detailed relationships, between the observed margin of the granite and the margin inferred from the gravity map are complex and will only be elucidated by more detailed mapping.

2.1.6 West Coast survey

During 1967, a survey of the West Coast region of Tasmania was carried out by myself with the assistance of B.F. Cameron and M.J. Rubenach. (Johnson, B.D., 1967).

This consisted of road traverses along the Lyell, Zeehan and Murchison Highways. Much of this region is extremely inaccessible except along these roads.

The survey was then extended into the north-western part of the state along the Savage River road and along the north coast.

A further road traverse was carried out along the Gordon River road leading to the new Gordon River damsite in the South West of Tasmania. A number of short traverses were also made in the National Park region along timber tracks.

The coverage thus obtained was therefore almost complete for all road access. A successful approach was made to the Broken Hill Co. Pty. Ltd. to assist the survey by making some helicopter time available. This enabled the establishment of over 200 gravity stations reasonably uniformly distributed throughout this otherwise inaccessible region of the state.

The regional survey has been carried out on the basis of availability. Much of the terrain that remains to be surveyed is highly inaccessible and requires not only helicopters but ground parties to cut landing areas.

2.1.7 More recent surveys (1968-1970)

Further surveys have been carried out, since 1968, by several authors, in order to define particular geological problems.

A survey of King Island (to the north west of Tasmania) was carried out by myself and G.M. Sheehan. The survey was interesting in that a reasonably uniform station coverage of the island was possible and that the geological structure was largely hidden due to recent sand cover.

A survey of the Sheffield region of northern Tasmania was carried out by G.M. Sheehan (1969).

Further work was carried out in the Longford-Cressy region by M.J. Longman of the Mines Department, Hobart (Longman & Leaman, 1967) which greatly extended the work of Hinch (1965). A major reinterpretation of this work has subsequently been carried out.

A detailed study of the dolerite distribution and structure, in the Hobart district, was undertaken by D.E. Leaman (1970).

The work is still continuing.

MAJOR SOURCES OF DATA FOR REGIONAL GRAVITY OF TASMANIA

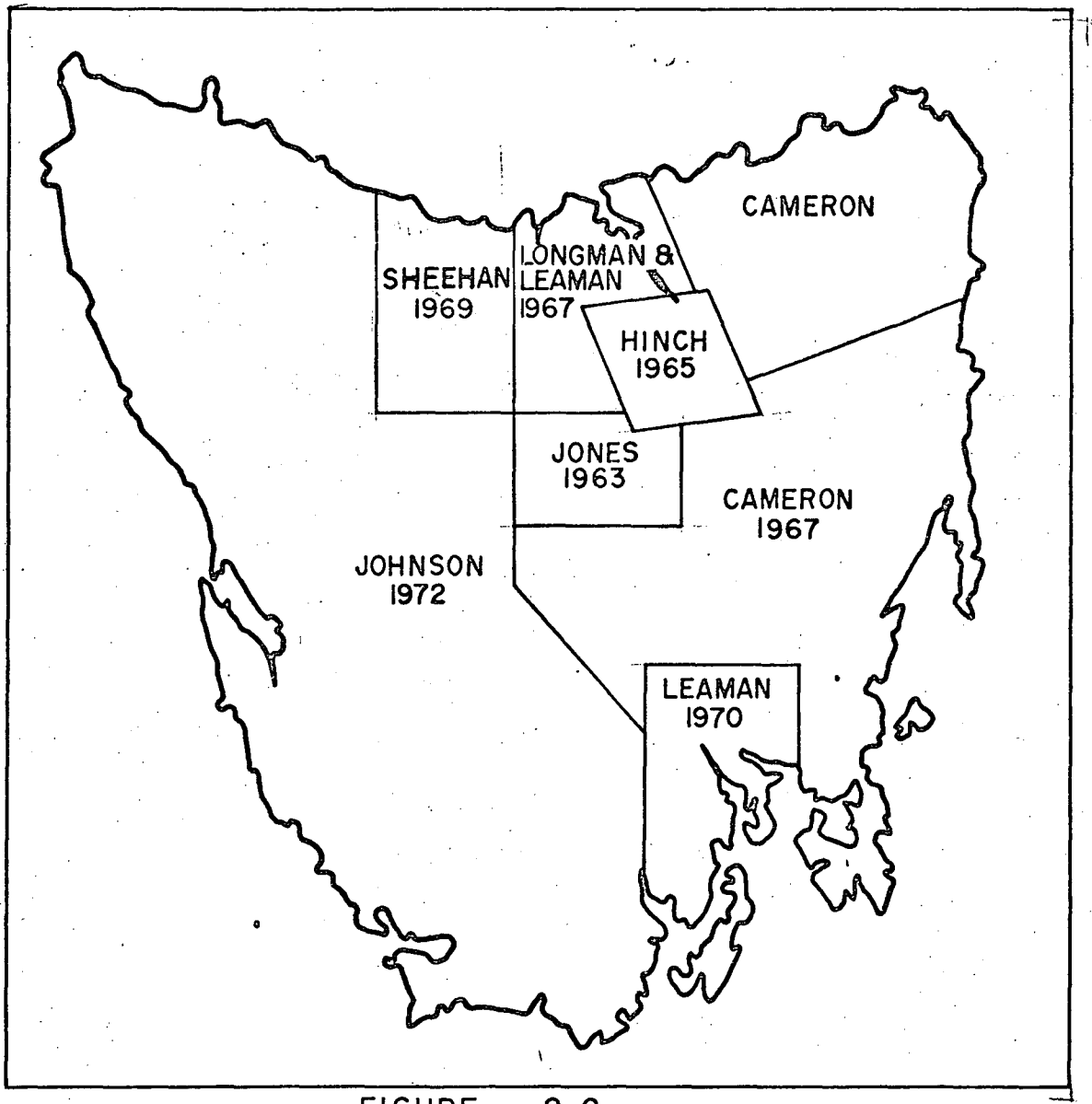

FIGURE 2·2

2.2 SURVEY METHODS

2.2.1 Instrumentation

2.2.1.1 *Gravity meters*

A number of gravity meters have been used during the period of the gravity survey of Tasmania. The main instrument was the Worden No. 273 of the Geology Department, University of Tasmania. This was originally purchased in 1960 and had an 80 mgal range dial on the fine adjustment spring. During 1967, the instrument was returned to Texas Instruments and fitted with a new 200 mgal range dial. This greatly improved the performance of the instrument since only occasional scale changes were required during the course of a survey.

During the absence of this instrument, the Worden Master No. 201 of the Geophysics Department, Australian National University was borrowed. This instrument was used only in restricted areas as it was found to have a relatively high drift rate.

The helicopter survey of the south western area of the State was made with a portable La Coste-Romberg meter, G101, on loan from the Bureau of Mineral Resources, Canberra. The instrument was chosen for its supposedly excellent drift characteristics. However, in subsequent surveys unpredictably high drift rates were observed (Barlow B.C.,

pers. comm.). It is possible that some errors have therefore been incorporated into the survey values. Drift rates were observed during the survey but these were regarded as not being serious, in view of the errors in position and elevation.

2.2.1.2 *Microbarometers*

Two types of microbarometers were used to establish levels for survey stations. The first, Askania microbarometers, were found to be very sensitive to wind conditions, difficult to operate over large elevation changes and were not really accurate enough for this kind of survey. The second, Mechanism microbarometers, were found to be reliable, easy to use and sufficiently accurate for regional surveys. All the earlier surveys were carried out using the Askania microbarometers. Certain difficulties arose due to the lack of precision of these instruments, but this could be overcome in part by surveying around the contour and between fixed level points as far as possible (Longman, M.J., pers. comm.). It is considered that the errors in the elevations are the major source of error in these surveys.

2.2.2 Survey Techniques

2.2.2.1 *Drift Control*

The organisation of a gravity survey is dependant upon the characteristics of the variation in time, or drift, of

the gravimeter spring.

It has been found that it is sufficient to assume linear variation of the spring in periods of the order of 1 hour. In order to account for this, repeated readings must therefore be taken at a number of the stations, the time interval being not much greater than 1 hour.

Since we are interested only in the relative differences between stations (even with a meter having a world wide range), it should only be used in the relative mode. It is a straightforward matter to determine the drift corrected gravity intervals. It is important, however, to establish a clearly defined routine method; since without this it is difficult for different people to arrive at the same answers.

Since, in all of these surveys, microbarometers were used to obtain levels, it was found convenient to reduce the barometric values in the same manner as the gravity values. In this case the pressure is varying with time and not the measuring device. Again the barometer was used in a relative sense between fixed levels, normally state permanent marks.

This process can be automated as in the Bureau of Mineral Resources System of reduction of gravity data (Barlow B.C., Pers. Comm.).

2.2.2.2 *Adjustment of Intervals*

The isogal survey stations were used as a fixed frame of reference and all the surveys are adjusted to these values.

In the eastern part of the state complex loop patterns were adjusted by standard least squares methods (e.g. see Cameron, B.F., 1967).

In the remainder of the state, most of the surveys were carried out between two isogal stations or were tied to only one of these stations. In the former case simple linear adjustment was carried out for the survey values. This was considered to be completely adequate as the largest misclosures obtained during the regional survey were 0.05 mgals. This is within the accurace of the isogal values.

The helicopter survey of the south west of Tasmania was directly connected to the isogal station at Strahan airport. As a check, connections were made at Port Davey, where a temporary base station had been established by air from Sydney, and at the Gordon River Road. Both of these observations tied in well considering the measured drift variation in the La Coste-Romberg instrument. (The differences in the observations were 0.15 mgals at Port Davey and 0.06 mgals at the Gordon River Road.)

2.2.2.3 *Reduction of Gravity Data*

Standard techniques of reduction of gravity data have been employed throughout this survey. These have been incorporated into a computer programme, U191, originally written by R. Green and considerably modified by subsequent users.

The base station value and survey parameters are initially read in. Each station is then treated separately and the following sequence of operations is carried out:

1. multiplication of scale readings by the calibration constant of the meter.
2. adjustment of gravity intervals (if applicable)
3. addition of base station value

   thus giving absolute values of the observed gravity at each station
4. calculation of theoretical gravity from International Gravity formula

   $(g(\phi) = 978049.0\ (1 + 0.0052884\ \sin^2\phi$

   $- 0.0000059\ \sin^2 2\phi)$ mgals

   where ϕ is latitude of station
5. calculation of free air anomaly

   $g_A = gh + 0.3086\ h - g(\phi)$ mgals

   g_A = free air anomaly

   gh = gravity at height h meters
6. Calculation of Bouguer anomaly

   $g_B = g_A - 0.04185\ \rho\ h$ mgals

   g_B = Bouguer gravity anomaly

   ρ = density (normally use 2.67 gms/cc)
7. print out consisting of:

   station number, position, elevation, theoretical gravity (4), observed gravity (3), free air anomaly (5), Bouguer anomaly (6).

2.2.2.4 *Location of gravity stations*

The gravity stations were located by means of topographic survey maps and in some cases air photographs. The quality of the positioning is very variable since the accuracy of the topographic surveys is extremely variable.

Cards giving the description of the location of most of the gravity stations are lodged with the Geology Department, University of Tasmania.

2.2.2.5 *Accuracy of gravity values*

The accuracy of the gravity values is a function of a number of different factors:

Calibration constant of the meter

All the instruments used in this survey were calibrated on the Hobart calibration range (Barlow, B.C., 1967). Although some doubt has recently been raised over the actual value of the gravity interval of the Hobart range (Barlow B.C., pers. comm.) this has been assumed to be not serious.

Errors of the order of 0.01 mgals may be attributable to errors in the calibration constant.

Latitude of the gravity station

Errors in the positioning, and in particular, the latitude of the station can be serious in areas of inadequate topographic surveying. At the latitude of Tasmania (42^{o}S), the change in gravity is 0.807 mgals/km, towards the south.

Thus an error in positioning may be directly related to errors in the gravity value.

Expected error in Positioning (km)	Error in Gravity (mgals)
0.01	0.008
0.1	0.081
1	0.807

Errors in positioning are generally better than 0.1 kms for the eastern parts of the state and for areas that have been mapped for the Hydro Electric Commission. Other areas in the South-west of the state and in other poorly mapped areas may well be in error by greater than 0.1 kms but are certainly better than 1 kms.

Errors in elevation

Errors in elevation of the gravity station often lead to the most serious errors in the Bouguer anomaly values.

The combined elevation correction (using a density of 2.67 gms/cc in the Bouguer correction) is 0.1967 mgals/m. Thus an error of 1 meter in elevation gives rise to an error of 0.2 mgals.

In well controlled barometric surveys the errors in elevation are generally less than 1 metre. In less well controlled barometric surveys, in particular those using the Askania barometers, the errors may be as high as 3 metres.

Effect of Terrain Correction

The work of St. John (1967), and St. John and Green (1967) has shown that topographic corrections should be rigorously applied in regions of rugged terrain, taking into account the curvature of the earth, the departure of the topography from the Bouguer approximation and effects of horizontal variations in density.

In general there are two distinct regions of influence affecting the terrain correction at a given point. The first part is due to extremely local terrain variations; where only spectacular topographic variations, within a distance of less than a kilometre or so, have any appreciable effect. The second part is due to the inadequacies of the normal topographic correction process. This second effect must vary very slowly from station to station as the masses causing the effect are at a cnnsiderable distance from the station. The effect is only serious for high mountainous regions, such as New Guinea, which are closely associated with deep oceanic regions.

This second source of topographic correction has been ignored in this work, any large scale topographic variations being included in the isostatic model developed in the interpretation of the regional field.

The Bouguer Anomaly values are therefore considered accurate to ±0.2 mgals in all regions and are generally accurate to ±0.5 mgals.

2.2.3 Data Files

2.2.3.1 *University of Tasmania File*

A file of the original field data and reduced data for all the surveys is held at the Department of Geology, University of Tasmania.

A system for collating the results of the reduction programme was initiated in 1968, by myself. This system uses the programme, U606 GRAVDECK, which takes the reduced data tapes from U191 and combines these values with those present in the tape files. Facilities exist for deleting, exchanging and overwriting surveys or individual stations. These paper tape files are also lodged at the University of Tasmania.

2.2.3.2 *B.M.R. Files*

The Bureau of Mineral Resources, Canberra, has for several years been carrying out a systematic gravity survey of mainland Australia. Some of this data has been placed on computer files and may be readily accessed.

During 1970, I worked at the Bureau of Mineral Resources for a short period, in order to place the Tasmanian data onto compatible data files. A magnetic tape file now exists of all the gravity data obtained in Tasmania in the period 1960-1969.

2.3 BOUGUER ANOMALY MAP OF TASMANIA

The results of all gravity surveys carried out during the period 1960-1970 have been compiled using a crustal density of 2.67 gms/cc and a Bouguer anomaly map of Tasmania has been drawn. Considerable assistance with this project was generously given by Mr. B.F. Cameron. A copy of this map at 1:500,000 scale is placed in the appendix to the thesis. (Figure A.1).

CHAPTER THREE

ANALYSIS OF GRAVITY DATA

3.0 ANALYSIS OF GRAVITY DATA

Before any meaningful interpretation can be made of the Bouguer anomalies, observed in Tasmania, consideration must be given as to the source of the anomalies.

The most striking feature of the Bouguer anomaly map is the regional effect due to the close proximity of the oceanic crustal structure. This causes the values, near to the coasts, to have a steep positive gradient of the order of 1 mgal/km toward the ocean.

Superimposed on this regional anomaly are many smaller scale anomalies that are due to structures which are shallower than the depth of the continental crust.

In order to separate these smaller scale anomalies from the broader regional anomalies, an effective method must be found in order to adequately represent the regional component. Once this has been carried out the regional component may be removed from the observed values to give the residual anomaly due entirely to shallow sources.

3.1 DETERMINATION OF REGIONAL FIELD

The complete set of the gravity data is extremely unevenly distributed. Surveys have been carried out in detail in restricted regions, along roads and vehicular tracks, and in isolated positions accessible only by helicopter.

Any kind of surface fitting procedure, of irregularly

spaced data, is biased towards fitting the surface to the data points. Hence, if we have a restricted region of complex data, and a large proportion of the data set is present in this region, then the surface in the area adjacent to the detailed region will also tend to reflect the complex nature of that region. The effect is thus to produce a highly complex surface in an area where there are few, if any, data points.

It is necessary therefore to remove this bias from the data set. This was carried out by averaging the original data set and producing a subset of more evenly spaced and smoothed data.

3.1.1 Averaged data set

The method chosen to obtain a smoothed subset of the data was by a form of convolution filtering.

The average value and position was calculated for all stations lying within each 20,000 yard (approx. 20 kms) grid square. This procedure was chosen to limit the amount of computer calculations involved. In any process of aerial smoothing, distances are normally calculated between every possible pair of data points. If the number of points, n, is large, then this can become prohibitive since there are of the order of n^2 calculations.

A much simpler process can however be devised with a large reduction in computer time. Each station position was

known in terms of the Transverse Mercator grid coordinates giving distances in yards north and east from a fixed point. A station can be defined to lie within a particular 20,000 yard square by carrying out an integral division of the coordinates by 20,000. It is then a simple matter to reference all the stations within a particular square, and to carry out averages of value and position. The number of calculations has been reduced to order n.

However this is not the end of the process since the averaging of the data set has introduced spurious effects into the data. The averaging process is approximately equivalent to the application of a two-dimensional sin xf/xf filter in frequency. The data must be further smoothed to eliminate the deleterious effects of the simple averaging process.

A second stage of filtering was therefore carried out on the averaged data set. The process chosen for this stage was to perform a convolution by averaging all the values within a distance, r, of each station. This is equivalent to applying a sin rf/rf filter in frequency. To reduce the effect of the side lobes, the process was repeated. The effects of repeated application of a convolution filter are well demonstrated in Bracewell (1965, p171).

Table 3.1 is the data set resulting from the averaging process and at each stage of the filtering. The square index

REGIONAL GRAVITY SURVEY OF TASMANIA

DATA AVERAGED OVER 20000 YD (20 KMS) GRID SQUARES

SQUARE INDEX	GRID COORDINATE NORTH	GRID COORDINATE EAST	UNFILTERED DATA NUMBER OF DATA POINTS	UNFILTERED DATA HEIGHT METRES	UNFILTERED DATA FREE AIR ANOMALY	UNFILTERED DATA BOUGUER ANOMALY	20 KMS FILTERED DATA NUMBER OF DATA POINTS	20 KMS FILTERED DATA HEIGHT METRES	20 KMS FILTERED DATA FREE AIR ANOMALY	20 KMS FILTERED DATA BOUGUER ANOMALY	40 KMS FILTERED DATA NUMBER OF DATA POINTS	40 KMS FILTERED DATA HEIGHT METRES	40 KMS FILTERED DATA FREE AIR ANOMALY	40 KMS FILTERED DATA BOUGUER ANOMALY
6244	636000	457900	1	.30	22.54	22.50	3	3.49	20.42	20.69	5	99.26	25.07	14.37
6246	634157	474793	3	.25	22.15	25.12	3	1.92	20.46	21.24	5	78.13	24.86	16.60
6440	649940	411886	7	5.70	-.04	-.79	2	17.69	.41	-1.57	5	95.30	14.98	4.31
6442	643200	432200	1	.30	15.35	15.32	2	6.30	18.02	17.31	7	126.48	20.50	6.49
6444	641900	447400	2	14.69	18.87	17.22	3	5.89	19.07	18.74	7	140.88	25.48	10.00
6446	641703	478943	3	.30	18.73	18.69	3	28.69	20.82	18.27	8	128.49	27.18	13.10
6448	655152	484852	5	.64	16.30	16.23	4	78.34	22.33	13.81	7	92.84	26.07	15.86
6450	655360	503650	1	.00	23.09	23.09	2	17.11	23.51	21.59	5	51.21	24.97	19.33
6638	667300	393367	3	10.78	24.47	23.26	2	4.73	24.08	23.55	6	40.19	13.26	8.76
6640	665634	414871	8	.04	-1.04	-1.05	3	43.70	.83	-4.07	8	116.48	16.05	3.01
6642	671365	425020	2	89.29	5.18	-4.82	3	99.03	3.41	-7.68	9	184.29	21.77	1.19
6644	673200	455750	1	1008.89	106.33	-6.56	2	790.66	78.10	-10.36	9	245.53	30.21	2.82
6646	672548	477270	5	320.73	38.98	3.09	4	126.41	24.32	9.95	8	203.15	30.32	7.69
6648	672760	489778	6	19.91	15.02	12.79	5	82.44	23.01	13.79	9	125.18	27.52	13.00
6650	670075	509147	6	39.00	25.40	21.04	4	34.53	24.22	20.36	8	63.56	25.53	18.47
6652	675520	520360	1	.00	27.56	27.56	3	30.05	26.52	23.15	6	43.44	27.15	22.29
6836	693800	375800	1	.30	26.22	26.18	3	2.69	25.87	26.57	6	53.86	21.74	15.71
6838	682300	386850	2	.46	22.84	22.79	3	3.29	24.66	24.29	7	61.42	16.93	10.06
6840	690600	408600	2	108.77	.00	-12.16	2	161.34	3.81	-14.24	9	160.56	17.74	-.24
6842	698950	425450	2	197.33	.82	-21.31	4	168.94	6.77	-12.13	8	234.95	22.02	-4.27
6844	685200	447000	2	572.44	49.88	-14.17	2	790.66	78.10	-10.36	8	281.71	29.15	-2.37
6846	699606	472994	5	205.29	27.18	4.21	3	150.00	23.22	6.44	8	219.31	28.88	4.45
6848	686004	493194	161	74.26	22.39	14.08	4	87.74	22.92	13.10	9	145.59	26.05	9.76
6850	696820	509314	72	187.27	38.19	17.23	4	86.87	26.38	16.65	9	78.84	25.23	16.41
6852	686050	521910	2	.00	25.82	25.82	3	60.66	28.72	21.93	8	53.06	27.31	21.38
6854	690506	556559	8	106.41	47.87	35.96	3	48.11	38.03	32.64	7	49.11	31.91	26.41
6856	693639	564544	9	40.00	38.51	34.04	4	44.50	37.09	32.11	4	40.02	33.68	29.20
7034	708800	355200	1	10.67	36.35	35.16	2	4.69	31.33	30.80	5	56.71	28.56	22.21
7036	705140	367620	2	.46	28.35	28.30	3	3.25	29.49	29.12	8	75.74	24.73	16.25
7038	709390	394000	1	39.62	2.70	-1.74	1	39.62	2.70	-1.74	9	124.99	20.50	6.51

REGIONAL GRAVITY SURVEY OF TASMANIA

DATA AVERAGED OVER 20000 YD (20 KMS) GRID SQUARES

SQUARE INDEX	GRID COORDINATE NORTH	GRID COORDINATE EAST	UNFILTERED DATA NUMBER OF DATA POINTS	UNFILTERED DATA HEIGHT METRES	UNFILTERED DATA FREE AIR ANOMALY	UNFILTERED DATA BOUGUER ANOMALY	20 KMS FILTERED DATA NUMBER OF DATA POINTS	20 KMS FILTERED DATA HEIGHT METRES	20 KMS FILTERED DATA FREE AIR ANOMALY	20 KMS FILTERED DATA BOUGUER ANOMALY	40 KMS FILTERED DATA NUMBER OF DATA POINTS	40 KMS FILTERED DATA HEIGHT METRES	40 KMS FILTERED DATA FREE AIR ANOMALY	40 KMS FILTERED DATA BOUGUER ANOMALY
7040	711980	416730	1	292.64	29.79	-2.96	3	281.42	23.74	-7.75	8	239.94	21.57	-5.28
7042	705950	422750	1	281.51	22.81	-8.70	3	243.77	17.71	-9.57	7	280.59	23.65	-7.75
7046	707989	475726	7	76.08	14.98	6.47	3	127.44	20.64	6.38	8	220.94	24.39	-.33
7048	705481	489664	14	56.58	12.56	6.23	3	88.71	13.97	9.05	9	147.35	21.50	5.01
7050	712780	514760	105	164.73	31.12	12.68	4	80.02	22.56	13.62	9	89.23	21.59	11.61
7052	713151	526816	55	8.69	17.18	16.21	3	71.17	20.31	12.34	9	59.77	24.56	17.87
7054	702925	552175	2	7.31	29.83	29.01	4	44.50	37.09	32.11	9	51.89	29.36	23.55
7056	709544	566556	9	32.44	34.47	30.84	4	43.04	35.29	30.47	6	44.86	31.15	26.13
7234	730728	354970	6	134.21	48.38	33.36	3	85.00	38.49	28.98	7	76.48	31.81	23.25
7236	735011	365600	7	146.52	22.22	5.82	3	110.83	25.91	13.50	9	109.46	26.10	13.85
7238	733664	394658	5	277.75	26.25	-4.83	3	224.33	21.27	-3.83	9	187.27	22.85	1.90
7240	729940	409007	20	339.46	31.75	-6.23	4	276.69	24.97	-5.99	9	278.76	23.49	-7.70
7242	730688	431299	18	422.80	34.58	-12.73	2	433.91	32.13	-16.43	8	338.92	25.87	-12.06
7244	732936	454344	23	371.36	29.77	-11.79	3	341.65	26.19	-12.04	7	313.76	24.28	-10.83
7246	735345	470000	8	258.33	24.11	-4.80	4	240.34	18.30	-8.60	8	230.05	19.69	-6.05
7248	734381	487183	9	124.01	5.02	-8.86	4	139.03	13.50	-7.65	9	162.91	17.20	-1.03
7250	726890	514419	59	15.23	7.74	6.03	4	65.97	19.51	12.12	9	117.96	18.37	5.17
7252	732488	532093	292	37.92	18.73	14.48	4	58.90	19.13	12.54	9	94.22	21.99	11.45
7254	728800	549800	5	48.80	25.93	20.47	3	47.67	24.98	19.65	9	80.35	26.13	17.14
7256	723783	561933	3	54.95	34.26	28.11	3	42.10	30.71	26.00	6	72.04	27.83	19.77
7432	756370	336955	2	.07	51.83	51.82	4	50.53	41.57	35.91	5	63.04	35.88	28.82
7434	745810	342940	2	.15	50.56	50.56	3	58.65	45.05	38.49	8	82.88	31.29	22.01
7436	750320	371708	4	68.96	3.84	-3.88	4	123.13	16.41	2.63	8	117.33	25.40	12.27
7438	748130	390575	2	104.02	13.72	2.08	3	170.99	17.01	-2.13	8	224.34	23.82	-1.29
7440	744760	414520	1	219.46	13.40	-11.16	2	230.89	23.94	-7.49	8	341.31	26.54	-11.65
7442	741445	438865	2	456.68	31.35	-19.75	4	422.26	30.77	-16.43	8	389.19	28.72	-14.83
7444	749766	443027	11	461.48	29.45	-22.19	2	443.58	30.84	-18.79	9	366.45	26.15	-14.86
7446	744509	471269	48	185.26	16.62	-4.11	4	189.03	13.50	-7.65	9	290.71	21.12	-11.41
7448	749913	487148	12	161.40	6.05	-12.01	3	173.30	11.71	-7.74	9	221.36	17.85	-6.97
7450	748084	510811	15	106.45	8.60	-3.31	2	92.18	13.36	3.05	9	185.31	19.11	-1.62

REGIONAL GRAVITY SURVEY OF TASMANIA

DATA AVERAGED OVER 20000 YD (20 KMS)² GRID SQUARES

SQUARE INDEX	GRID COORDINATE NORTH	GRID COORDINATE EAST	UNFILTERED DATA NUMBER OF DATA POINTS	UNFILTERED DATA HEIGHT METRES	UNFILTERED DATA FREE AIR ANOMALY	UNFILTERED DATA BOUGUER ANOMALY	20 KMS FILTERED DATA NUMBER OF DATA POINTS	20 KMS FILTERED DATA HEIGHT METRES	20 KMS FILTERED DATA FREE AIR ANOMALY	20 KMS FILTERED DATA BOUGUER ANOMALY	40 KMS FILTERED DATA NUMBER OF DATA POINTS	40 KMS FILTERED DATA HEIGHT METRES	40 KMS FILTERED DATA FREE AIR ANOMALY	40 KMS FILTERED DATA BOUGUER ANOMALY
7452	746597	527884	117	99.62	15.98	4.83	3	78.25	14.61	5.85	9	160.92	22.11	4.10
7454	752284	550432	19	137.82	25.27	9.85	2	95.31	21.27	10.61	9	130.67	23.93	9.31
7456	755585	561463	4	52.81	17.28	11.37	2	95.31	21.27	10.61	6	111.90	24.44	11.91
7632	774130	335555	2	78.42	48.58	39.80	4	50.15	35.94	30.33	6	78.22	32.10	23.35
7634	770485	351024	12	71.46	27.02	19.82	5	73.57	30.56	22.32	9	106.67	28.37	16.44
7636	762030	361880	2	169.76	10.26	-8.75	3	102.44	18.82	7.35	8	168.23	23.02	4.20
7640	776020	415680	1	331.78	16.37	-20.76	2	604.04	40.16	-27.43	6	410.99	29.61	-16.38
7642	761620	425460	1	876.30	63.95	-34.11	2	604.04	40.16	-27.43	8	475.19	34.12	-19.05
7644	774066	450011	13	339.87	17.29	-20.74	3	400.42	24.61	-20.19	9	460.12	32.19	-19.29
7646	769519	467567	14	141.26	-3.03	-18.84	3	314.75	17.31	-17.91	9	398.40	28.02	-16.56
7648	770915	486788	11	354.17	28.74	-10.89	3	330.35	21.73	-15.23	9	340.32	25.57	-12.51
7650	770783	507444	17	265.63	18.05	-11.67	2	351.79	31.45	-7.91	9	304.44	26.22	-7.84
7652	774108	526750	8	407.21	41.74	-3.83	5	375.37	34.80	-7.20	9	262.13	28.84	-2.49
7654	778375	543800	2	296.72	28.91	-4.29	4	365.30	34.60	-6.28	9	204.64	25.28	2.38
7656	772650	573358	9	45.90	15.59	10.45	2	29.88	12.81	9.47	7	159.93	23.11	5.21
7832	789909	332746	7	2.69	37.63	37.33	4	65.20	28.81	21.51	6	96.75	24.62	13.79
7834	788994	350079	15	88.33	13.46	3.57	4	102.33	23.73	12.27	9	133.73	22.35	7.39
7836	789210	365810	1	266.15	14.20	-15.58	2	142.20	18.45	2.54	8	213.41	20.29	-3.59
7838	783695	392105	2	345.70	25.33	-13.36	1	345.70	25.33	-13.36	7	332.20	24.52	-12.65
7842	794189	432413	15	674.16	55.93	-19.51	3	641.80	50.12	-21.70	8	579.00	42.95	-21.84
7844	791535	451435	29	576.41	39.30	-25.20	5	560.09	40.39	-22.28	9	505.11	42.80	-22.97
7846	790392	467077	13	533.81	39.32	-20.41	2	562.72	40.48	-22.48	9	543.90	40.04	-20.82
7848	789555	487982	17	444.48	33.51	-16.22	2	356.31	25.43	-14.44	9	479.82	36.26	-17.43
7850	788907	516268	6	465.19	39.88	-12.17	3	394.74	36.37	-7.80	9	416.87	33.82	-12.83
7852	789061	527606	17	401.08	36.44	-8.44	4	385.10	36.02	-7.07	9	345.08	31.31	-7.30
7854	788828	549566	16	319.79	32.89	-2.89	4	346.91	33.28	-5.54	9	270.68	28.52	-1.76
7856	786591	575809	9	18.24	12.43	10.39	3	25.59	11.43	8.57	8	204.32	25.52	2.65
7858	795603	581000	3	18.94	6.82	4.70	3	27.10	10.96	7.93	6	142.67	21.32	5.36
8032	809594	333569	9	3.82	11.43	11.00	3	83.65	22.17	12.81	6	134.06	17.57	2.57
8034	811532	349621	9	209.94	20.32	-3.17	3	140.43	16.97	1.26	9	172.00	16.73	-2.52

REGIONAL GRAVITY SURVEY OF TASMANIA

DATA AVERAGED OVER 20000 YD (20 KMS) GRID SQUARES

SQUARE INDEX	GRID COORDINATE NORTH	GRID COORDINATE EAST	UNFILTERED DATA NUMBER OF DATA POINTS	UNFILTERED DATA HEIGHT METRES	UNFILTERED DATA FREE AIR ANOMALY	UNFILTERED DATA BOUGUER ANOMALY	20 KMS FILTERED DATA NUMBER OF DATA POINTS	20 KMS FILTERED DATA HEIGHT METRES	20 KMS FILTERED DATA FREE AIR ANOMALY	20 KMS FILTERED DATA BOUGUER ANOMALY	40 KMS FILTERED DATA NUMBER OF DATA POINTS	40 KMS FILTERED DATA HEIGHT METRES	40 KMS FILTERED DATA FREE AIR ANOMALY	40 KMS FILTERED DATA BOUGUER ANOMALY
8036	814971	369843	11	278.87	8.84	-22.36	2	249.27	9.89	-18.00	8	242.13	17.04	-10.05
8038	809536	390851	8	408.01	21.39	-23.66	2	533.86	37.63	-22.11	6	336.79	21.96	-15.72
8040	805993	410497	10	659.71	53.27	-20.55	2	533.86	37.63	-22.11	5	522.52	37.71	-20.76
8042	809518	431076	22	706.55	59.23	-19.83	3	675.06	53.45	-22.09	6	693.10	53.14	-24.42
8044	806289	449004	23	727.38	56.45	-24.94	3	647.71	50.17	-22.30	8	711.90	53.85	-25.80
8046	812148	469601	33	790.33	60.14	-28.29	3	861.47	66.77	-29.62	9	685.66	51.62	-25.11
8048	812951	485221	46	786.96	61.47	-26.59	3	840.29	64.92	-29.10	9	583.36	43.10	-22.18
8050	808107	506329	10	804.24	74.21	-15.78	1	804.24	74.21	-15.78	9	472.20	35.54	-17.30
8052	814517	533400	7	214.32	11.12	-12.86	3	279.95	20.10	-11.23	9	375.32	30.35	-11.65
8054	805143	548171	7	294.78	25.43	-7.56	4	316.76	27.90	-7.54	9	309.96	29.18	-5.50
8056	800600	560800	2	469.85	47.40	-5.18	3	343.81	32.70	-5.77	9	237.58	26.97	.38
8058	808350	586285	14	13.94	6.77	5.22	4	68.42	15.45	7.79	8	163.93	22.79	4.45
8060	814070	603786	8	22.31	14.79	12.30	3	29.22	11.90	8.64	5	111.23	19.14	6.69
8232	834353	327775	4	93.68	8.85	-1.64	2	165.44	13.19	-5.32	6	168.40	15.78	-3.06
8234	830222	352748	6	192.70	15.07	-6.50	4	203.01	12.23	-10.49	9	198.45	14.73	-7.47
8236	820543	370083	4	242.30	8.87	-18.24	3	237.40	10.65	-15.91	7	246.23	14.65	-12.90
8244	832110	454158	27	1000.10	75.51	-36.40	4	1019.97	80.19	-33.94	7	777.67	58.07	-28.94
8246	831009	469871	54	1010.53	81.09	-31.99	5	950.05	74.48	-31.83	9	720.71	52.38	-28.27
8248	831506	488969	31	799.96	58.72	-30.79	3	862.54	66.62	-29.90	9	572.87	38.73	-25.37
8250	835328	515456	18	230.62	4.49	-21.31	4	219.15	5.29	-19.23	9	435.19	28.40	-20.29
8252	834237	532110	23	197.71	3.98	-18.15	5	258.89	13.90	-15.07	9	353.52	24.83	-14.73
8254	830541	549451	16	567.03	63.66	.21	2	330.99	25.70	-11.34	9	330.96	28.67	-8.36
8256	823988	569576	13	565.27	77.75	14.50	2	265.79	40.39	10.65	9	281.02	29.66	-1.78
8258	827566	585092	13	91.26	21.96	11.75	5	163.67	25.75	7.44	9	191.50	25.26	3.84
8260	827393	601952	10	14.11	7.26	5.68	4	65.57	16.70	9.37	6	130.21	21.16	6.59
8432	844966	335104	9	219.53	21.03	-3.53	3	185.28	12.19	-8.54	6	208.76	22.34	-1.02
8434	849892	349839	10	209.64	4.46	-19.00	4	226.01	10.84	-14.45	8	243.79	18.07	-9.21
8436	856517	363997	3	277.91	.21	-30.89	3	282.70	10.60	-21.03	5	270.11	15.25	-14.97
8444	843290	453230	10	1128.30	85.84	-40.42	3	1050.17	82.71	-34.90	6	693.04	47.37	-30.18
8446	847075	467171	91	1045.85	87.75	-29.28	4	1019.97	80.19	-33.94	9	618.60	40.58	-28.64

REGIONAL GRAVITY SURVEY OF TASMANIA

DATA AVERAGED OVER 20000 YD (20 KMS) GRID SQUARES

SQUARE INDEX	GRID COORDINATE NORTH	GRID COORDINATE EAST	UNFILTERED DATA NUMBER OF DATA POINTS	UNFILTERED DATA HEIGHT METRES	UNFILTERED DATA FREE AIR ANOMALY	UNFILTERED DATA BOUGUER ANOMALY	20 KMS FILTERED DATA NUMBER OF DATA POINTS	20 KMS FILTERED DATA HEIGHT METRES	20 KMS FILTERED DATA FREE AIR ANOMALY	20 KMS FILTERED DATA BOUGUER ANOMALY	40 KMS FILTERED DATA NUMBER OF DATA POINTS	40 KMS FILTERED DATA HEIGHT METRES	40 KMS FILTERED DATA FREE AIR ANOMALY	40 KMS FILTERED DATA BOUGUER ANOMALY
8448	851992	494456	38	204.28	-9.18	-32.04	3	187.56	-4.64	-25.63	9	467.14	26.68	-25.59
8450	850075	509203	64	177.13	-3.96	-23.78	4	195.97	-1.02	-22.95	9	354.51	18.58	-21.09
8452	849604	527266	43	188.33	4.66	-16.42	4	219.15	5.29	-19.23	9	313.81	18.24	-16.88
8454	851438	551453	16	217.14	-.12	-24.42	3	373.77	22.63	-19.19	9	333.39	25.06	-12.25
8456	850296	570010	8	224.33	2.80	-22.30	4	334.90	22.69	-14.79	9	297.19	27.52	-5.74
8458	844267	583583	6	332.09	40.85	3.69	3	239.08	24.34	-2.41	9	215.64	25.59	1.46
8460	844700	606825	2	9.57	10.07	9.00	3	15.66	13.94	12.19	6	149.82	22.51	5.75
8630	872110	317300	4	73.53	28.78	20.55	2	198.10	41.10	18.94	4	241.50	34.47	7.45
8632	876750	324507	3	265.89	46.72	16.97	3	255.60	43.99	15.39	6	273.67	33.92	3.30
8636	869223	366187	6	386.01	23.93	-19.26	2	311.57	10.80	-24.06	5	367.77	30.24	-10.91
8644	875675	451122	42	283.52	1.17	-30.55	4	264.55	4.96	-24.64	7	441.52	24.21	-25.20
8646	872395	470095	33	378.58	16.74	-25.62	3	276.53	6.49	-24.45	9	420.06	22.07	-24.94
8648	870668	490349	119	179.28	-9.86	-29.92	4	171.35	-2.82	-21.99	9	320.14	13.61	-22.21
8650	871758	507718	104	158.14	.04	-17.66	4	188.17	4.27	-16.79	9	277.14	12.16	-18.86
8652	870546	527246	34	223.93	14.55	-10.51	3	270.81	16.56	-13.74	9	299.51	17.39	-16.13
8654	867317	556417	3	696.27	51.50	-26.41	3	423.22	26.08	-21.28	9	350.16	25.99	-13.20
8656	869550	568379	7	418.62	37.43	-9.41	3	396.15	26.81	-17.52	8	329.30	28.58	-8.27
8658	875510	590670	5	233.48	26.48	.35	2	116.74	19.99	6.92	8	224.60	25.57	.44
8660	862700	608400	1	.00	20.99	20.99	2	6.34	14.15	13.44	5	138.99	21.99	6.44
8832	888961	330447	9	340.02	57.87	19.82	3	362.49	49.78	9.22	4	307.55	41.65	7.23
8834	892556	349467	9	505.94	44.73	-11.88	3	470.14	53.70	1.09	6	394.36	42.02	-2.11
8836	892340	364918	4	625.16	62.71	-7.25	3	509.25	55.19	-1.79	5	436.40	42.74	-6.09
8840	899500	410350	1	410.84	28.36	-17.61	2	292.64	16.43	-16.32	5	256.06	16.44	-12.22
8842	882320	437760	1	241.40	-2.41	-23.43	3	255.04	4.32	-24.22	7	256.19	11.92	-16.75
8844	890461	451478	80	242.83	8.76	-18.41	5	233.02	5.65	-20.43	8	260.30	10.99	-18.14
8846	886896	469398	72	217.15	2.71	-21.59	4	229.10	4.18	-21.45	9	253.99	9.69	-18.53
8848	888449	489821	83	161.13	-2.03	-20.06	5	169.63	1.20	-17.78	9	215.50	7.58	-16.53
8850	888420	508060	92	126.74	6.21	-7.97	4	142.39	2.04	-13.90	8	222.64	9.70	-15.22
8852	885421	530051	16	408.45	35.63	-10.08	3	354.61	28.33	-12.47	7	276.55	16.56	-14.39
8854	892743	548345	4	498.35	40.46	-15.30	2	415.15	34.13	-12.33	6	353.01	25.70	-13.81

REGIONAL GRAVITY SURVEY OF TASMANIA

DATA AVERAGED OVER 20000 YD (20 KMS) GRID SQUARES

SQUARE INDEX	GRID COORDINATE NORTH	GRID COORDINATE EAST	UNFILTERED DATA NUMBER OF DATA POINTS	UNFILTERED DATA HEIGHT METRES	UNFILTERED DATA FREE AIR ANOMALY	UNFILTERED DATA BOUGUER ANOMALY	20 KMS FILTERED DATA NUMBER OF DATA POINTS	20 KMS FILTERED DATA HEIGHT METRES	20 KMS FILTERED DATA FREE AIR ANOMALY	20 KMS FILTERED DATA BOUGUER ANOMALY	40 KMS FILTERED DATA NUMBER OF DATA POINTS	40 KMS FILTERED DATA HEIGHT METRES	40 KMS FILTERED DATA FREE AIR ANOMALY	40 KMS FILTERED DATA BOUGUER ANOMALY
8856	890068	569388	5	273.41	21.36	-9.24	1	273.41	21.36	-9.24	6	299.06	25.87	-7.60
8860	890400	600900	1	.00	13.49	13.49	2	116.74	19.99	6.92	5	101.83	19.16	7.76
9036	911800	366481	8	517.18	61.23	3.36	4	446.81	49.84	-.05	6	381.04	41.97	-.67
9038	916800	380000	1	466.68	46.55	-5.67	4	378.27	44.14	1.81	7	332.16	33.56	-3.61
9040	902567	417330	6	213.64	8.85	-15.06	3	254.70	13.85	-14.65	6	195.50	10.69	-11.19
9042	905047	431926	16	194.67	5.54	-16.24	3	200.64	10.56	-11.89	9	185.85	9.39	-11.41
9044	906053	450056	36	128.13	11.69	-2.65	4	153.51	7.45	-9.72	8	170.17	6.99	-12.36
9046	905914	477722	5	170.93	9.11	-10.02	2	125.30	3.14	-10.88	7	167.17	5.44	-13.27
9048	908304	492222	40	69.58	-2.45	-10.23	4	126.68	2.21	-11.96	7	158.55	6.02	-11.72
9050	907517	504217	15	119.71	7.17	-6.23	3	125.70	3.15	-10.92	7	171.17	9.40	-9.75
9058	914810	591053	4	90.52	9.84	-.29	2	49.01	15.04	9.56	6	123.67	20.06	6.22
9060	909894	607624	5	27.10	15.98	12.96	3	39.19	18.79	14.41	4	61.66	18.41	11.52
9236	931006	370622	5	342.84	46.54	8.18	5	329.66	40.14	3.25	7	249.62	31.74	3.81
9238	930600	384700	10	299.45	32.87	-.64	4	287.78	35.89	3.69	7	258.14	30.74	1.86
9240	935189	403870	7	7.08	1.90	1.11	1	7.08	1.90	1.11	7	199.14	18.83	-3.45
9242	927002	431054	18	24.89	3.33	.55	2	46.15	7.08	1.92	6	148.34	8.60	-8.00
9244	926776	450053	49	34.63	8.98	5.11	3	80.79	7.63	-1.40	5	136.16	6.80	-8.44
9250	926463	514608	4	150.19	17.05	.25	2	125.29	12.77	-1.25	5	129.41	9.18	-5.18
9252	931201	532941	7	112.51	10.91	-1.68	4	117.55	11.40	-1.76	5	124.65	10.69	-3.26
9254	926018	549613	4	194.31	11.29	-10.45	2	136.32	11.33	-3.92	5	125.57	13.52	-.53
9256	931951	570342	9	257.23	22.37	-6.41	2	134.46	18.27	3.23	5	114.74	17.47	4.63
9260	924375	609350	2	.00	25.69	25.69	3	24.86	24.96	22.18	5	55.69	21.62	15.39
9426	957500	279300	1	89.00	41.00	31.04	3	42.66	32.79	28.01	4	38.89	30.79	26.44
9428	955267	292083	6	41.76	29.55	24.87	4	38.06	31.11	26.85	6	37.02	28.77	24.63
9430	954935	312730	6	60.55	28.53	21.75	2	35.93	25.10	21.08	5	36.80	25.62	21.50
9434	956080	355250	3	119.58	19.14	5.76	3	84.74	18.34	8.86	5	122.80	22.96	9.22
9436	949681	372380	10	70.36	23.15	15.27	4	166.87	26.12	7.45	6	160.51	24.87	6.91
9438	943810	390387	10	8.14	7.77	6.86	3	180.16	26.28	6.12	5	193.22	25.21	3.59
9452	945635	530370	2	19.92	6.98	4.75	2	92.72	10.25	-.12	4	114.80	10.77	-2.07
9456	949420	579270	2	47.24	13.10	7.82	3	105.11	17.85	6.09	4	116.41	17.30	4.28

REGIONAL GRAVITY SURVEY OF TASMANIA

DATA AVERAGED OVER 20000 YD (20 KMS) GRID SQUARES

SQUARE INDEX	GRID COORDINATE NORTH	GRID COORDINATE EAST	UNFILTERED DATA NUMBER OF DATA POINTS	UNFILTERED DATA HEIGHT METRES	UNFILTERED DATA FREE AIR ANOMALY	UNFILTERED DATA BOUGUER ANOMALY	20 KMS FILTERED DATA NUMBER OF DATA POINTS	20 KMS FILTERED DATA HEIGHT METRES	20 KMS FILTERED DATA FREE AIR ANOMALY	20 KMS FILTERED DATA BOUGUER ANOMALY	40 KMS FILTERED DATA NUMBER OF DATA POINTS	40 KMS FILTERED DATA HEIGHT METRES	40 KMS FILTERED DATA FREE AIR ANOMALY	40 KMS FILTERED DATA BOUGUER ANOMALY
9458	951921	587267	7	45.58	20.93	15.83	2	81.55	17.91	9.79	5	80.82	21.23	12.19
9460	944083	610383	3	31.60	37.18	33.64	2	17.68	28.86	26.88	3	47.01	24.57	19.31
9626	960350	278550	1	1.83	29.05	28.84	3	42.66	32.79	28.01	4	38.89	30.79	26.44
9628	972267	295633	3	25.71	28.30	25.43	4	27.65	26.58	23.49	7	34.62	27.82	23.95
9630	969946	309808	9	26.60	25.08	22.10	5	27.12	23.40	20.37	6	34.04	25.04	21.23
9632	957408	329563	6	25.50	13.73	10.88	3	33.77	17.70	13.92	6	49.71	21.57	16.01
9634	965075	347320	2	10.97	8.73	7.51	3	46.67	15.57	10.35	4	88.35	20.23	10.34
9830	980100	305300	1	3.05	21.32	20.98	3	23.67	24.78	22.14	4	31.82	23.73	20.17

is derived by integral division of the grid coordinates by 20,000. The grid coordinates given are the position within each square of the average value for that square. The number of data points is the number of data values used in that stage of the calculation.

Figure 3.1 is the distribution of the averaged data set. Figures 3.2, 3.3 and 3.4 are maps of the data set averaged, filtered to 20 kms and filtered to 40 kms.

3.1.2 Choice of Interpolation Method

The process of obtaining an averaged smoothed subset of the gravity data, described in the previous section, leaves us with a data set that is irregularly spaced and with an irregular boundary.

The normal surface fitting techniques, employing the use of Fourier Series or polynomials, are inapplicable, since they require the data set to be evenly distributed for orthogonality. The property of orthogonality is necessary since, in any of these methods, the surface is defined by terminating the coefficients of the function set at some limit and reconstructing the surface from these coefficients. The addition or removal of any coefficient would change the value of all of the remainder in the non-orthogonal case.

For irregularly distributed data therefore a surface fitting process can best be achieved by employing functions which are orthogonal to the data set.

DISTRIBUTION OF AVERAGED DATA SET

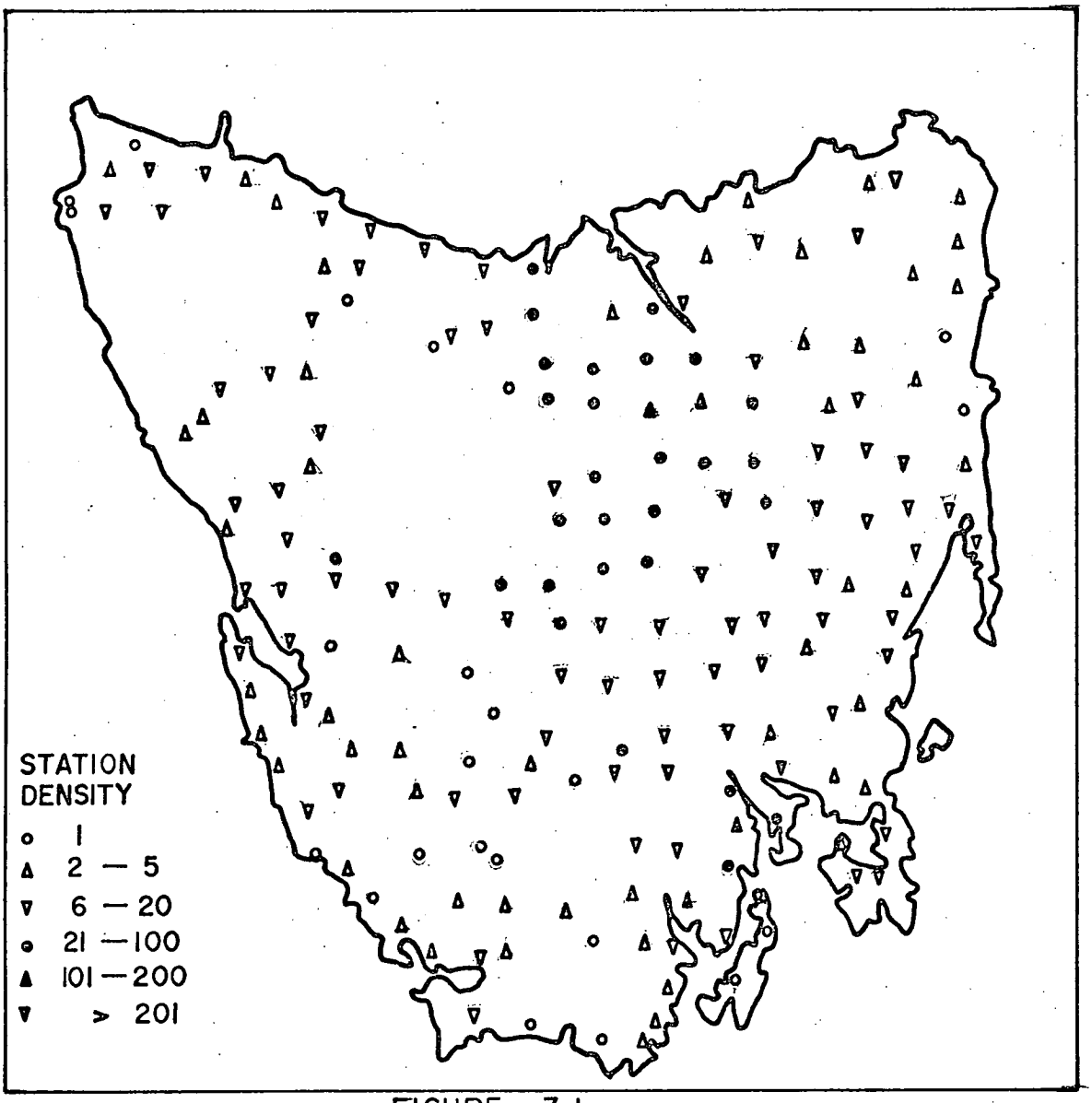

FIGURE 3·1

REGIONAL GRAVITY SURVEY OF TASMANIA AVERAGE DATA

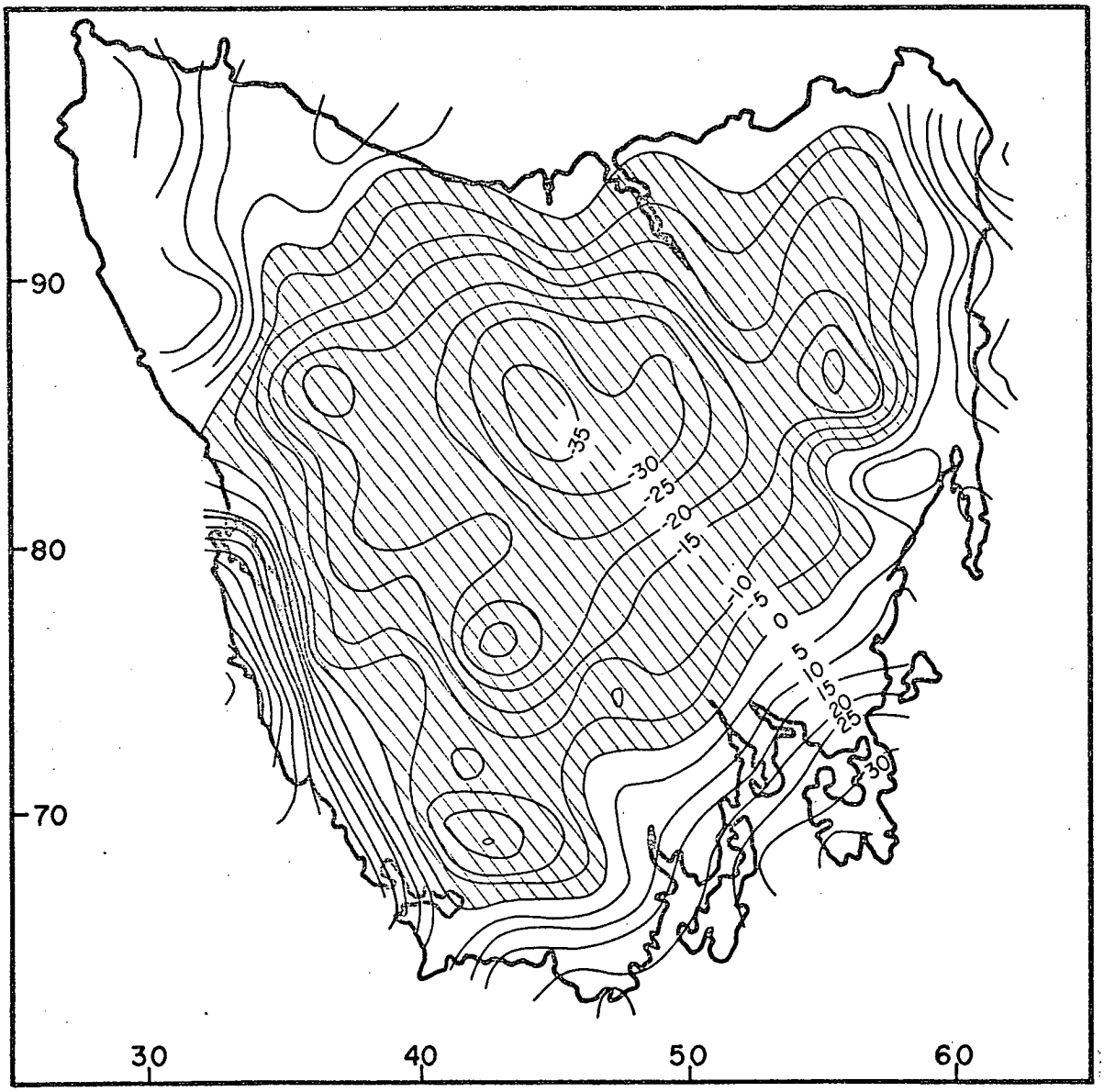

FIGURE 3·2

REGIONAL GRAVITY SURVEY OF TASMANIA
FILTERED TO 20kms

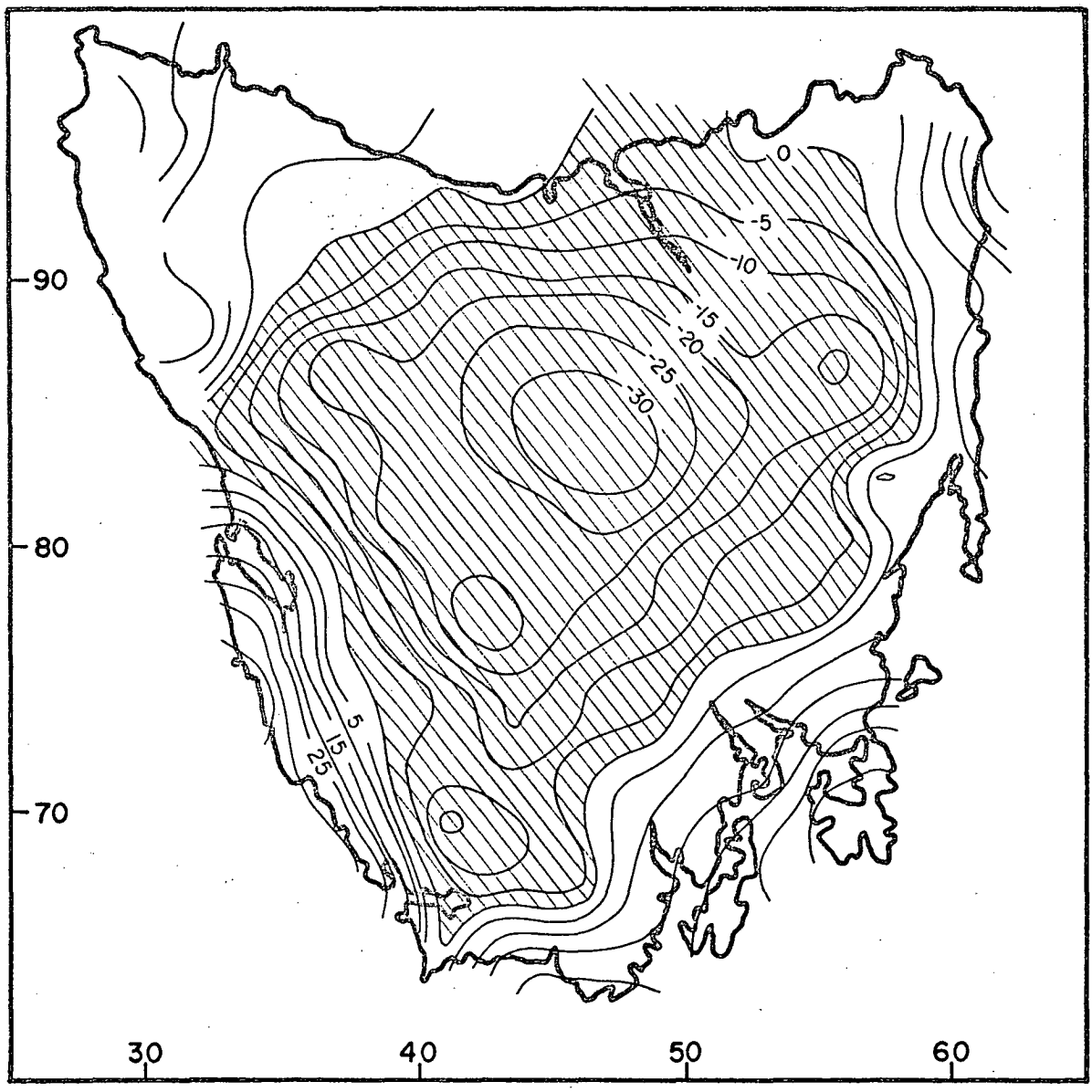

FIGURE 3·3

REGIONAL GRAVITY OF TASMANIA
FILTERED TO 40kms

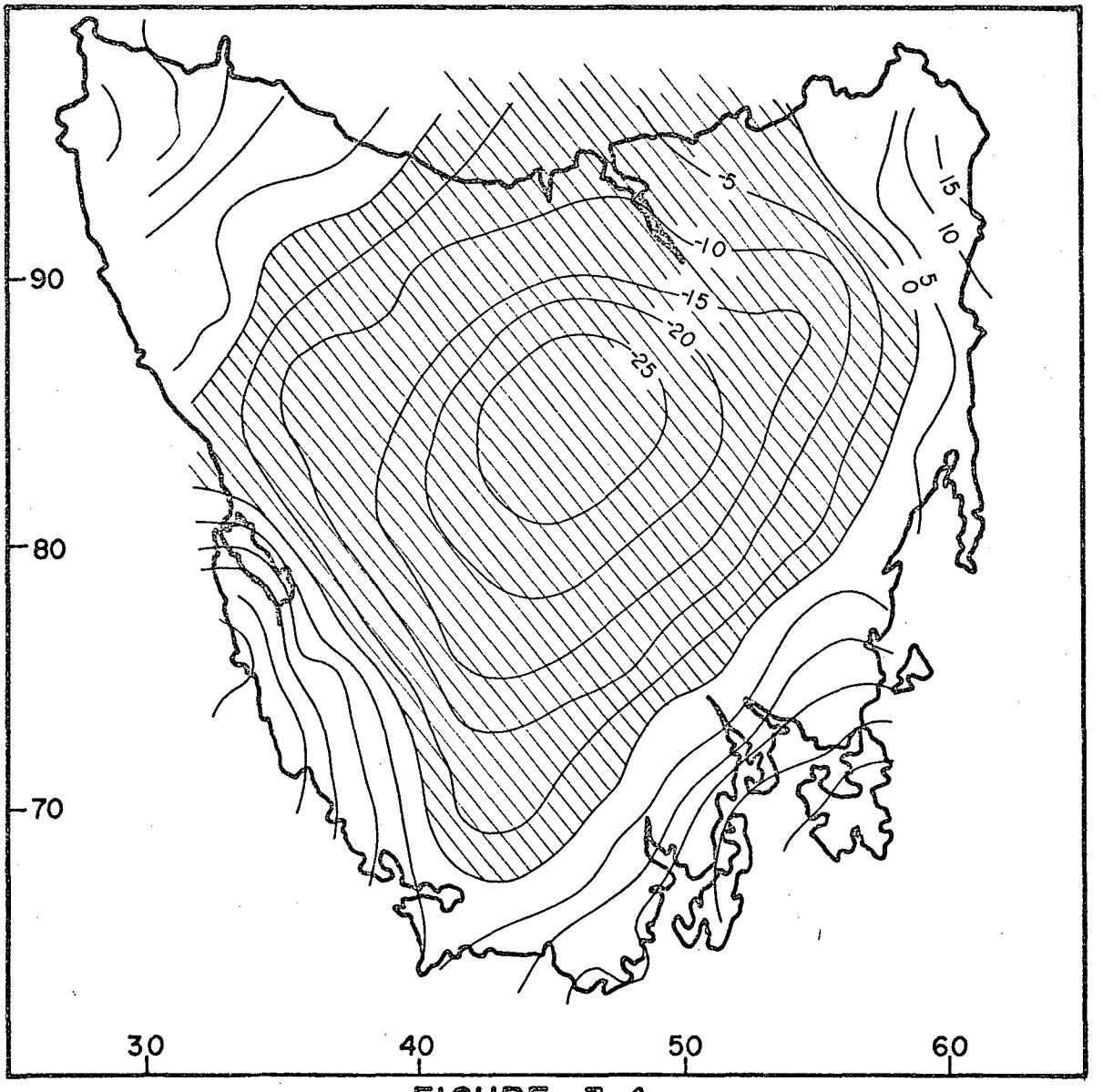

FIGURE 3·4

A function set which is linearly independant can be transformed into a new function set, which is orthogonal to a defined distribution, by the Gram-Schmidt process. (Davis and Rabinowitz, 1954; Davis, 1963; Lanczos, 1957, pp.358). The successful application of this technique to the interpolation of various kinds of geophysical data has been described (Jones and Gallet, 1962; Fougere, 1963, 1965; Crain and Bhattacharyya, 1967; Parkinson, 1971)

The work of Anderson (1970), has assisted in the appreciation of problems encountered in the interpolation of non-equispaced data.

3.1.3 Gram Schmidt Orthogonalisation

Let there be N data points each having rectangular coordinates (x_k, y_k) and having values $\zeta(x_k, y_k)$. Let us define a function set that is orthogonal to an evenly distributed set of data points. Such a function set can be defined by the sequence

Gi(x,y) = {1, cos x, sin x, cos y, sin y, cos x cos y, cos x sin y, sin x cos y, sin x sin y, ...}

which is the function set of the two dimensional Fourier series. The number of functions in this sequence, kmax, is defined in terms of the maximum wave numbers of the nonorthogonal functions. In more general terms

$$Gi\ (x,y) = \left\{ \begin{array}{l} \cos mx \cos ny \\ \cos mx \sin ny \\ \sin mx \cos ny \\ \sin mx \sin ny \end{array} \right\} \begin{array}{l} i = i(m,n) \\ \\ m = 0,1,.....mmax \\ \\ n = 0,1,.....nmax \end{array}$$

The relationship between, i, the number of the function, and m and n is given in Table 3.2, and in Figure 3.5. It can be seen that radial symmetry has been preserved as far as possible in order that no undue directional bias be introduced into the data.

The Gram Schmidt orthogonalisation produces a new set of functions, F, which are orthogonal with respect to the data distribution. In this process each function is computed, by ensuring its orthogonality with all the previous functions, at each data point (x_k, y_k)

Hence, $F_1(x_k,y_k) = G_1(x_k,y_k)$; $k = 1, ... N$

and for successive functions, $i = 2, ... imax$

$$F_i(x_k,y_k) = G_i(x_k,y_k) - \sum_{j=1}^{i-1} a_{ij}\ F_j\ (x_k,y_k);$$

$$k = 1, ... N$$

where $$a_{ij} = \frac{\sum_{k=1}^{N} G_i\ (x_k,y_k)\ F_j\ (x_k,y_k)}{\sum_{k=1}^{N} (F_j\ (x_k,y_k))^2}$$

The coefficients of the orthogonal functions are then computed by multiplying the data values by the function sets.

Table 3.2 Function Set Chosen for Gram Schmidt Orthogonalisation Process

Wave number	$G_i(x, y)$			
0	$G_1 = 1$			
1	$G_2 = \cos x$	$G_3 = \sin x$	$G_4 = \cos y$	$G_5 = \sin y$
	$G_6 = \cos x \cos y$	$G_7 = \cos x \sin y$	$G_8 = \sin x \cos y$	$G_9 = \sin x \sin y$
2	$G_{10} = \cos 2x$	$G_{11} = \sin 2x$	$G_{12} = \cos 2y$	$G_{13} = \sin 2y$
	$G_{14} = \cos 2x \cos y$	$G_{15} = \cos 2x \sin y$	$G_{16} = \sin 2x \cos y$	$G_{17} = \sin 2x \sin y$
	$G_{18} = \cos x \cos 2y$	$G_{19} = \cos x \sin 2y$	$G_{20} = \sin x \cos 2y$	$G_{21} = \sin x \sin 2y$
3	$G_{22} = \cos 3x$	$G_{23} = \sin 3x$	$G_{24} = \cos 3y$	$G_{25} = \sin 3y$
	$G_{26} = \cos 3x \cos y$	$G_{27} = \cos 3x \sin y$	$G_{28} = \sin 3x \cos y$	$G_{29} = \sin 3x \sin y$
	$G_{30} = \cos 2x \cos 2y$	$G_{31} = \cos 2x \sin 2y$	$G_{32} = \sin 2x \cos 2y$	$G_{33} = \sin 2x \sin 2y$
	$G_{34} = \cos x \cos 3y$	$G_{35} = \cos x \sin 3y$	$G_{36} = \sin x \cos 3y$	$G_{37} = \sin x \sin 3y$
4	$G_{38} = \cos 4x$	$G_{39} = \sin 4x$	$G_{40} = \cos 4y$	$G_{41} = \sin 4y$
	$G_{42} = \cos 4x \cos y$	$G_{43} = \cos 4x \sin y$	$G_{44} = \sin 4x \cos y$	$G_{45} = \sin 4x \sin y$
	$G_{46} = \cos 3x \cos 2y$	$G_{47} = \cos 3x \sin 2y$	$G_{48} = \sin 3x \cos 2y$	$G_{49} = \sin 3x \sin 2y$
	$G_{50} = \cos 2x \cos 3y$	$G_{51} = \cos 2x \sin 3y$	$G_{52} = \sin 2x \cos 3y$	$G_{53} = \sin 2x \sin 3y$
	$G_{54} = \cos x \cos 4y$	$G_{55} = \cos x \sin 4y$	$G_{56} = \sin x \cos 4y$	$G_{57} = \sin x \sin 4y$
	$G_{58} = \cos 4x \cos 2y$	$G_{59} = \cos 4x \sin 2y$	$G_{60} = \sin 4x \cos 2y$	$G_{61} = \sin 4x \sin 2y$
	$G_{62} = \cos 3x \cos 3y$	$G_{63} = \cos 3x \sin 3y$	$G_{64} = \sin 3x \cos 3y$	$G_{65} = \sin 3x \sin 3y$
	$G_{66} = \cos 2x \cos 4y$	$G_{67} = \cos 2x \sin 4y$	$G_{68} = \sin 2x \cos 4y$	$G_{69} = \sin 2x \sin 4y$

Figure 3.5 Ordering of Fourier Coefficients to Preserve Approximately Circular Symmetry

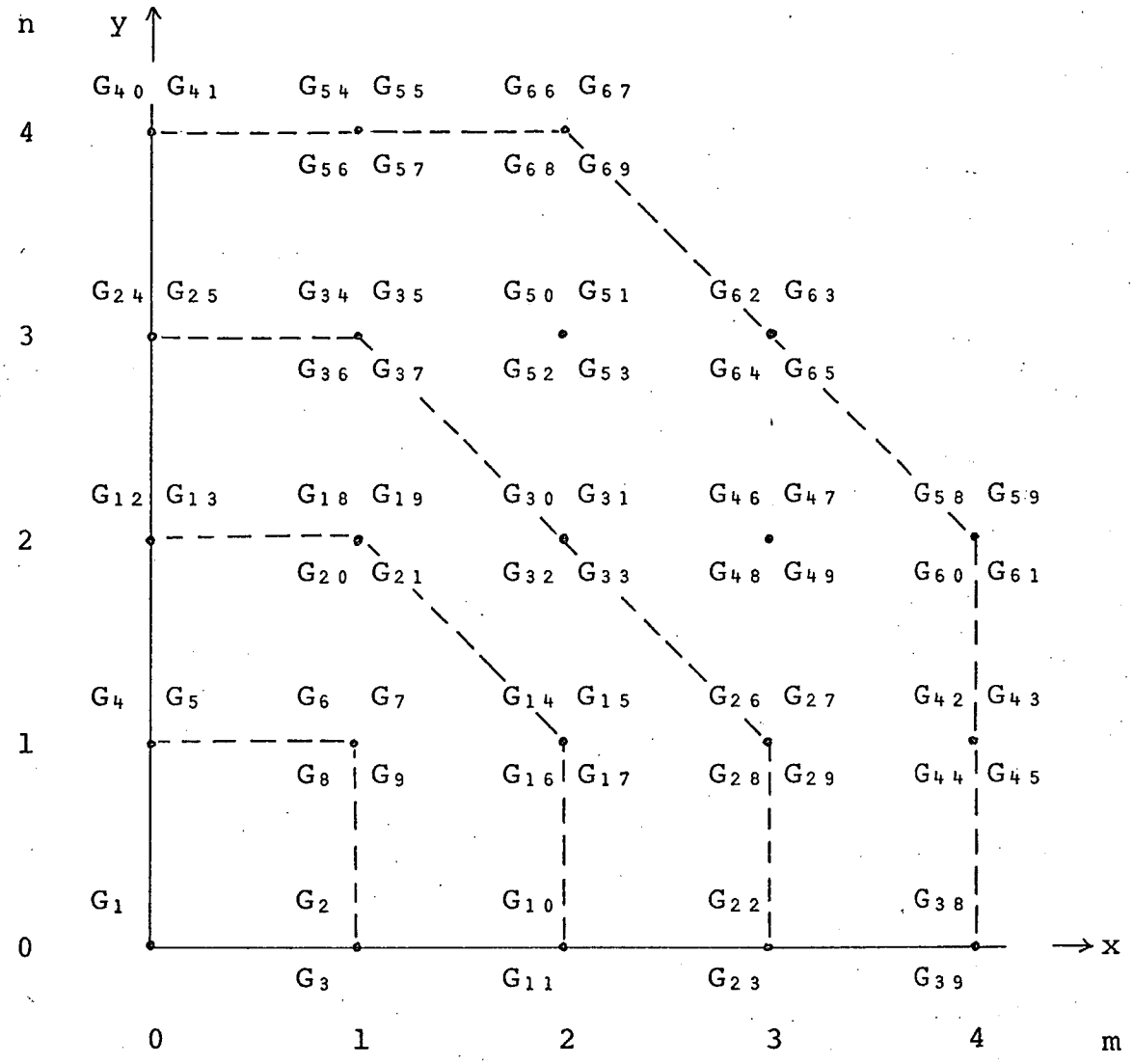

a) Plot of Fourier coefficient sequence in wavenumber space

cos mx cos ny cos mx sin ny

sin mx cos ny sin mx sin ny

b) Distribution of terms around a point representing wavenumber m in x direction and n in y direction

$$C_i = \frac{\sum_{k=1}^{N} F_i(x_k,y_k) \cdot \zeta_k(x_k,y_k)}{\sum_{k=1}^{N} (F_i(x_k,y_k))^2} \qquad i = 1,.....kmax$$

The coefficients may be transformed in terms of the original non-orthogonal function set. This is carried out by the following transformation; for i = 1, ... kmax;

$$b_{ii} = 1$$

$$b_{ij} = -\sum_{n=j}^{i-1} a_{in}\, b_{nj} \; ; \quad j = 1, 2, ... (i - 1)$$

the new coefficient set being obtained by

$$d_i = \sum_{j=i}^{kmax} c_j b_{ji}$$

The stepwise approximation to the data, $\bar{\zeta}_m(x_k,y_k)$, of the first m terms of the orthogonal function set is computed from the following relationship

$$\bar{\zeta}_m(x_k,y_k) = \sum_{i=1}^{m} C_i\, F_i(x_k,y_k) \; ; \; k = 1, ... N$$

The estimate of the variance of the residuals can also be calculated, at that stage, using

$$Var_m = \frac{\sum_{k=1}^{N} (\zeta(x_k,y_k))^2 - \sum_{k=1}^{m} C_i^2 \left[\sum_{k=1}^{N} (F_i(x_k,y_k))^2 \right]}{N - m}$$

3.1.4 Orthoganility

Orthogonalisation procedures are often limited in their effectiveness due to accumulated errors in the computations (e.g. Jones and Gallett, 1962); it is wise therefore to test the orthogonality of the function set before proceeding with the analysis.

Two artificial data sets were produced to test the effectiveness of the orthogonalisation process. The first, was on a regular basis, the central region having a smaller sampling interval. The second, was similarly produced except the coordinates were chosen from consecutive pairs of a random number requence. The distributions, referred to as REGULAR and RANDOM, were chosen to simulate the bias in sampling in the real data. The values given to the data points were calculated from a double Fourier series synthesis, the amplitudes being unity up to a given frequency and zero above. Figure 3.6 shows the distributions of the two artificial sets of data.

Two different approaches have been used to test for orthoganility. The first method is to test for the difference between the coefficient sets after stages of reorthogonalisation. This technique was used by Jones and

REPEATED ORTHOGONALISATION TEST

GRAM-SCHMIDT ORTHOGONALISATION			FIRST REORTHOGONALISATION		SECOND REORTHOGONALISATION	
	NON-ORTHOGONAL FUNCTIONS	ORTHOGONAL FUNCTIONS	ORTHOGONAL FUNCTIONS	PERCENTAGE CHANGE	ORTHOGONAL FUNCTIONS	PERCENTAGE CHANGE
K	D	C1	C2	(C2-C1)/C1	C3	(C3-C2)/C2
1	1.000	.2008120+01	.2008120+01	.0000	.2008120+01	.0000
2	1.000	.1408602+01	.1408602+01	.0000	.1408602+01	.0000
3	1.000	.1464590+01	.1464590+01	.5087-06	.1464590+01	.0000
4	1.000	.1167017+01	.1167017+01	-.1277-05	.1167017+01	-.1915-05
5	1.000	.1409064+01	.1409064+01	.2644-05	.1409364+01	.0000
6	1.000	.7436761-00	.7436761-00	-.3006-05	.7436761-00	.1002-05
7	1.000	.9413300-00	.9413300-00	.5145-05	.9413300+01	.0000
8	1.000	.7984195-00	.7984195-00	-.4666-06	.7984195-00	-.4666-06
9	1.000	.9999998-00	.9999998-00	.7451-06	.9999998-00	.0000
10	.000	-.1928964-07	-.5036740-07	.6170+02	-.4793184-07	-.5081+01
11	.000	-.1128460-07	-.6765442-08	-.6680+02	-.9742768-08	.3056+02
12	.000	.3296917-07	.2888325-07	-.1415+02	.2714556-07	-.6401+01
13	.000	.1041320-06	.9387959-07	-.1092+02	.9649294-07	.2708+01
14	.000	.1079380-06	.7541361-07	-.4313+02	.7863030-07	.4091+01
15	.000	-.8869010-07	-.8337931-07	-.6369+01	-.8675991-07	.3895+01
16	.000	-.2076876-06	-.2106530-06	.1408+01	-.2062578-06	-.2131+01
17	.000	-.2623771-06	-.2902203-06	.9594+01	-.2912784-06	.3633-00
18	.000	-.8552091-07	-.5287294-07	-.6175+02	-.5460671-07	.3175+01
19	.000	-.2306305-06	-.2219471-06	-.3912+01	-.2305147-06	.3717+01
20	.000	.7774534-07	.5557474-07	-.3989+02	.5406077-07	.2800+01
21	.000	-.4818753-08	-.6191871-07	.9222+02	-.6605771-07	.6266+01
22	.000	-.9556118-07	-.8406431-07	-.1368+02	-.9186953-07	.8496+01
23	.000	.8127604-07	.8333077-07	.2466+01	.8093358-07	-.2962+01
24	.000	-.7534161-07	-.7142106-07	-.5489+01	-.7062148-07	-.1132+01
25	.000	.1323339-06	.1218592-06	-.8596+01	.1260076-06	.3292+01
26	.000	-.1925694-08	-.1502041-07	.8718+02	-.1104864-07	-.3605+02
27	.000	-.8780599-07	-.7532377-07	-.1657+02	-.6779139-07	-.1111+02
28	.000	-.2030589-07	-.4702417-07	.5682+02	-.4981474-07	.5802+01
29	.000	-.6513771-08	.1880111-07	.1346+03	.1783885-07	-.5394+01
30	.000	.1927782-08	-.1517939-09	.1370+04	-.9411222-08	.9839+02
31	.000	.3011137-07	-.2519780-09	.1205+05	.1385879-08	.1182+03
32	.000	-.1776683-06	-.1238046-06	-.4351+02	-.1370055-06	.9635+01
33	.000	-.3670935-06	-.3628381-06	-.1173+01	-.3614197-06	-.3925-00
34	.000	.8173533-07	.1010233-06	.1909+02	.1056068-06	.4340+01
35	.000	-.2187563-07	.1048832-07	.3086+03	.7791321-08	-.3462+02
36	.000	-.1064155-06	-.1064515-06	.3383-01	-.1154803-06	.7819+01
37	.000	.1641446-06	.1643003-06	.9479-01	.1725525-06	.4782+01

DISTRIBUTION OF ARTIFICIAL DATA SETS

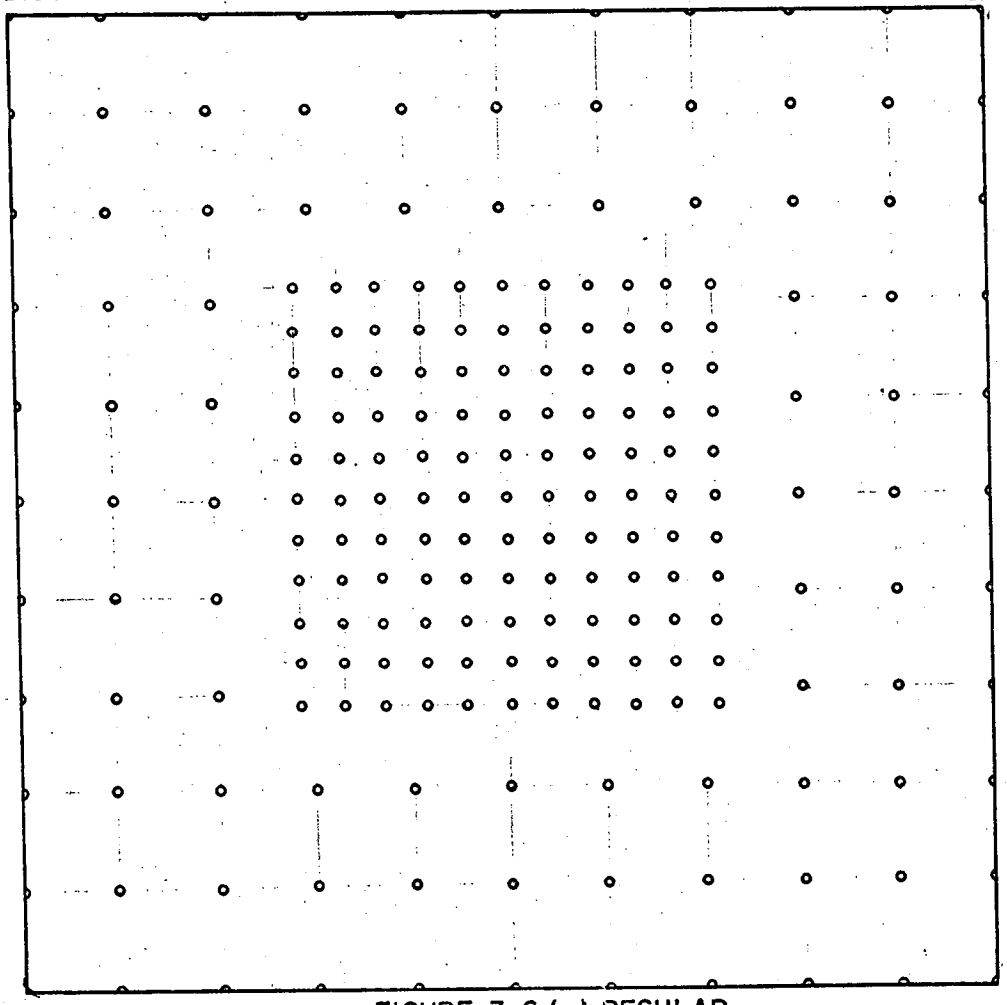

FIGURE 3·6 (a) REGULAR

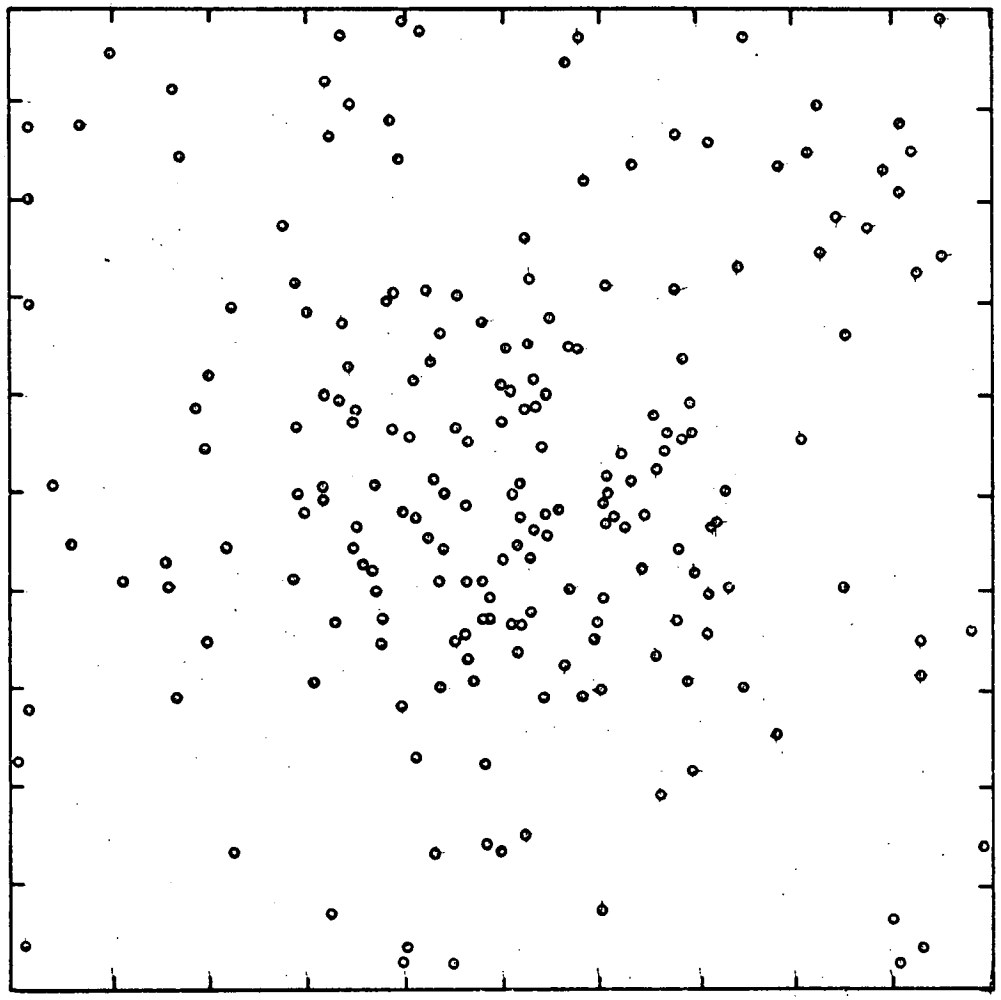

FIGURE 3·6 (b) RANDOM

Gallett (1962) who found that a second stage of orthogonalisation was required. However their data distribution was very uneven in comparison to the data distribution in this study.

The results of calculating the percentage change between successive stages of orthogonalisation, for the RANDOM data set are given in Table 3, it can be seen that no dramatic improvement can be observed even after one stage of reorthogonalisation.

This second approach used was to calculate the degree of the orthogonality of the function set. The procedure is that of Davis (1963, p.77).

Given a set of elements $F_n(k)$, we may define an inner product, such that

$$(x_i,x_j) = \sum_k F_i(k)\ F_j(k)$$

The matrix of such inner products is known as the Gram matrix and may be written

$$((x_i,x_j)) = \begin{pmatrix} x_1x_1 & x_1x_2 & \cdots\cdots\cdots & x_1x_n \\ x_2x_1 & x_2x_2 & \cdots\cdots\cdots & x_2x_n \\ \vdots & \vdots & & \vdots \\ x_nx_1 & x_nx_2 & \cdots\cdots\cdots & x_nx_n \end{pmatrix}$$

The determinant of this matrix is known as the Gram determinant, $|(x_i,x_j)|$. Where the set of elements $F_n(k)$

are linearly independant, and normalised, the value of this determinant is unity. For dependant sets of elements the determinant is zero. Hence, in general a non-orthogonal function set of elements will have a determinant of intermediate value.

Table 3.3 shows the values of the Gram determinant before and after orthogonalisation for the two artificial data sets REGULAR and RANDOM.

Table 3.3

Summary of results from Gram Determinant Calculations to Test Orthoganality

Data	Gram Determinant of Non-orthogonal function set →	Gram Determinant of Orthogonal function set
REGULAR	1.2914×10^{-4}	$1.000 \times 10^{+0}$
RANDOM	-2.4588×10^{-10}	$1.000 \times 10^{+0}$

On the basis of these tests, it was confirmed that a single orthogonalisation procedure was entirely adequate for the type of data distribution involved. In the analysis of Jones and Gallett (1962), a second stage of orthogonalisation

was required due to the extreme irregularity of the distribution of ionospheric observatories.

3.1.5 Analysis of Averaged Data Set

3.1.5.1 *Computational restrictions*

The Gram Schmidt orthogonalisation technique was programmed for the University of Tasmania/Hydro Electric Commission Elliott 503 computer. Severe restrictions were placed on the design of the programme by the capabilities of this computer.

The non-orthogonal G array is a rectangular array of k rows and n columns; where k is the number of data points used and n is the number of functions used. The number of functions used is a function of wave number, a sshown in Table 3.2, and summarized in Table 3.4

Table 3.4

Total Number of functions for each additional wave number

Wave number	Number of functions
1	9
2	21
3	37
4	69

This if we have 200 data points, this requires a core storage of 13,800 words.

The array size is far in excess of the available area in the 8,000 word main store, and therefore had to be placed in the backing store. This is a separate storage module of 16,000 words which can only be addressed by machine language instructions.

The orthogonalisation process is a stepwise procedure operating by columns in such a way that each column of the G array can be overwritten by the corresponding column of the orthogonal F array.

Figure 3.7

COMPUTATIONAL PROCEDURE OF GRAM-SCHMIDT ANALYSIS

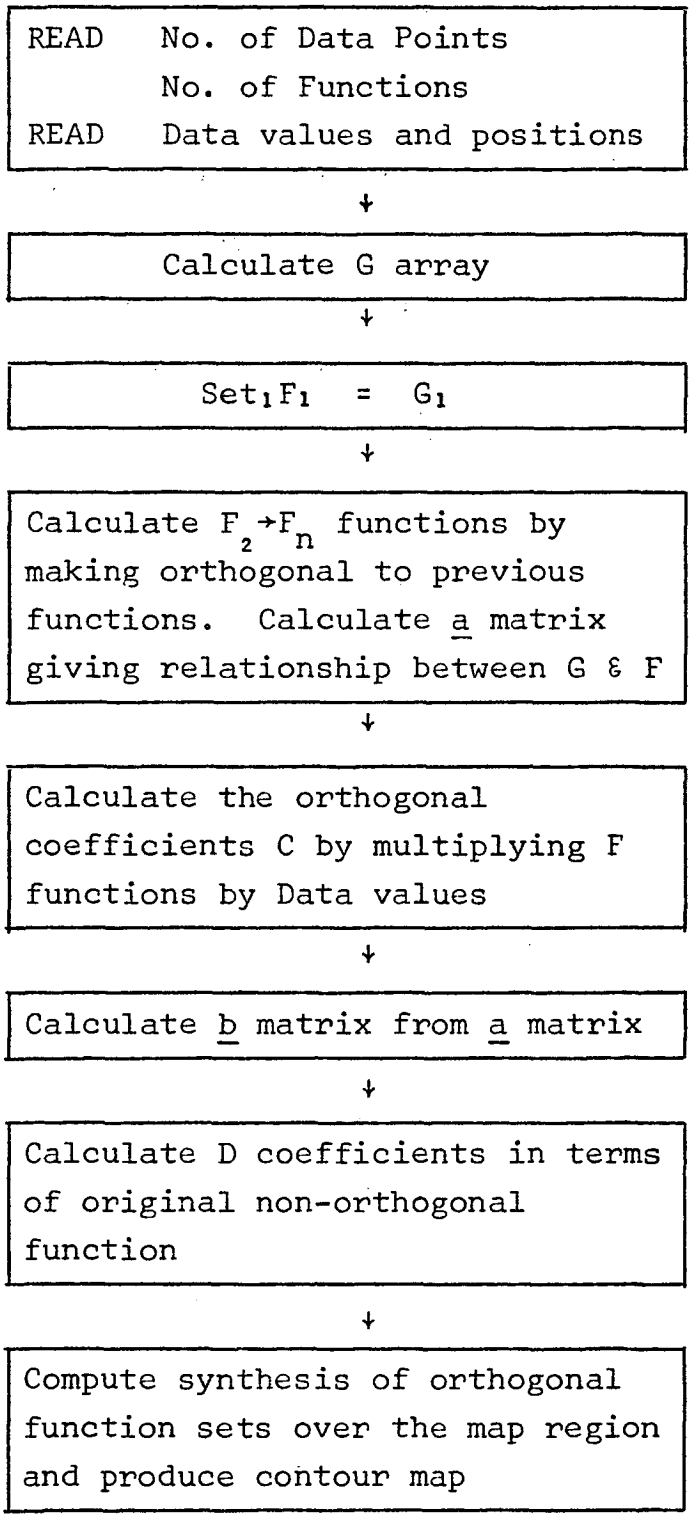

The transformation matrix, a, between the G and F arrays, is calculated at each stage of the orthogonalisation. This is a triangular array requiring half of an nxn array. The square array would occupy 4761 words of store, but the storage requirements were halved by linearly addressing the array (viz, $a'_1 = a_{11}$, $a'_2 = a_{21}$, $a'_3 = a_{22}$, $a'_4 = a_{31}$, $a'_5 = a_{32}$, $a'_6 = a_{33}$, etc). The a array and subsidiary storage was therefore able to be placed in the main store. The remainder of the computer store was required by the operating system. The programme to carry out the full scale Gram Schmidt analyses was necessarily written in Elliott Machine Language and has therefore not been included with this thesis. However, a more general version of this program, for one dimensional variable data, is included as an appendix.

The computational procedure for an analysis is given as a flow sheet (Figure 3.7).

The final result is a map of the synthesis of the synthesis of the functions that were derived during the analysis. This provides an easy method of estimating the effectiveness of the procedure.

3.1.5.2 *Coordinate Transformation*

The coordinates of the data points, used in the analysis, are known in terms of the Tasmanian Mercator grid. The map area was chosen such that it was bounded on the north by the grid value 1,000,000 yds N, to the south by 600,000 yds N, to

the west by 250,000 yds E and to the east by 650,000 yds E. This achieved a square map area, with the data positions in terms of rectangular coordinates, which would not have been the case had latitudes and longitude coordinates been used. The coordinates were also scaled such that the boundaries corresponded to +Π and -Π.

3.1.5.3 *Terminating the approximation*

The most difficult aspect of an analysis of this type is to determine the "best" approximation to the data. The normal method is to adopt some kind of statistical test and accept all the coefficients of the orthogonal functions which contribute significantly to the approximation. Parkinson (1971), in an analysis of Geomagnetic Diurnal variation, used a significance test to reject or accept each coefficient. Crain and Bhattacharyya (1967) examined several different indicators to assist them in terminating the series at a specific wave number. The statistic that was found to be most useful was the ratio of variance of the residuals before and after the addition of a group of coefficients, corresponding to the addition of one wave number.

In general, it is found that the variance drops appreciably, with the addition of functions, until it arrives at a certain level where it levels out and often rises again. The statistic used in this analysis was to examine the variance after each additional wave number had been completed.

3.1.5.4 *Boundary problems*

The choice of Fourier series terms for the original non-orthogonal functions has placed a severe restriction on the approximation. That is that the opposite boundaries of the map area must be made to be identical. This is most noticeable in certain of the syntheses where large "anomalies" have been forced into the data free portions of the map. These anomalies are in certain cases large enough to influence the approximating surface at opposite coastlines.

Two attempts have been made to overcome this effect. The first is to remove the boundary of the map area to a further distance away from the data. This has particularly disastrous effects in that the boundary anomalies, noticed previously, have become much more enhanced. This is due to the increase in the size of the data free area.

The second approach to the problem was to attempt the analysis with polynomials in x and y. Due to computational problems this approach was not fully developed and only a preliminary study was undertaken. A detailed study of the relative merits of different sets of non-orthogonal functions is planned as a next stage to this analysis.

3.1.5.5 *Analysis of Average Bouguer Gravity*

Six different analyses were carried out using Fourier Series coefficients on the three data sets; averaged, filtered to 20 kms, and filtered to 40 kms. The series of

orthogonal functions was terminated after wave number 3 for the first 3 analyses and after wave number 4 for the second 3. Figures 3.8 to 3.13 are syntheses of these analyses. The contour interval is 10 mgals between +50 and -50 and 50 mgals beyond these values. The shaded portions are negative.

In general the surface is smooth and well behaved within the data area and is badly behaved in the data free areas.

The unsmoothed data set

The main features of the synthesis (Figure 3.8) are a good comparison to the Bouguer anomaly map. The detail however is of too shallow an origin (viz. the southward protruding negative lobe and the northward extension of the northeast negative anomaly). There is also some degree of interference from the pseudo anomalies generated at the east and west margins. The aim therefore is to produce a smoother surface with less interference.

The series of orthogonal functions was terminated after wave number 3 and a new synthesis made (Figure 3.9). This is a much smoother field but the surface reflects the general character less well than the more complex surface.

It is very difficult, at this stage, to arrive at some reliable criterion for judging the quality of a mpa. The main criteria that have been used are an examination of the coastal gradients and the size and position of the central negative.

UNSMOOTHED AVERAGE DATA FROM GRAVITY SURVEY
ANALYSIS TO K=3 SYNTHESIS TO K=3

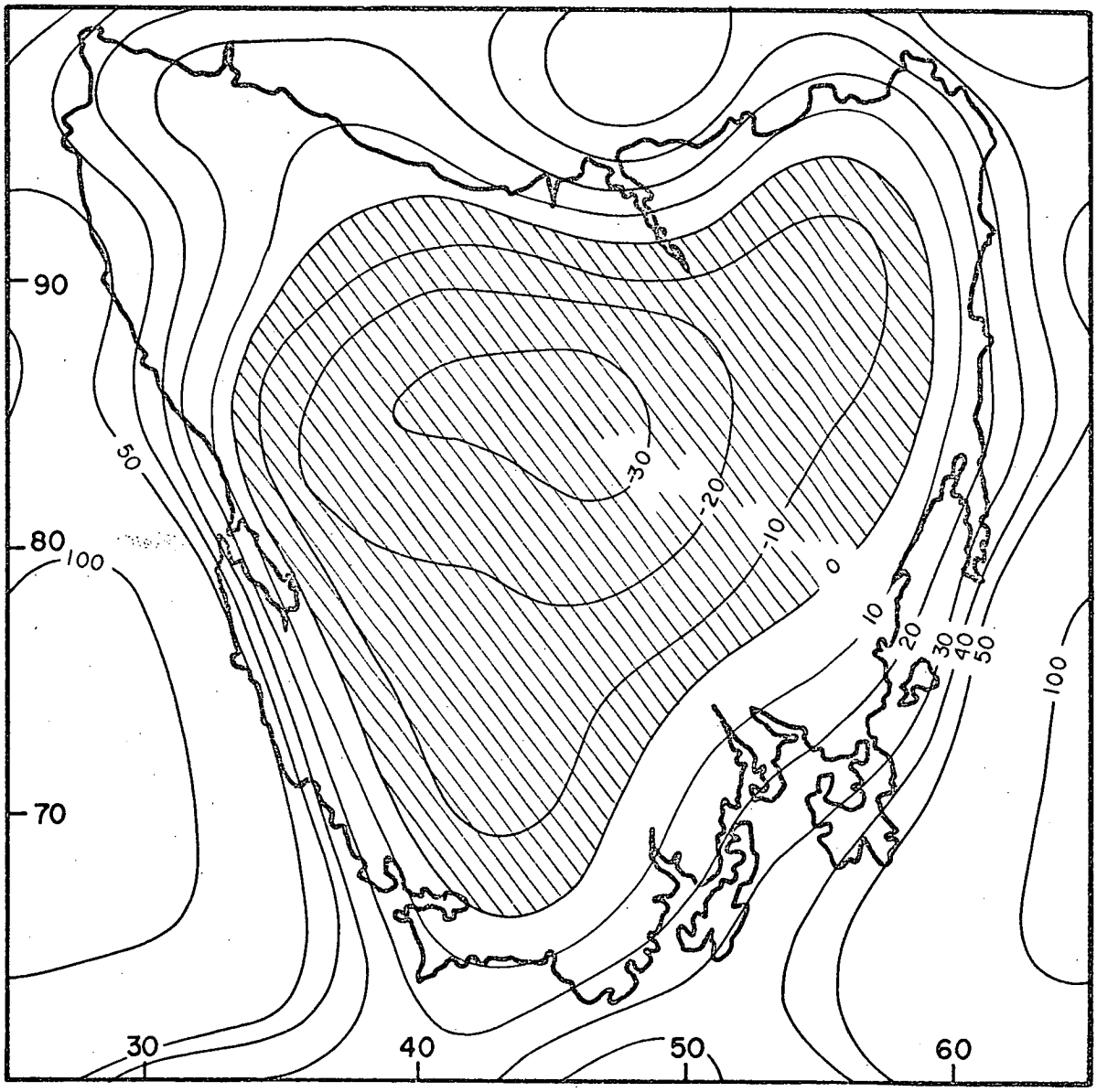

FIGURE 3·8

UNSMOOTHED AVERAGE DATA FROM GRAVITY SURVEY
ANALYSIS TO K=4 SYNTHESIS TO K=4

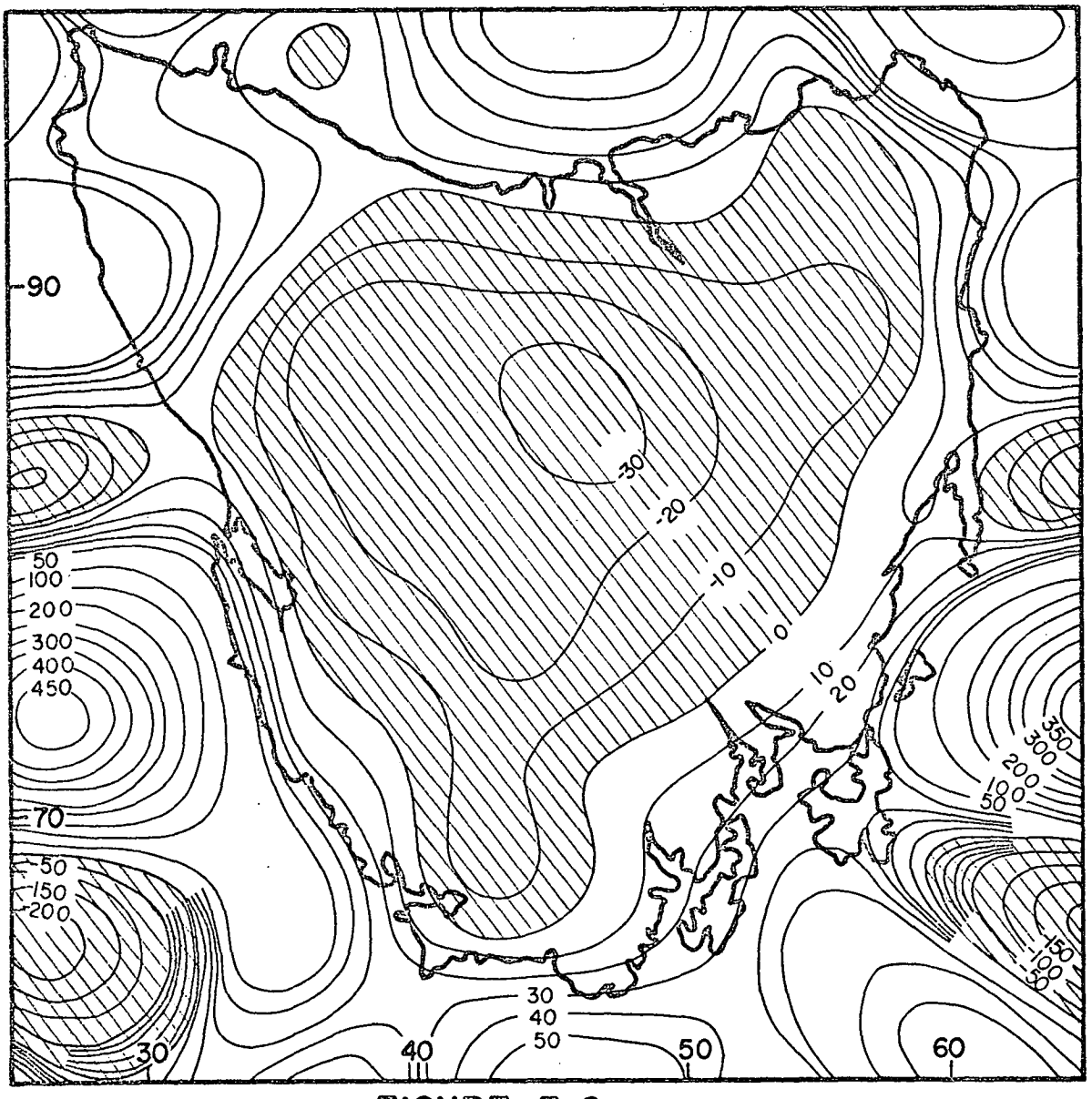

FIGURE 3·9

AVERAGE DATA FROM GRAVITY SURVEY FILTERED TO 20kms
ANALYSIS TO K=3 SYNTHESIS TO K=3

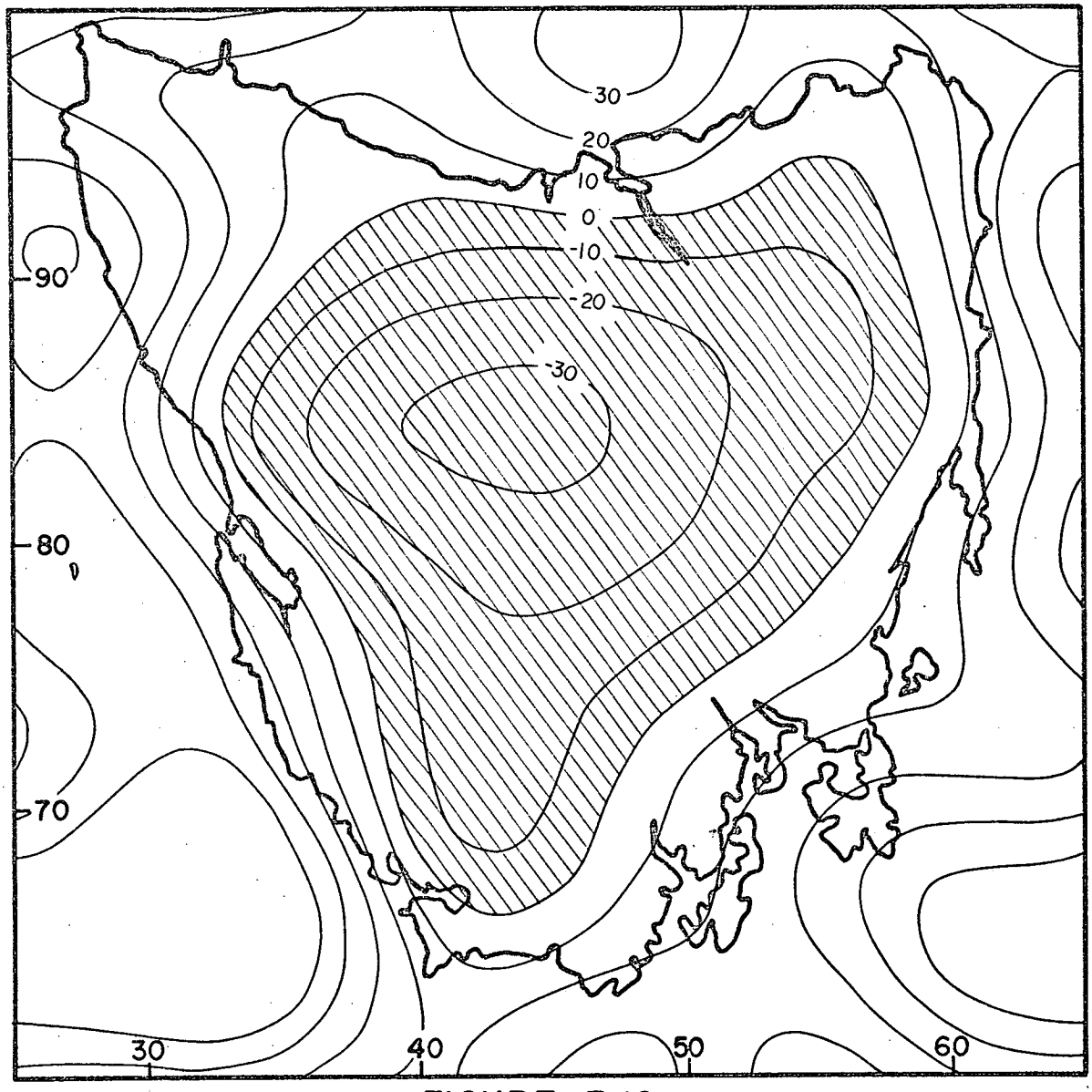

FIGURE 3·10

AVERAGE DATA FROM GRAVITY SURVEY FILTERED TO 20kms ANALYSIS TO K=4 SYNTHESIS TO K=4

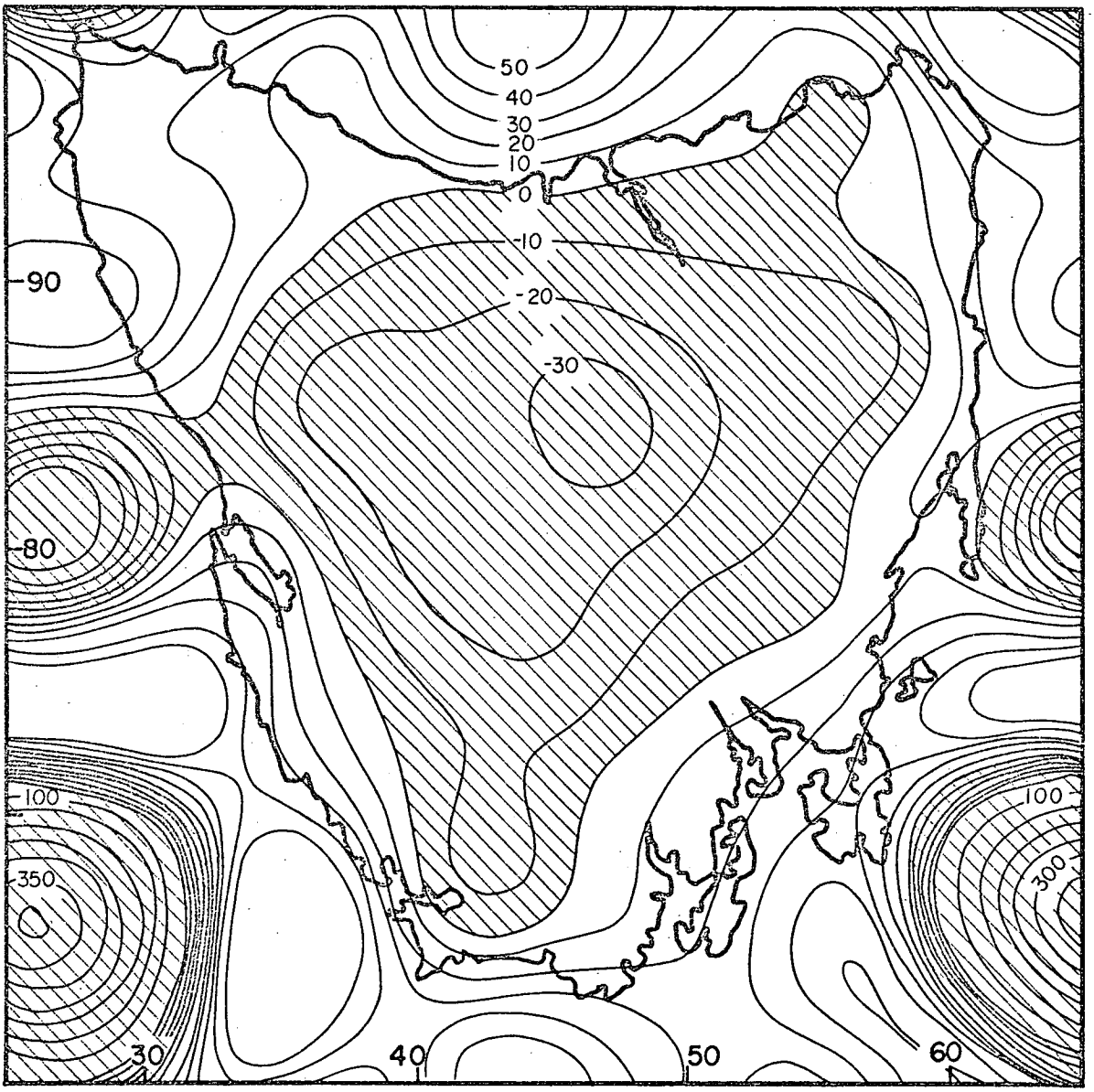

FIGURE 3·11

AVERAGE DATA FROM GRAVITY SURVEY
FILTERED TO 40kms ANALYSIS TO K=3 SYNTHESIS TO K=3

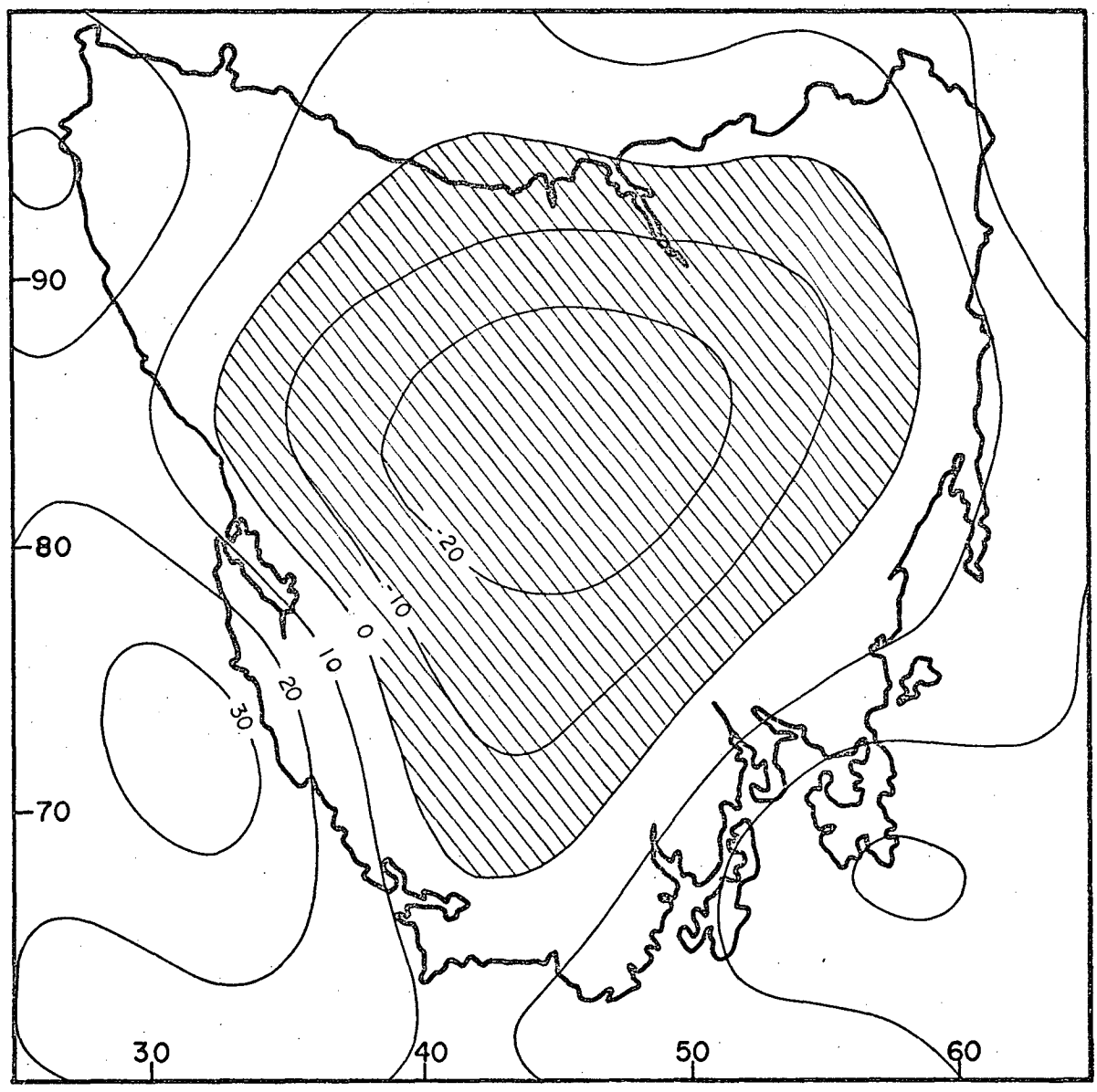

FIGURE 3·12

AVERAGE DATA FROM GRAVITY SURVEY FILTERED TO 40kms ANALYSIS TO K=4 SYNTHESIS TO K=4

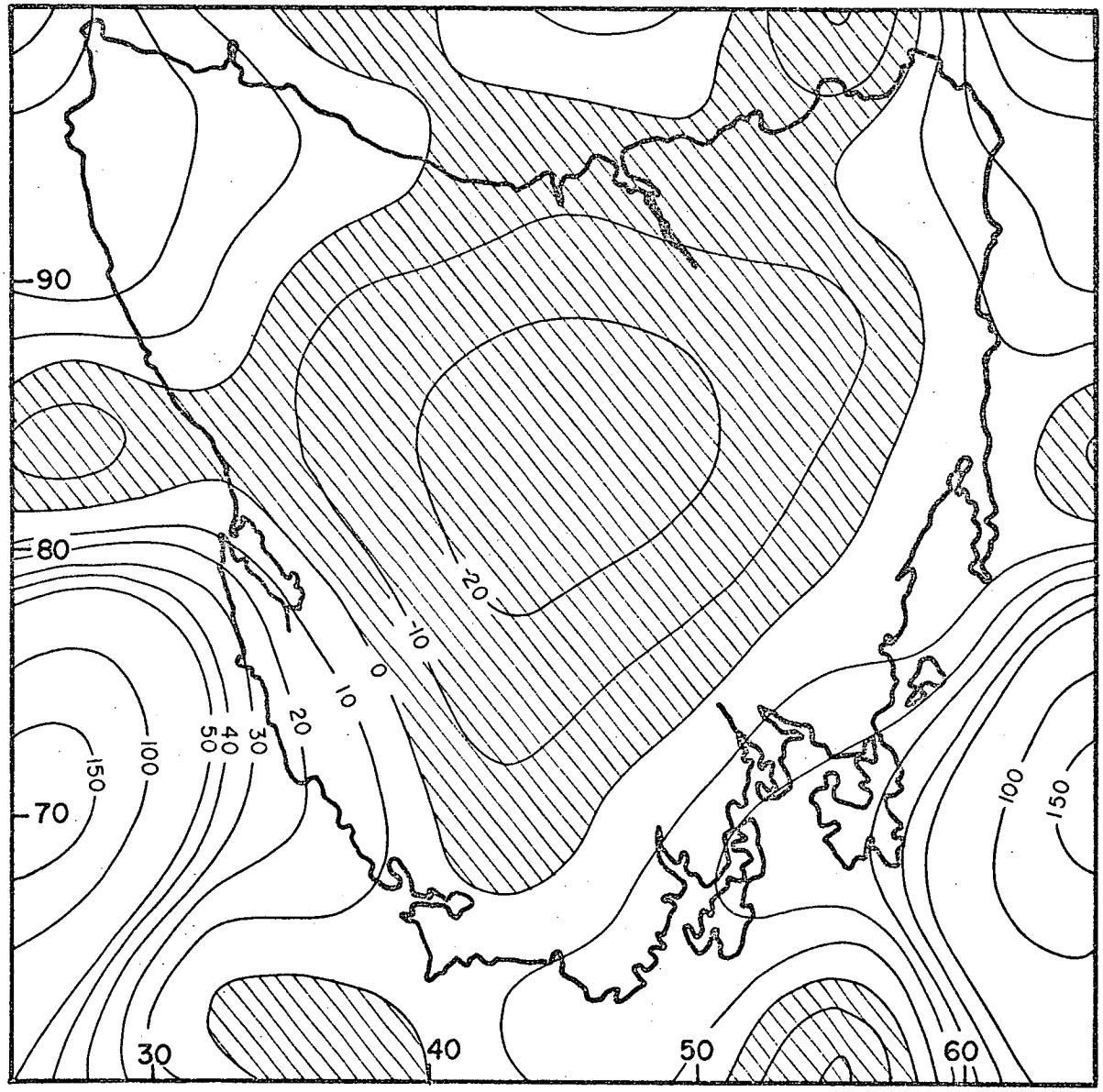

FIGURE 3·13

The data filtered to 20 kms

A synthesis of the analysis made to wave number 4 (Figure 3.10) reveals a map which is better behaved in the central region. It is however badly effected by the generation of psuedo anomalies and the necessity for the boundaries to be identical.

When the synthesis is terminated at wave number 3 a much more realistic map is produced (Figure 3.11). The position of the coastal gradients and the size of the negative anomaly are approximately correct.

The data filtered to 40 kms

The synthesis made including up to wave number 4, of this data, produces a completely unrealistic map (Figure 3.12). In particular the northern boundary is very poorly represented.

The synthesis made up to wave number 3 is much more sensible (Figure 3.13). However the data has apparently been oversmoothed and it does not sufficiently represent the regional surface.

3.1.5.6 *Behaviour of residuals*

A table of the non-orthogonal and orthogonal coefficients for each of the six analyses is included (Table 3.5, 3.6, 3.7). The variance of the residuals with the addition of each subsequent orthogonal function is calculated as a fraction of the variance of the residuals from the mean.

GRAM-SCHMIDT ORTHOGONALISATION

UNSMOOTHED AVERAGED GRAVITY DATA SET

WAVE NUMBER	FUNCTION NUMBER	ORTHOGONAL FUNCTION COEFFICIENTS	NORMALISED VARIANCE	NON-ORTHOGONAL FUNCTION COEFFICIENTS D(J) SERIES TERMINATED AT WAVE NUMBER	
				4	3
K	J	C(J)	V(J)/V(1)		
0					
	1	-.361436	1.000000	28.716030	27.132472
1					
	2	-13.632030	.812672	-1.157302	-14.955383
	3	-3.548279	.699348	-24.262362	-23.298060
	4	-22.345380	.291511	-40.098787	-39.416181
	5	-1.502869	.280505	-2.247783	-6.308472
	6	-8.553010	.262176	-44.157803	-17.947621
	7	-2.612652	.259786	-23.913608	-7.621840
	8	11.414673	.217080	20.282775	20.159702
	9	-1.278296	.217562	6.323158	5.071060
2					
	10	.323925	.218687	-3.166680	-.048822
	11	-2.225061	.214863	-35.475644	-1.138430
	12	3.515610	.207674	10.391739	11.057186
	13	5.803011	.176894	5.406795	10.336091
	14	11.048467	.143526	16.286781	7.979202
	15	2.884313	.140256	19.301086	6.015342
	16	-3.797670	.137931	58.179164	-4.568602
	17	3.010884	.133026	16.261653	1.807330
	18	-.483313	.133747	20.393820	2.866775
	19	3.687651	.129571	27.548779	7.059288
	20	4.953743	.125304	3.656840	3.362286
	21	-2.508713	.123873	-8.666561	-5.004266
3					
	22	1.791921	.122204	-28.235921	1.081333
	23	-.145735	.122939	-2.325757	-1.951792
	24	-1.705900	.122023	1.090132	-2.148998
	25	-1.355264	.121630	.858950	-.951965
	26	-3.068967	.120298	46.729355	-1.735275
	27	-2.920238	.117872	-1.909436	-2.316931
	28	1.301694	.116321	3.384586	4.286235
	29	2.289902	.116433	-2.819305	1.887175
	30	-.134038	.117167	-4.122303	1.783382
	31	-6.064250	.107024	-20.797044	-3.933862
	32	-4.613048	.104386	-45.468519	-4.439045
	33	-.111398	.105036	-21.904231	-3.059337
	34	.342140	.105662	-12.571189	-.550588
	35	-8.150139	.091887	-20.943926	-7.565951
	36	-1.783728	.092189	-.817667	-1.092389
	37	1.205287	.092525	5.450570	1.205287

GRAM-SCHMIDT ORTHOGONALISATION

UNSMOOTHED AVERAGED GRAVITY DATA SET

WAVE NUMBER	FUNCTION NUMBER	ORTHOGONAL FUNCTION COEFFICIENTS	NORMALISED VARIANCE	NON-ORTHOGONAL FUNCTION COEFFICIENTS D(J) SERIES TERMINATED AT WAVE NUMBER	
K	J	C(J)	V(J)/V(1)	4	3
4					
	38	2.548857	.089543	5.050740	
	39	1.795192	.088363	7.750709	
	40	-1.711049	.087530	-1.812327	
	41	.322647	.087840	-1.062674	
	42	3.015303	.087233	-5.892239	
	43	.644765	.087705	1.813195	
	44	.282575	.088303	-10.061310	
	45	-1.115608	.088445	.947902	
	46	-7.098054	.084268	-33.361667	
	47	1.329088	.084359	-2.241778	
	48	-2.436072	.084313	2.646406	
	49	-5.024174	.081184	2.598244	
	50	2.979856	.080315	9.221509	
	51	1.601805	.081119	11.088678	
	52	2.201452	.081365	17.227400	
	53	4.342305	.079802	12.752864	
	54	-4.538763	.078867	2.471876	
	55	2.493895	.078602	6.297222	
	56	3.321559	.078500	-.302365	
	57	-6.558903	.078029	-4.445069	
	58	4.871896	.072137	5.772543	
	59	-.514212	.072637	.997037	
	60	-.743028	.073139	4.112117	
	61	-3.998393	.071330	-2.548740	
	62	4.232161	.070879	9.559674	
	63	1.351626	.071095	3.101891	
	64	-2.761630	.071175	-1.741944	
	65	1.823724	.071370	-.925762	
	66	-2.933035	.071185	-4.714120	
	67	-4.663283	.070092	-5.286381	
	68	-2.189366	.070456	-3.091121	
	69	-4.727281	.069833	-4.727281	

GRAM-SCHMIDT ORTHOGONALISATION

GRAVITY DATA SET SMOOTHED TO 20 KMS

WAVE NUMBER	FUNCTION NUMBER	ORTHOGONAL FUNCTION COEFFICIENTS	NORMALISED VARIANCE	NON-ORTHOGONAL FUNCTION COEFFICIENTS D(J) SERIES TERMINATED AT WAVE NUMBER	
K	J	C(J)	V(J)/V(1)	4	3
0					
	1	-.336011	1.000000	-3.433480	16.322601
1					
	2	-13.033306	.783944	-2.130695	-14.911788
	3	-8.443453	.664907	11.820715	-13.012302
	4	-21.133324	.235770	15.027079	-23.952384
	5	-1.789772	.225967	.145823	-6.042151
	6	-7.563577	.200336	-39.560916	-11.069617
	7	-2.404126	.197560	-3.260735	-.125396
	8	10.345682	.156174	-42.101670	2.216093
	9	-1.700099	.154221	-3.248414	2.066435
2					
	10	-.061037	.155084	4.403652	-.088568
	11	-2.045016	.150382	-25.703132	1.475681
	12	2.078655	.148246	-23.225910	1.918270
	13	4.381409	.125941	-5.422755	6.539840
	14	9.234198	.099041	2.359954	4.340826
	15	1.718473	.090979	3.493149	1.543643
	16	-1.872015	.086535	43.677962	-7.028126
	17	2.855470	.080395	5.665905	-.967129
	18	-1.045441	.091189	16.733425	-.344945
	19	2.174224	.089677	10.108794	1.387276
	20	6.453432	.080191	41.123191	11.006439
	21	-2.787364	.077381	5.488952	-1.464311
3					
	22	1.608530	.075536	-19.063043	3.271532
	23	-.746849	.075509	.656535	-2.663808
	24	-1.600240	.074221	12.661278	.392508
	25	.433191	.074489	8.310109	1.400566
	26	-4.291787	.070341	30.171661	-4.393024
	27	-2.490333	.068036	1.853790	-1.083669
	28	.335736	.068438	-4.038655	3.052987
	29	3.273533	.062478	1.381663	3.395540
	30	1.172967	.062815	5.465573	3.127152
	31	-3.148934	.059529	-7.570733	-1.520203
	32	-.892112	.059758	-35.258260	-.932504
	33	1.974604	.059032	-9.940189	.051363
	34	-.062961	.059415	-9.018178	-.992350
	35	-2.620811	.059002	-7.414653	-3.334242
	36	-1.802441	.056039	-14.710258	-3.072350
	37	-2.194776	.057339	-8.184364	-2.194776

GRAM-SCHMIDT ORTHOGONALISATION

GRAVITY DATA SET SMOOTHED TO 20 KMS

WAVE NUMBER	FUNCTION NUMBER	ORTHOGONAL FUNCTION COEFFICIENTS	NORMALISED VARIANCE	NON-ORTHOGONAL FUNCTION COEFFICIENTS D(J) SERIES TERMINATED AT WAVE NUMBER	
				4	3
K	J	C(J)	V(J)/V(1)		
4					
	38	1.751099	.055704	2.913785	
	39	1.098834	.055285	4.406043	
	40	-.724682	.055354	-2.334873	
	41	-.259616	.055697	-4.427644	
	42	4.021910	.053523	-2.660827	
	43	-.351577	.053346	.745242	
	44	-.061726	.054220	-5.386546	
	45	.244182	.054572	.840755	
	46	-6.592126	.050026	-24.878041	
	47	.613316	.050313	-3.960292	
	48	.104499	.047350	8.420672	
	49	-4.922806	.046774	.798637	
	50	1.739042	.046766	2.239552	
	51	-.770541	.047012	3.982080	
	52	.548787	.047333	12.102094	
	53	3.392741	.046185	7.722242	
	54	-3.116054	.044550	-.638695	
	55	-1.351570	.044326	2.353712	
	56	.670359	.044624	1.948554	
	57	-.332307	.044955	.168226	
	58	3.418056	.043979	4.001541	
	59	-1.472910	.043917	.447819	
	60	-1.376052	.043718	1.134646	
	61	-4.190398	.044270	-1.855809	
	62	3.585880	.040417	7.251412	
	63	3.286537	.039572	4.654869	
	64	-3.806040	.038741	-2.728178	
	65	-.725463	.038851	-2.459197	
	66	.997473	.038197	-.312950	
	67	-3.712442	.038255	-3.915000	
	68	-1.424749	.038463	-1.814246	
	69	-2.041831	.038517	-2.041831	

GRAM-SCHMIDT ORTHOGONALISATION

GRAVITY DATA SET SMOOTHED TO 40 KMS

WAVE NUMBER	FUNCTION NUMBER	ORTHOGONAL FUNCTION COEFFICIENTS	NORMALISED VARIANCE	NON-ORTHOGONAL FUNCTION COEFFICIENTS D(J) SERIES TERMINATED AT WAVE NUMBER	
K	J	C(J)	V(J)/V(1)	4	3
0					
	1	-.867979	1.000000	13.504829	7.805329
1					
	2	-11.800643	.759300	-7.448586	-9.166147
	3	-7.880563	.595157	-22.462377	-8.592180
	4	-13.454219	.113016	-29.443187	-15.356897
	5	-1.469428	.112775	-2.882366	-1.750357
	6	-4.930672	.096547	-3.581359	-7.840562
	7	-1.751215	.094130	-3.153601	-2.600397
	8	7.114824	.065707	22.833287	-2.682541
	9	-2.156654	.059534	-.682413	-2.270662
2					
	10	-.108757	.059349	-10.342597	-1.052618
	11	-1.221049	.057581	-4.786151	-2.223009
	12	.583885	.057512	11.426047	-.863213
	13	2.564461	.046419	3.277774	2.309235
	14	3.837259	.039568	13.420598	1.477785
	15	.929556	.039216	.558479	.528122
	16	.254069	.039420	4.442077	.989810
	17	3.058756	.029560	6.658273	2.916950
	18	-1.771849	.029320	-8.954518	-1.196313
	19	.537970	.028307	2.979074	1.171770
	20	4.706137	.020803	-13.447052	6.362236
	21	-1.870344	.018795	-3.854652	-.623173
3					
	22	.595623	.018452	.635636	.763659
	23	-.533573	.018208	1.473919	-.218242
	24	-.632255	.017930	-5.289953	-.022498
	25	.028419	.018039	.431701	.567649
	26	-1.041055	.017760	1.489655	-.634923
	27	-.240192	.017833	2.560648	.482057
	28	-2.035109	.016743	-2.731232	-.745654
	29	1.006814	.015979	.601408	.704464
	30	.130466	.016076	-3.837675	1.219810
	31	-.638852	.015972	-1.464819	-.317562
	32	.015921	.016074	.799231	-.048207
	33	-.931024	.015821	-6.039863	-1.600123
	34	.673072	.015752	2.961836	.299981
	35	-1.149534	.015361	-4.404099	-1.360065
	36	-.825056	.015352	3.769420	-1.230550
	37	-.700813	.015295	2.110638	-.700813

GRAM-SCHMIDT ORTHOGONALISATION

GRAVITY DATA SET SMOOTHED TO 40 KMS

WAVE NUMBER	FUNCTION NUMBER	ORTHOGONAL FUNCTION COEFFICIENTS	NORMALISED VARIANCE	NON-ORTHOGONAL FUNCTION COEFFICIENTS D(J) SERIES TERMINATED AT WAVE NUMBER	
				4	3
K	J	C(J)	V(J)/V(1)		
4					
	38	.451109	.015204	.405893	
	39	.440797	.015122	-.499768	
	40	-.859485	.014807	.793166	
	41	.209910	.014675	-.159468	
	42	1.177356	.014460	-1.010976	
	43	-.414981	.014468	-.490024	
	44	-.396108	.014532	1.026575	
	45	.731741	.014284	.409493	
	46	-1.996353	.013733	-3.136045	
	47	-.827708	.013653	-2.247464	
	48	-1.953745	.013104	-.727978	
	49	-2.113674	.012068	-1.287753	
	50	.220093	.012147	3.951126	
	51	-.859035	.012065	2.446563	
	52	-1.270480	.011965	-.415258	
	53	.854930	.011917	3.699779	
	54	-.450308	.011946	-.101645	
	55	.733895	.011909	1.654485	
	56	-1.254821	.011811	-2.953924	
	57	-2.507039	.011087	-1.914720	
	58	1.323781	.010887	1.738185	
	59	.493819	.010806	.676049	
	60	.030949	.010981	.256317	
	61	-.641542	.010972	-.413373	
	62	-.581605	.011027	.264254	
	63	-.054475	.011114	.448430	
	64	-1.190983	.011047	-.326511	
	65	1.043709	.010922	.406490	
	66	-1.033834	.010848	-1.346708	
	67	-.722292	.010868	-1.173736	
	68	.232317	.010955	-.174376	
	69	-2.131975	.010624	-2.131975	

COMPARISON OF VARIANCE OF RESIDUALS AFTER THE ADDITION OF EACH WAVE NUMBER

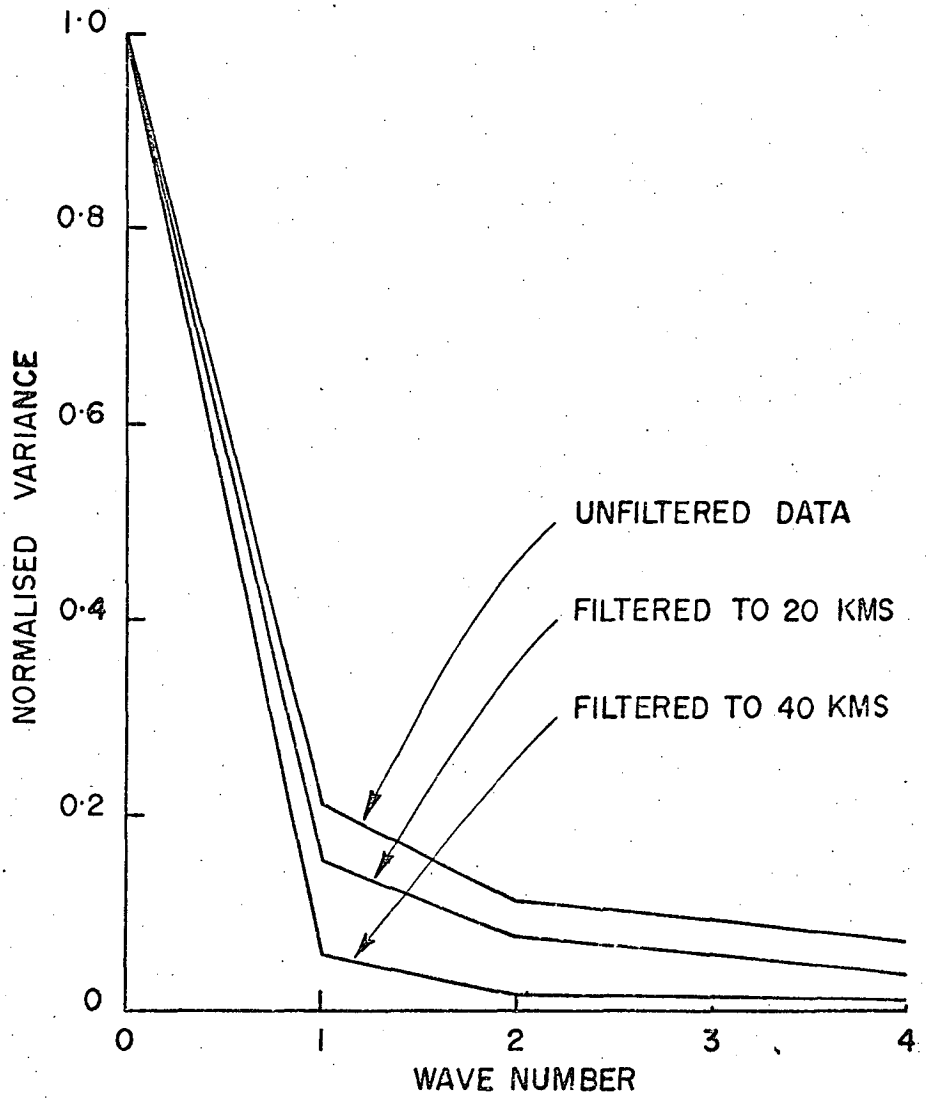

FIG. 3·14

The variance is seen to decrease more rapidly with data sets that have been prefiltered. It is also evident that, for example, the data set filtered to 40 kms can be realistically represented by the functions up to wave number 3 and that any further functions do not materially decrease the residuals.

It should be noted that although the orthogonal coefficients remain the same, regardless of the point of termination, the non-orthogonal coefficients are all different. The difference between the non-orthogonal coefficients for different points of termination is a measure of the irregularity of the distribution of data points and of the necessity for the use of an orthogonalisation procedure.

Figure 3.14 is a comparison of the variance of the residuals after the addition of each wave number, for the 3 data sets.

3.1.6 Regional Gravity Map

The coefficient set chosen to define the regional gravity map of Tasmania was that derived from the data set filtered to 20 kms and synthesised up to wave number 3.

Figure 3.15 is a map of the regional Bouguer gravity map showing also the location of the data points used in the analysis.

REGIONAL GRAVITY MAP OF TASMANIA

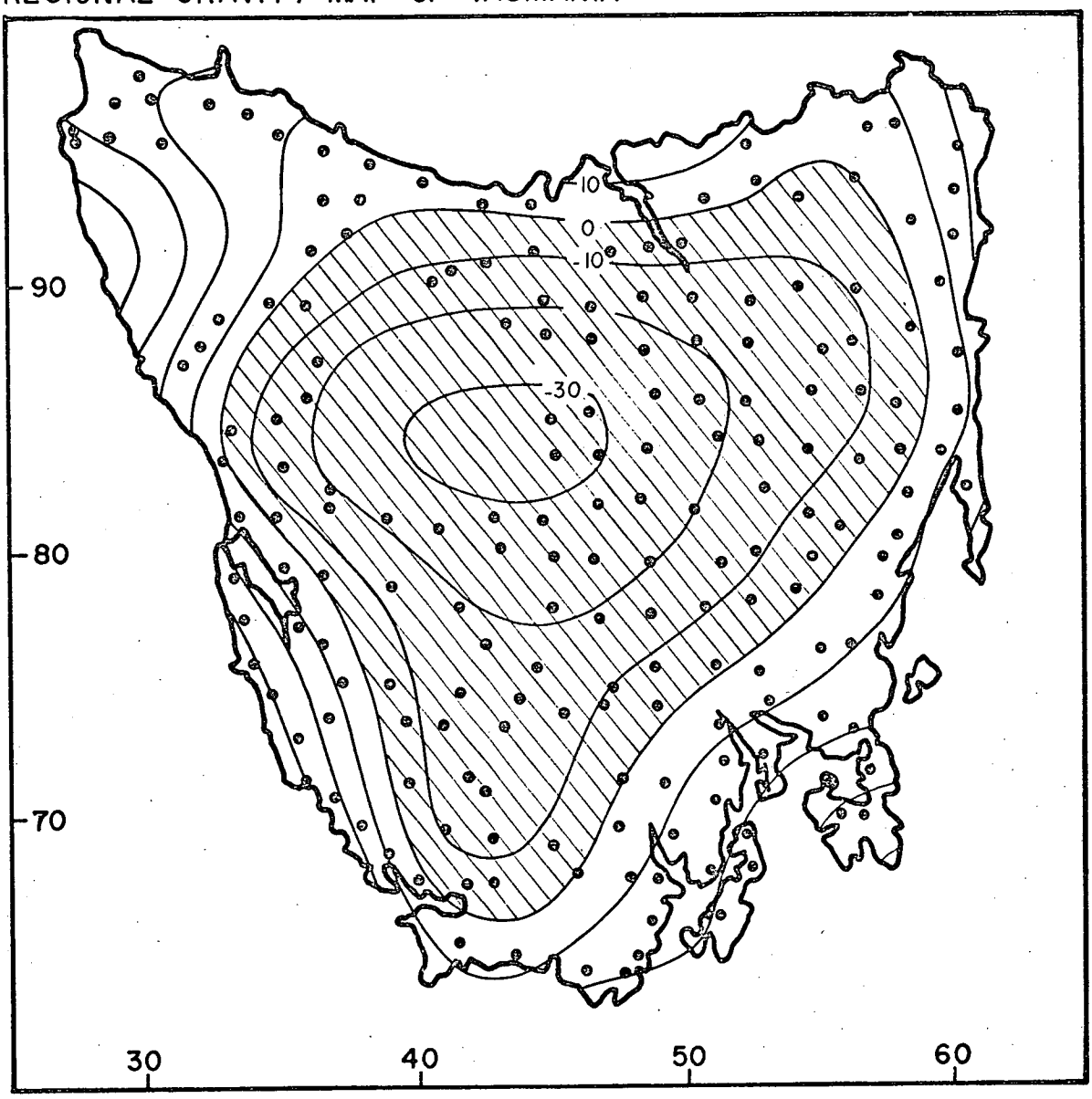

FIGURE 3·15

CHAPTER FOUR

INTERPRETATION OF THE GRAVITY DATA

4.0 INTERPRETATION OF THE GRAVITY DATA

Following from the analysis of the gravity data, in the previous section, the chosen regional field was subtracted from the observed Bouguer anomalies to give a residual Bouguer anomaly map. (Figure A.2, in Appendix).

Considerable difficulty was encountered, at this stage in the project, in finding a suitable machine contouring programme for the residual map. It has been found that many of the present systems for contouring irregularly spaced data do not produce realistic maps. The contour maps of irregularly spaced data in this thesis were prepared using a modification of a programme developed by I. Briggs (Bureau of Mineral Resources, Canberra). The problem of contouring irregularly spaced data has been examined by several authors (e.g. Crain, 1970), but much more work remains to be done.

4.1 INTERPRETATION OF THE RESIDUAL FIELD

The interpretation of the shallow source anomalies was carried out using both the observed Bouguer anomaly and the residual Bouguer anomaly maps. A map of the essential elements of the residual Bouguer anomaly field is given in Figure 4.1, to assist in the description.

The interpretations are described in terms of the dominant rock types or structures causing the anomalies.

ELEMENTS OF RESIDUAL GRAVITY MAP

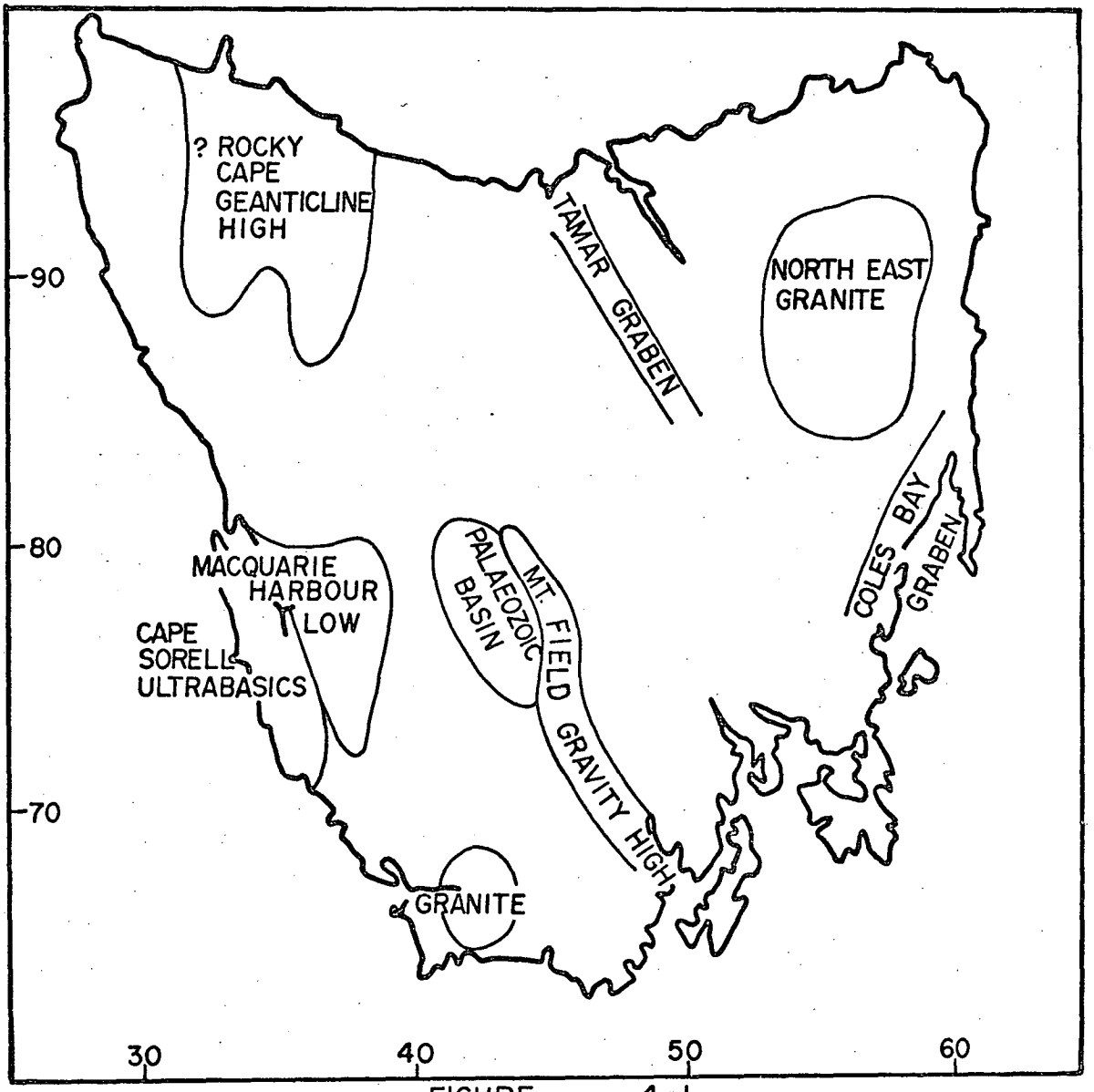

FIGURE 4·1

4.1.1 Anomalies associated with Dolerite Bodies

Dolerite is a very common intrusive rock found in much of the eastern part of Tasmania. As its normal density is appreciably higher than typical surrounding rocks it normally causes sharp positive anomalies.

4.1.1.1 *The Mt. Field Gravity High*

The most dominant anomaly that is associated with dolerite is the sharply positive gravity feature trending NW-SE through the Mt. Field National Park region. To the south it appears to continue but offset towards the SW. To the north it seems to disappear in the Lake King William - Lake St. Clair region (although it may continue as there are no observations to the north of Lake St. Clair).

The direction of the feature corresponds closely to the dominant directions of Tertiary faulting in many parts of the state. The structure is obviously very major and it must be seriously thought of in terms of a possible feeder for the large quantity of dolerite in the South East of Tasmania. The total length of the gravity feature is of the order of 160 kms, the width is variable but of the order of 8 kms wide.

A detailed gravity map, of the region at the southern end of the Mt. Field National Park, shows the part of the feature that has been surveyed in greatest detail. (Figure 4.2). The rather large gaps in the coverage are due to the extreme ruggedness and inaccessibility of the region.

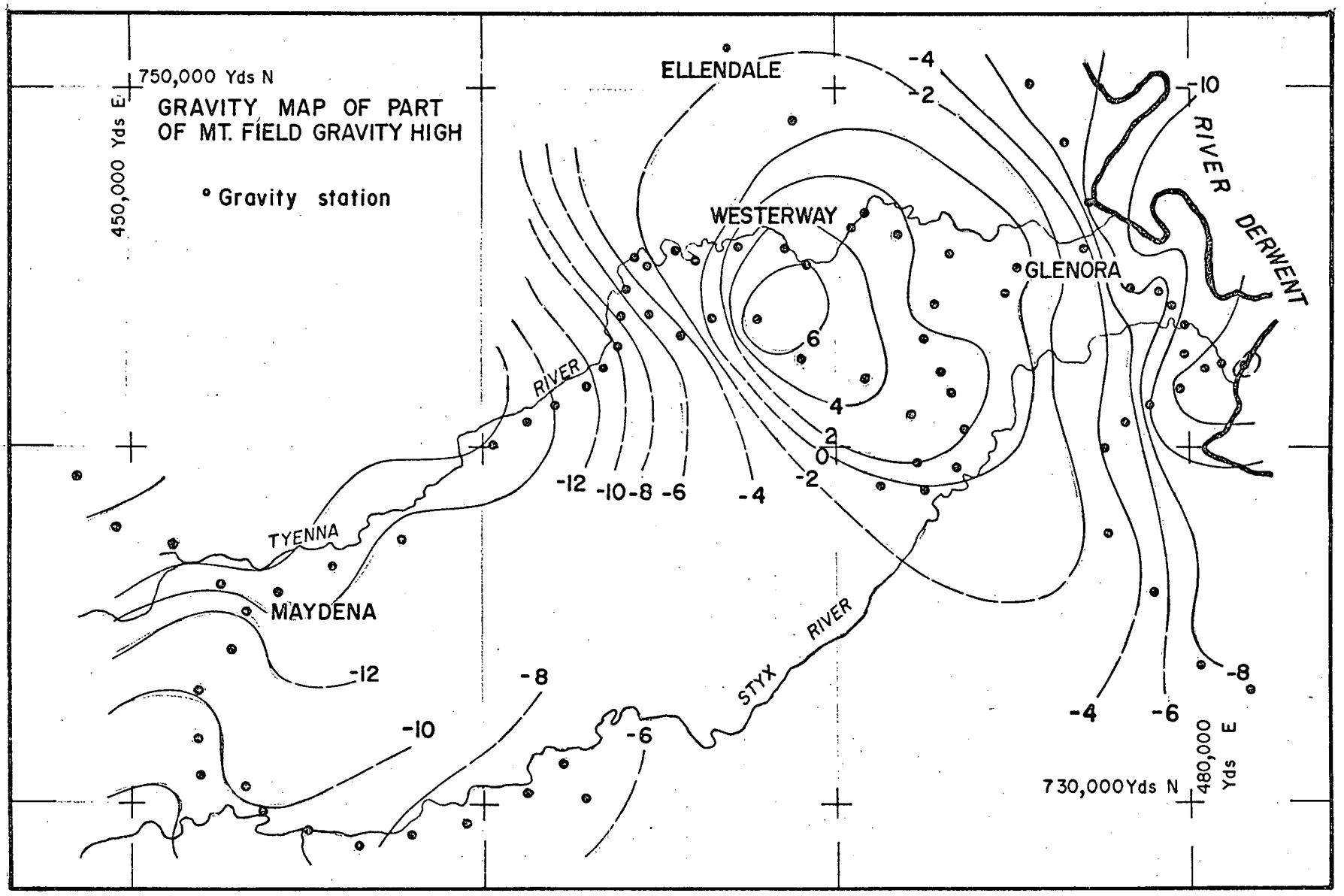
750,000 Yds N
450,000 Yds E
GRAVITY MAP OF PART
OF MT. FIELD GRAVITY HIGH
° Gravity station
ELLENDALE
WESTERWAY
GLENORA
RIVER DERWENT
RIVER
TYENNA
MAYDENA
STYX RIVER
-4
2
10
6
4
2
0
-2
-12
-10
-8
-6
-4
-12
-10
-8
-6
-4
-6
-8
730,000Yds N
480,000 Yds E

FIGURE 4·2

Gravity observations have been made along all the relatively navigable timber tracks - any further work will have to be carried out on foot or in part by helicopter.

Model studies have been carried out on the profile made along the Maydena Road. The values have been projected on to a theoretical traverse bearing N60^{o}E from Maydena. The deviation from the regional gradient is +20 mgals. The most reasonable fitting model, Figure 4.3, is 10 kms wide, 3 kms deep at the eastern end and possibly extending to depth at the western end.

The density contrast chosen for the gravity modelling was +0.3 gms/cc. This is a maximum probable contrast although the major effect is probably due to the density contrast between sediments (of the order of 2.60 gms/cc), and the dolerite (2.90 - 2.93 gms/cc).

The Mt. Field Gravity High therefore represents an extremely large body of dolerite. The detailed relationships of this body to the structure and evolution of the dolerites of south eastern Tasmania will undoubtedly prove to be a very interesting study.

4.1.1.2 *The Great Lake Anomaly*

The conclusions of Jones' original survey of the Great Lakes Gravity High anomaly (Jones, Haigh and Green, 1966) has not been changed very greatly since that time. Further work to the north and east by the Tasmanian Mines Department has

Fig 4.3

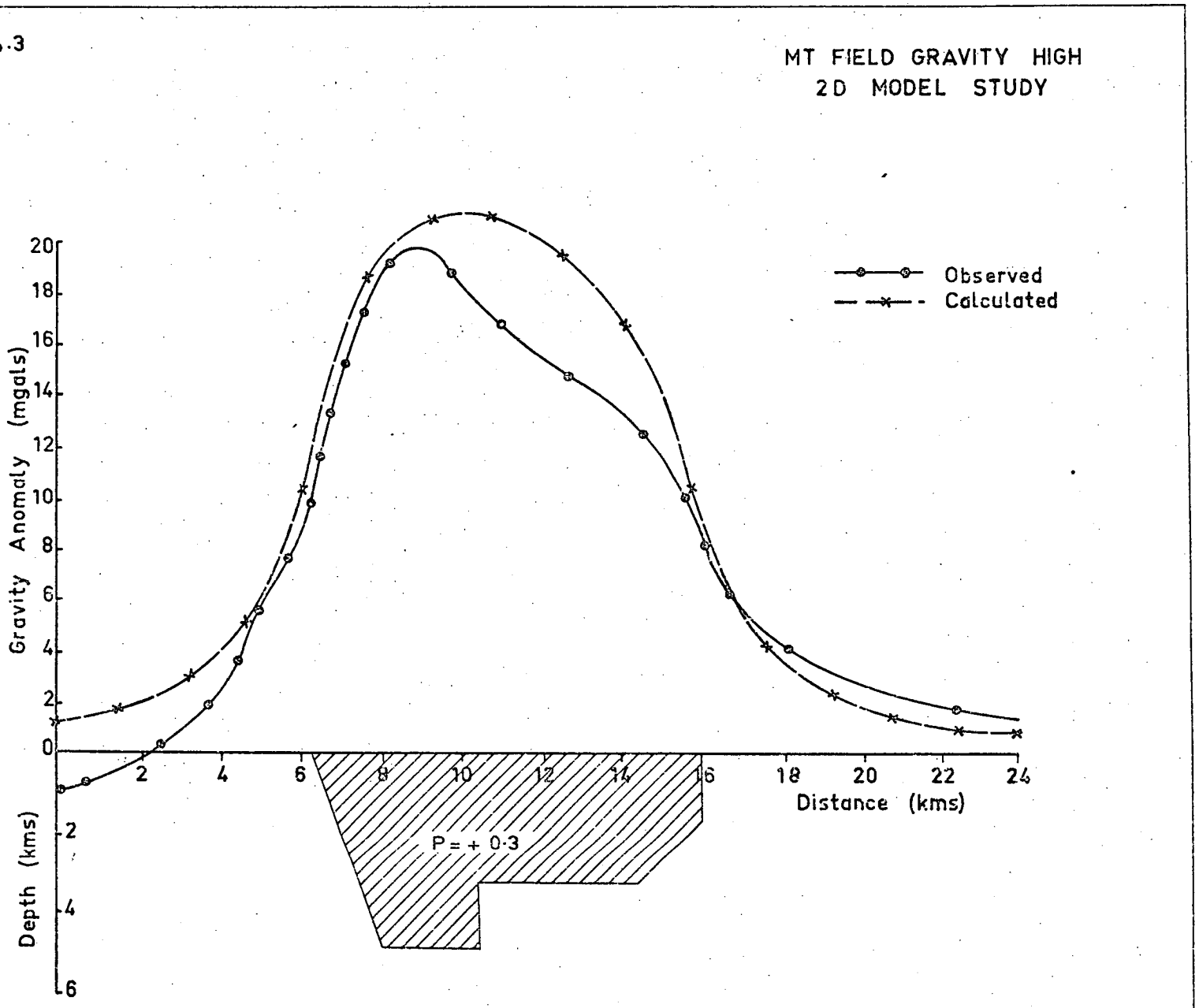
MT FIELD GRAVITY HIGH
2D MODEL STUDY
Observed
Calculated
Gravity Anomaly (mgals)
20
18
16
14
12
10
8
6
4
2
0
2
4
6
8
10
12
14
16
18
20
22
24
Distance (kms)
Depth (kms)
2
4
6
P = + 0·3

had no appreciable effect on the interpretation of the observed gravity high.

Camerons' (1967) reinterpretation of the data showed that there was a possibility of an extension to depth although this could not be confirmed. The present interpretation of this feature is a boss or neck of dolerite of the order of 1.2 kms deep and approximately 13 kms in diameter. This is certainly a rather simplified model but the details of geology and gravity information are not available.

4.1.1.3 *Dolerite structure in the Hobart region*

During 1968-1969, D.E. Leaman, from the Mines Department, Hobart, undertook a detailed survey of the Hobart region (Leaman, 1970). This comprised a gravity survey at a 1 mile station interval and some detailed geological mapping.

Leaman was able to establish detailed structural relationships in the dolerites and identified four distinct phases of intrusion.

One of the unusual features of the Tasmanian dolerite bodies is that the gravity anomaly is commonly the only way to determine whether an outcropping body is part of a sill or dyke.

Much of the terrain, in eastern Tasmania, is controlled by the presence or absence of dolerite and this creates problems in the interpretation of the gravity data.

4.1.1.4 *The Lake Leake Gravity High*

This anomaly, observed by Cameron (1967), is important only in its relationship to the surrounding anomalies. Firstly it interrupts the dominant SW-NE trend of the Bouguer anomaly contours. Secondly, it has a very steep gradient to the north, in the Avoca region. Thirdly, there is an indication of a negative gravity anomaly to the east trending N30^{o}E and passing through Oyster Bay. To the west, there is a rather abrupt termination of the anomaly, the structural significance of which is not clear.

The source of this positive anomaly is an intrusion of dolerite, the structural form of which has not been elucidated.

4.1.1.5 *General comments on dolerite structures*

There are many minor features on the Bouguer anomaly map that are due to dolerite bodies. These all contribute to give the map a grain reflecting the dominant direction of elongation of the bodies. This direction is commonly in the NW-SE Jurassic and Tertiary faulting direction. There is also a subsidiary N-S faulting direction.

This fault pattern is consistent over most parts of the state and must reflect a large scale deformation pattern. It is probably not coincidental that the dominant direction is almost parallel with several other large scale features in this region of the world. The elongation direction of the Sydney Basin; the observed magnetic lineation off the east

coast of Tasmania (Finney & Shelley, 1967); the Flinders Island-Bassian Rise (in eastern Bass Straits); the linearty of magnetic anomalies in the Tasman Sea (Ringis, 1970): these are all in the same dominant direction and are therefore thought to be related. The work of Griffiths (1971) should lead to some useful conclusions.

4.1.2 Anomalies associated with ultrabasic bodies

There are several regions in Tasmania where the gravity survey has crossed known bodies of ultrabasic or ultramafic rocks. Many of these bodies have no gravity expression whatsoever, since the rocks have been at least partially serpentinized. Normal ultrabasic rocks have densities of the region of 3.0 gms/cc and serpentine has a density of 2.0 gms/cc. It is therefore relatively common in partially serpentinized ultrabasic bodies to find a density close to that of the surrounding rocks.

4.1.2.1 *Ultrabasic bodies with no gravity expression*

A narrow band of superficially serpentinized ultrabasic rocks occurs on the Gordon River Road. Although this is quite narrow this body should have shown up on the gravity profile as the rock samples indicate a reasonable density contrast. It must therefore be more greatly serpentinized at depth or it does not extend to depth as the geology

indicates (K.D. Corbett, pers. comm.)

The Serpentine Hill body (Rubenach, 1967) is a large ultrabasic feature which has been very largely converted to serpentine. A single road traverse was made along the best known section of the body, and again this body does not have any gravity expression.

4.1.2.2 *Bald Hill Ultramafic Complex*

This is a large ultramafic complex of variable composition and is situated east of the Savage River Mines. A single profile across the body was made and a large positive anomaly was observed. The survey was carried out with the assistance of M.J. Rubenach who was carrying out petrological investigations in the region (Rubenach, in preparation).

A gravity profile across the body and the model interpretation is shown in Figure 4.4. The model interpretation is consistent with a synclinal feature with densities decreasing to the east. The detailed mapping of the body, by Rubenach, has not been able to reveal much indication of the depth continuation of the body. The interpretation is, at best, consistent with the known data; other equally consistent interpretations may be readily obtained.

Fig 4.4

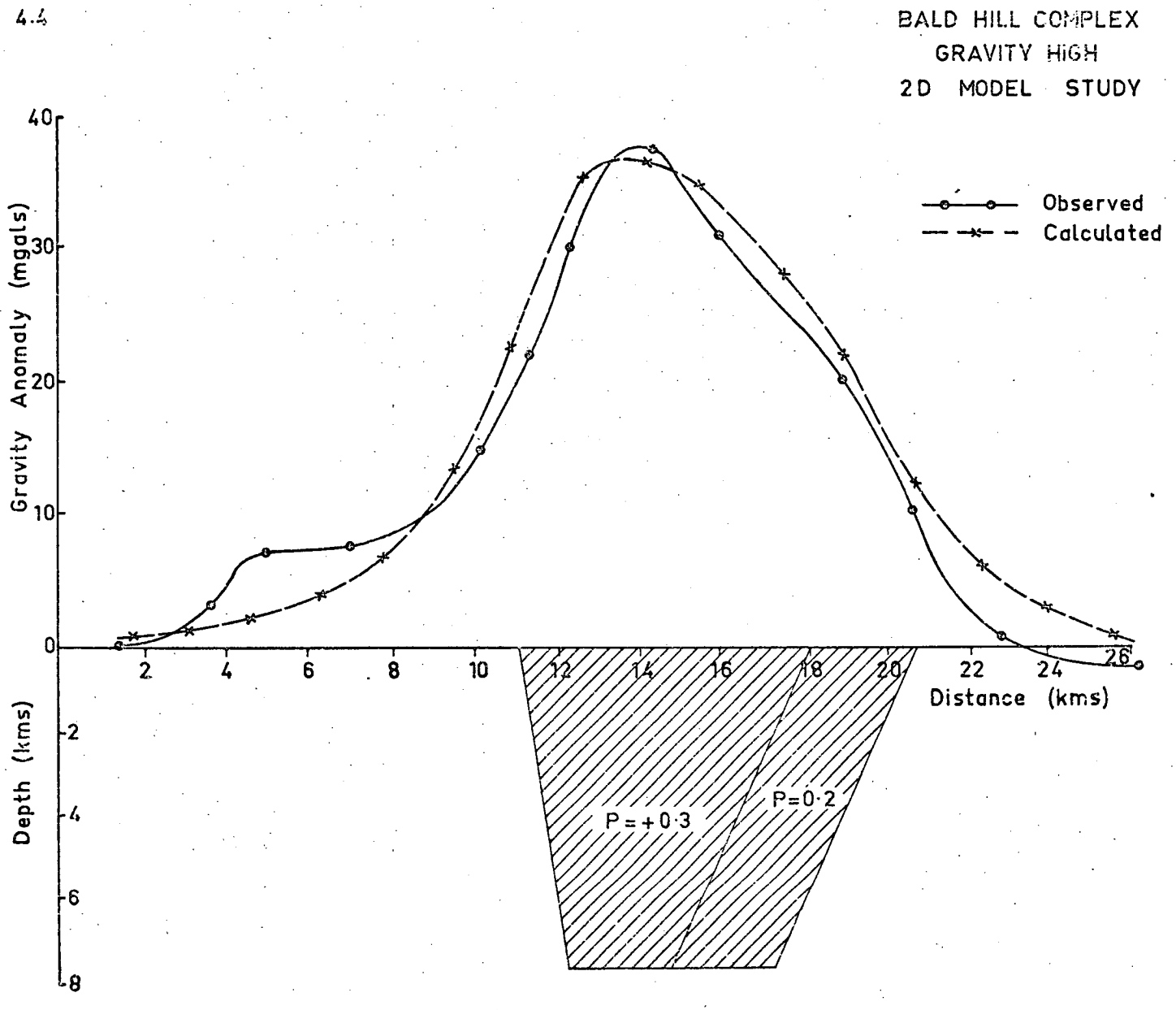
BALD HILL COMPLEX
GRAVITY HIGH
2D MODEL STUDY
Observed
Calculated
Gravity Anomaly (mgals)
40
30
20
10
0
2
4
6
8
10
12
14
16
18
20
22
24
26
Distance (kms)
Depth (kms)
2
4
6
8
P = +0·3
P=0·2

4.1.2.3 *Macquarie Harbour Ultrabasics*

Extremely high positive gravity values are observed in the Macquarie Harbour - Cape Sorell - Point Hibbs region of Western Tasmania. These are partially due to the high regional values observed near the west coast. In this region, these values have been augmented by the presence of relatively high density rocks. Detailed mapping by the Geological Staff of B.H.P. have revealed small ultrabasic bodies with relatively little serpentinization. The final result of this mapping has not been made available at this stage.

4.1.3 Anomalies associated with granite bodies

There are several granitic bodies in Tasmania - the largest of which is in the north east, and the remainder being mainly in the western part of the state.

4.1.3.1 *The North-east Granite Anomaly*

This anomaly, first identified by the work of B.F. Cameron (1967), is of very large extent (70 kms x 100 kms), and coincides in gross detail with the known position of granites in the north eastern part of the state.

There are several unusual features about this anomaly which should be explained. Firstly, although the general location of the gravity anomaly coincides with the surface geology, the detailed positioning of the margin of the body, as derived from gravity, does not. This is probably due to

non-vertical boundaries at shallow levels, (and therefore not effecting the gravity anomaly) which become near vertical at depth.

Estimates of the depth extent of this body depend largely on the chosen level of the regional field. Providing that a density contrast of -0.05 gms/cc is realistic then the body probably extends to a depth of the order of 10 kms. However the densities of the surface exposures are very variable and indicate many different granite compositions (Groves, pers. comm.)

4.1.3.2 *The Cox's Bight granite anomaly*

During the survey of the extreme south western part of the state a small negative anomaly was defined between Bathurst Harbour and Cox's Bight. Since alluvial tin is found in the drainage near Malaleuka Inlet (D. King, pers. comm.) this negative anomaly is interpreted as a small granite body with only a small surface outcrop at Cox's Bight. A single station on South West Cape has also a remarkably low gravity value and it is possible that the very small outcrop is part of an extension of the granite feature off the end of South West Cape. If that is the case, then one may be able to find a tin bearing granite in Antarctica, probably in the Ross Sea region.

4.1.3.3 *The Heemskirk granite anomaly*

The Heemskirk granite is a large granite body on the west coast of Tasmania and is readily accessible only along the Trial Harbour Road. Gravity values obtained along this road and along the ocean beach north of Strahan indicate that the granite contact dips to the south before becoming nearly vertical. An approximate estimate of the depth extent of the granite is of the order of 10 kms.

4.1.3.4. *The Meredith granite anomaly*

To the north-east of the Heemskirk is another large body of granite: the Meredith granite. The Savage River Road crosses the northernmost tip of this granite body. Although the surface expression of this body is only 2 kms wide the preliminary calculations on the observed negative gravity anomaly indicate a depth extent of the order of 10 kms and thus forming a dyke like extension of the main granite. In the Mt. Cleveland area just to the west the sloping upper surface of the granite has been mapped by estimating the lower termination of magnetic features (Glasson, 1967).

4.1.4 Anomalies associated with graben structures

There are two main graben-type anomalies in Tasmania. The first is in the north, the Tamar graben in the Launceston region, and this has been studied in detail by Hinch (1965) and later by Longman and Leaman (1967).

The second anomaly is that due to the Macquarie Harbour graben. This is a Tertiary graben structure which runs south-east down the length of Macquarie Harbour and turns south at the eastern end of the harbour. The graben becomes thinner and shallower as it proceeds southwards until it appears to bifurcate and turn once more south-eastwards (McHall, pers. comm.). The gravity anomaly is very clear and corresponds closely with the surface indications of the extent of the graben. At the ocean beach at Strahan the gravity anomaly indicates a depth of 3 kms for the sediments.

The other major graben, the Derwent graben, does not have a prominent gravity anomaly but detailed work has been carried out in this region by Leaman (1970).

4.2 INTERPRETATION OF THE REGIONAL FIELD

The regional field has been defined, in this work, as the anomaly due to the horizontal variation in the crust-mantle structure.

It remains therefore, to model the crustal structure by choosing some isostatic system, and then comparing the gravity effect of this model with the observed regional values.

4.2.1 Choice of isostatic model

A simple Airy isostatic system was chosen to model the crustal structure of Tasmania. In this model topography

above sea level is compensated for by a crustal root extending below some standard crustal depth. Similarly any topography below sea level is compensated for by a mantle antiroot rising above the standard crustal depth.

The densities of the portions of the crust and mantle which depart from the standard crustal model must be chosen in order to calculate the thickness of the root and antiroot. The upper crustal density was chosen to be 2.67 gms/cc. The lower crustal density was estimated to be 2.8 gms/cc and the underlying mantle 3.3 gms/cc; this giving a density contrast of 0.5 gms/cc at the base of the crust. Since the isostatic model anomalies are being compared to Bouguer anomalies, then the only regions contributing to the gravity anomalies are the roots and antiroots. Figure 4.5 pictorially describes the isostatic model system.

The use of the concept of a standard crust does lead to a major uncertainty. That is, the actual depth of the crust is unknown. In practice, it can be seen that the model anomalies computed for different standard crustal thicknesses are very similar.

It is also possible to vary the isostatic model system by letting the density contrast in the antiroot be different from that of the root. This appears to be feasible, since both the mantle and the crust may be expected to have variations in their physical properties over the range of

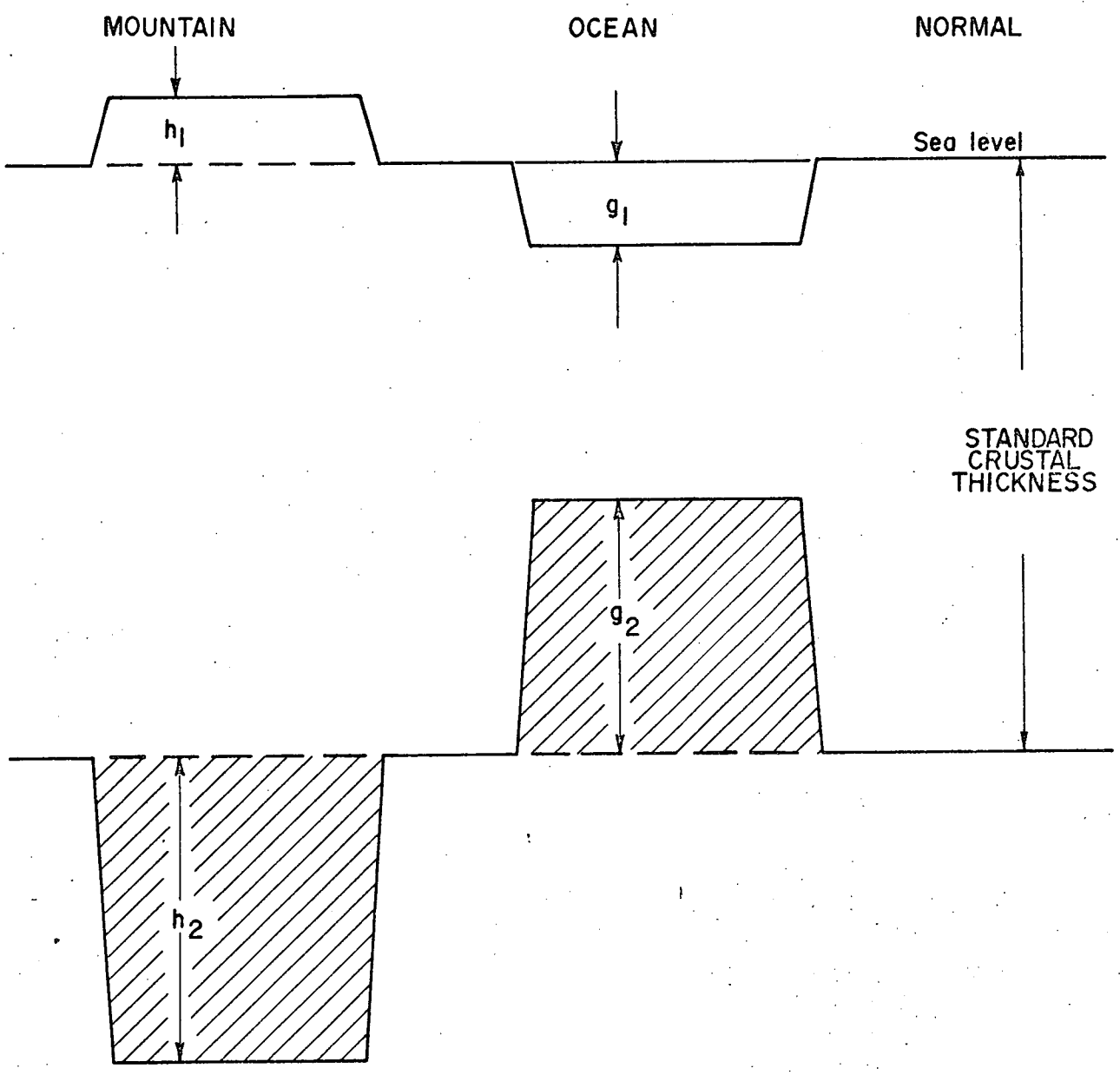
ISOSTATIC MODEL SYSTEM
MOUNTAIN
OCEAN
NORMAL
h_1
Sea level
g_1
STANDARD CRUSTAL THICKNESS
g_2
h_2
ROOT
ANTIROOT
$h_2 = h_1 \frac{2{\cdot}67}{0{\cdot}5}$
$g_2 = g_1 \frac{2{\cdot}67 - 1{\cdot}03}{0{\cdot}5}$
$-0{\cdot}5$ gms/cc
$+ \ 0{\cdot}5$ gms/cc

FIGURE 4 · 5

depths concerned. However it can be shown that, even with a root density contrast of only 0.3 gms/cc, and an antiroot density of 0.5 gms/cc, the gravity anomaly is not sensitive to this variation (as the total mass of the compensation must remain constant).

4.2.2 Calculation of isostatic model

A digital model of the topography and bathymetry of Tasmania was prepared. The size of the topographic blocks used is variable but is based on a 50 kms square. Larger blocks were used where the variation is small and smaller blocks were used for rapid changes in elevation.

A three dimensional gravity programme based on the formulation of Nagy (1966) was developed for the purpose of modelling crustal structure. In this programme the elevation of the topography is used to define a block representing the root (or antiroot), the vertical dimension of which is defined by the densities assumed for the crust and mantle.

Figures 4.6 and 4.7 are maps of the gravity field calculated for the crustal model of Tasmania using 30 kms and 35 kms respectively as the thickness of the standard crust.

4.2.3 Comparison of isostatic model with the regional anomaly

It is difficult from the maps of the isostatic model gravity field, to compare the adequacy (or otherwise) of the

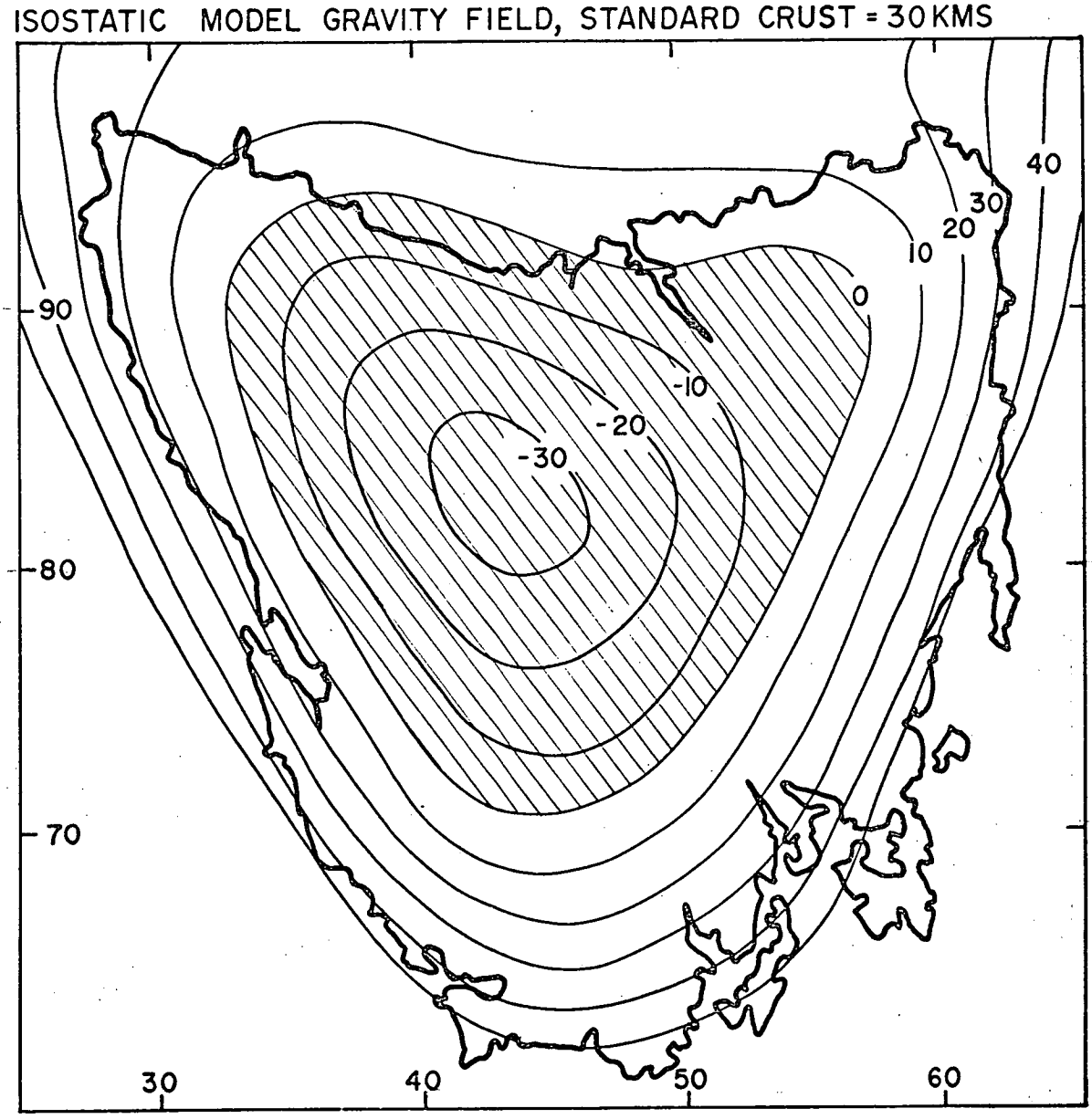
ISOSTATIC MODEL GRAVITY FIELD, STANDARD CRUST = 30 KMS
40
30
20
10
0
-10
-20
-30
-90
-80
-70
30
40
50
60

FIGURE 4 · 6

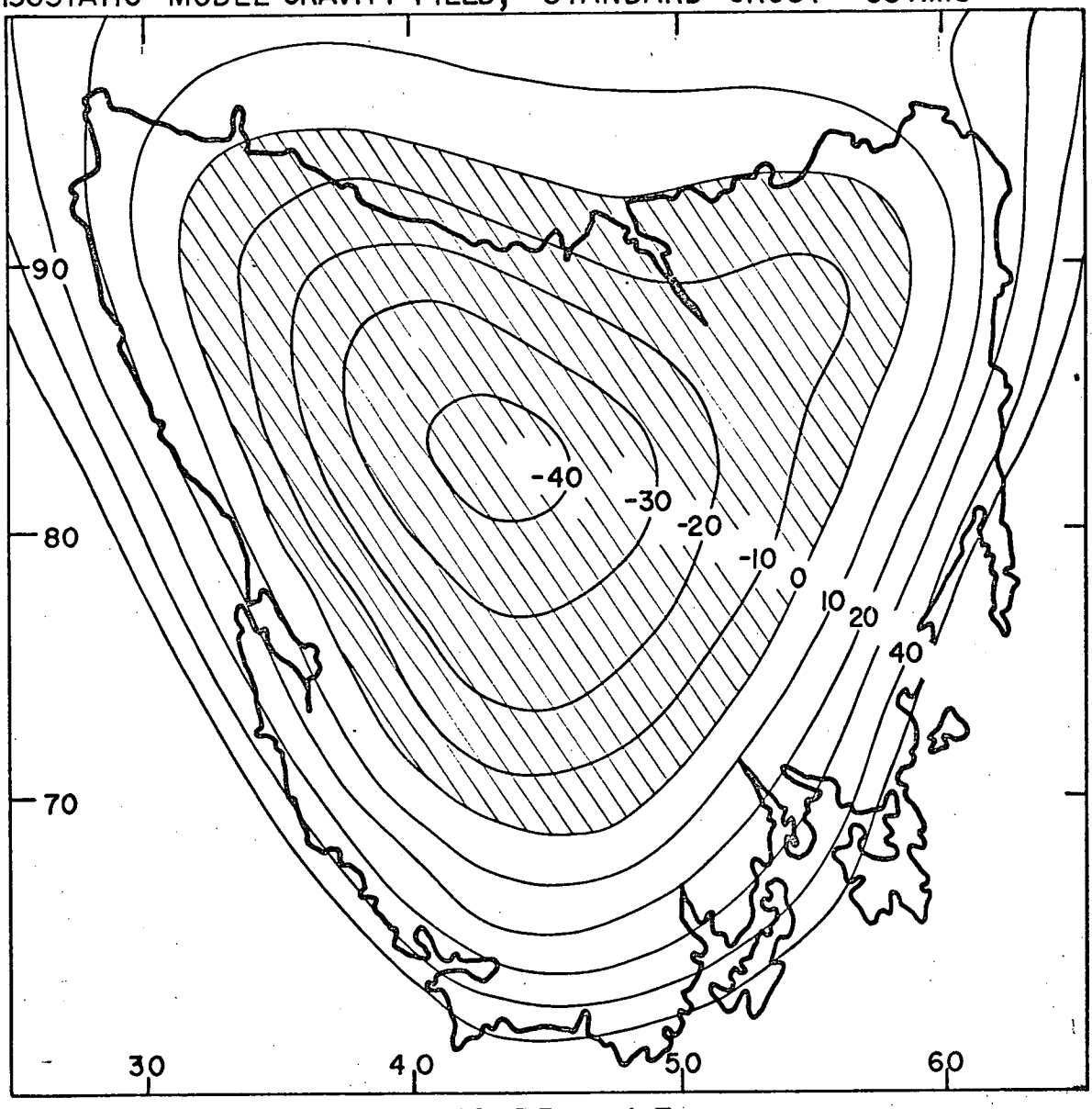
ISOSTATIC MODEL GRAVITY FIELD, STANDARD CRUST = 35 KMS
90
80
70
30
40
50
60
-40
-30
-20
-10
0
10
20
40

FIGURE 4·7

isostatic model.

A series of east-west profiles, Figures 4.8 to 4.13, were thus prepared showing the model crustal structure underneath the profile and the calculated gravity anomaly. On each of these profiles, the gravity anomaly was calculated with standard crustal thicknesses of 30 and 35 kms.

In order to compare the isostatic model field with the regional values, obtained by the Gram-Schmidt synthesis, the latter values have been superimposed as a series of figure 1's. The figure 2's are values of the actual observed Bouguer anomalies, where they are available. (The centres of the figures indicate the position of the data values).

Thus, we have diagrams indicating the isostatic crustal structure, for different standard crustal thicknesses, and a comparison of the calculated model anomalies with the observed anomalies.

4.2.3.1 *Line 650000 North (Figure 4.8)*

This line is the southernmost of the calculated profiles and lies just north of the southern edge of the exposed landmass of Tasmania. There is a marked discrepancy between the model anomalies, for both the 30 kms and 35 kms standard crusts, and the observed anomalies.

There are several possible reasons for this poor correlation. Firstly, the extent of the granitic bodies, in the south-west, may be greater than appears to be the case

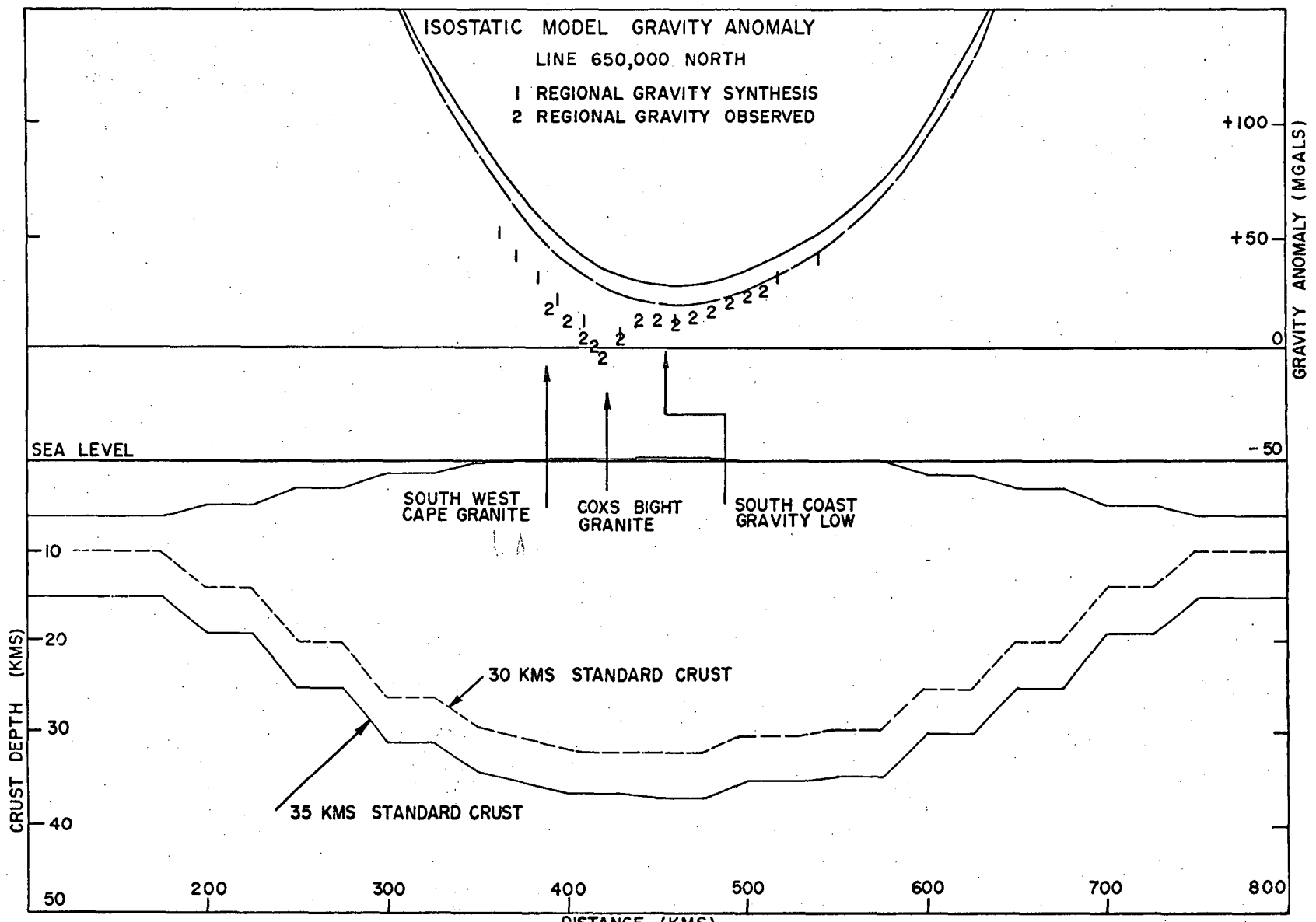
ISOSTATIC MODEL GRAVITY ANOMALY
LINE 650,000 NORTH
1 REGIONAL GRAVITY SYNTHESIS
2 REGIONAL GRAVITY OBSERVED
+100
+50
0
-50
GRAVITY ANOMALY (MGALS)
SEA LEVEL
SOUTH WEST CAPE GRANITE
COXS BIGHT GRANITE
SOUTH COAST GRAVITY LOW
10
20
30
40
CRUST DEPTH (KMS)
30 KMS STANDARD CRUST
35 KMS STANDARD CRUST
50
200
300
400
500
600
700
800
DISTANCE (KMS)

FIGURE 4·8

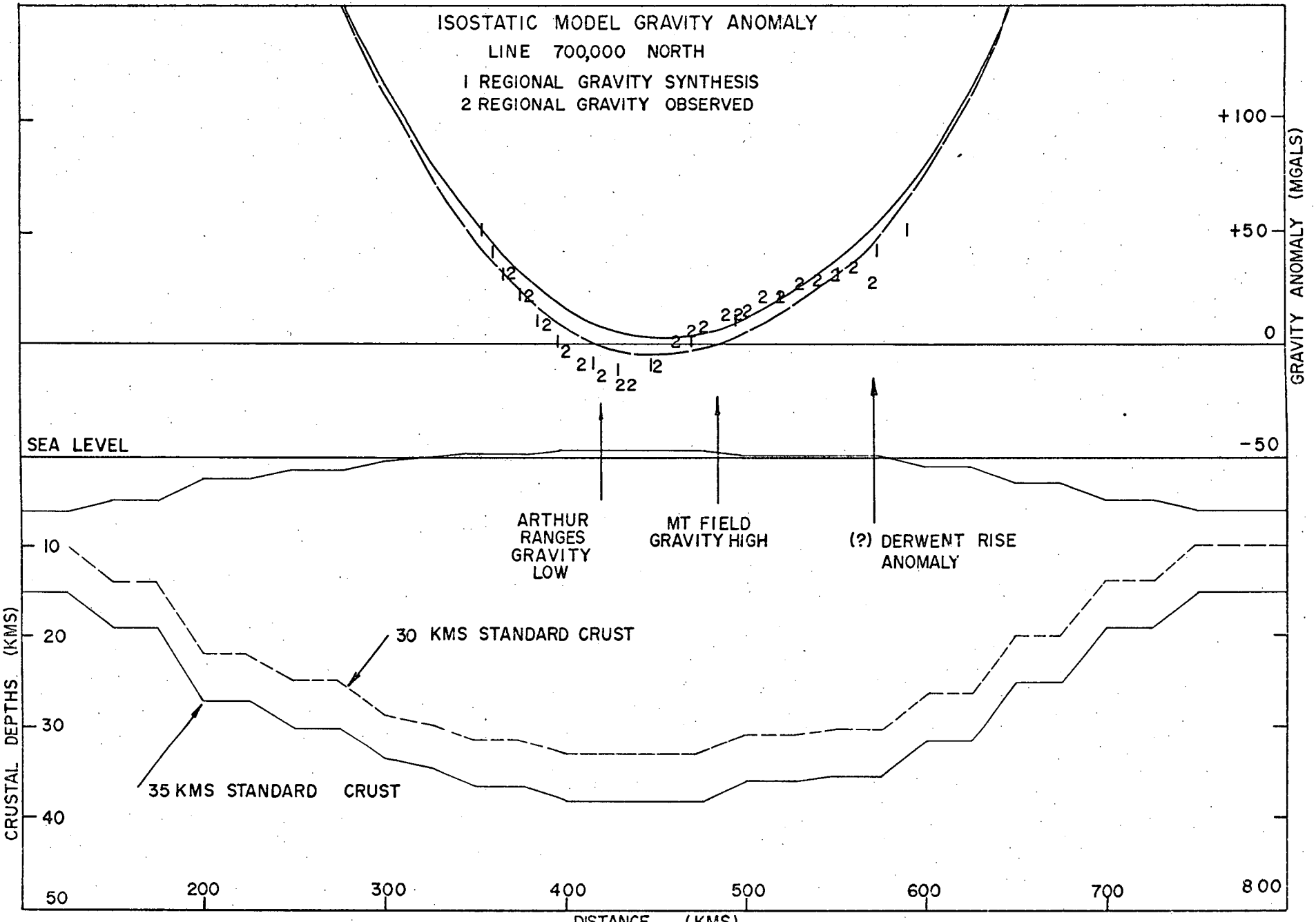
ISOSTATIC MODEL GRAVITY ANOMALY
LINE 700,000 NORTH
1 REGIONAL GRAVITY SYNTHESIS
2 REGIONAL GRAVITY OBSERVED
+100
+50
0
-50
GRAVITY ANOMALY (MGALS)
SEA LEVEL
ARTHUR RANGES GRAVITY LOW
MT FIELD GRAVITY HIGH
(?) DERWENT RISE ANOMALY
10
20
30
40
50
CRUSTAL DEPTHS (KMS)
30 KMS STANDARD CRUST
35 KMS STANDARD CRUST
200
300
400
500
600
700
800
DISTANCE (KMS)

FIGURE 4·9

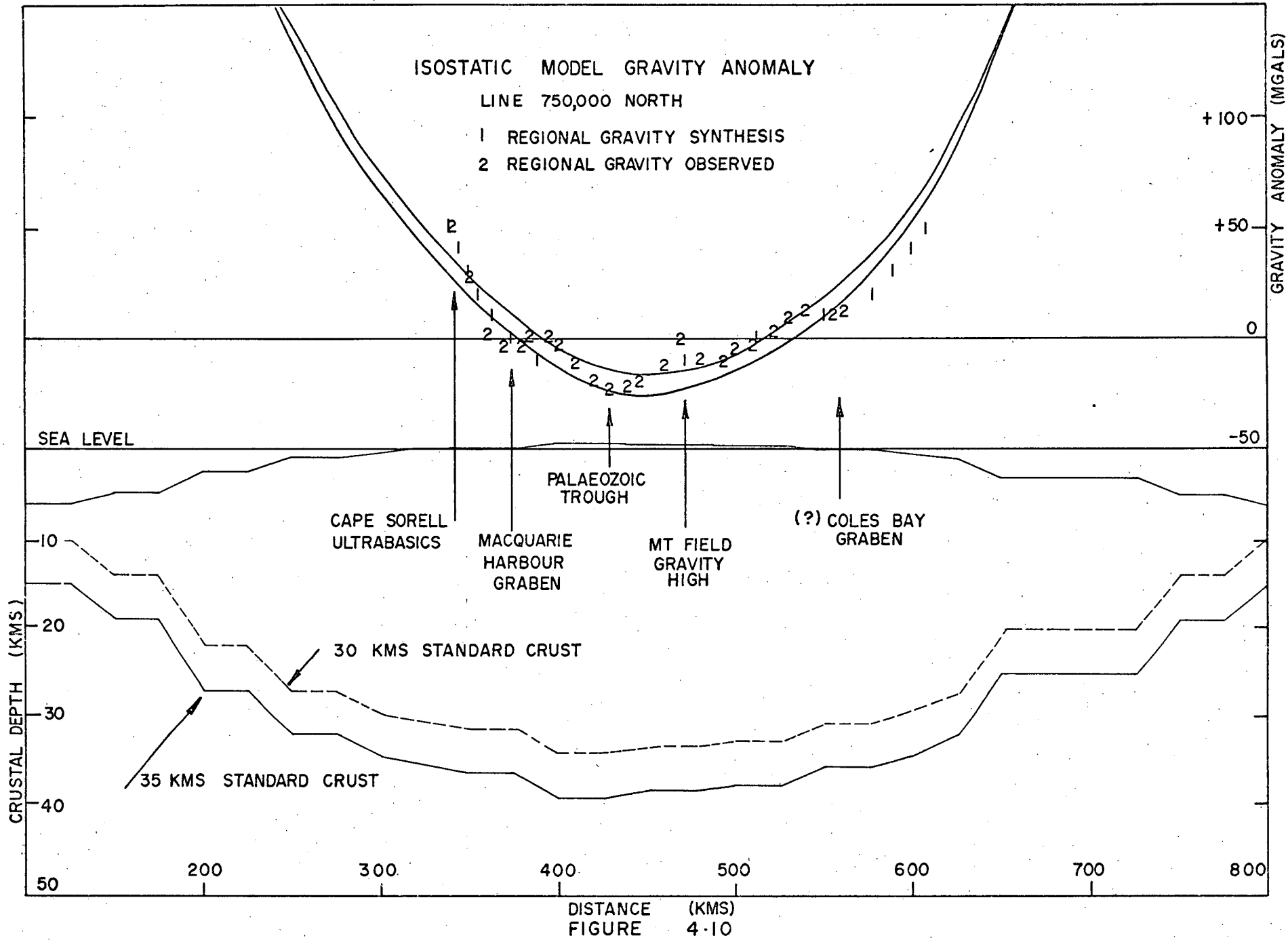
ISOSTATIC MODEL GRAVITY ANOMALY
LINE 750,000 NORTH
1 REGIONAL GRAVITY SYNTHESIS
2 REGIONAL GRAVITY OBSERVED
+100
+50
0
-50
GRAVITY ANOMALY (MGALS)
SEA LEVEL
CAPE SORELL ULTRABASICS
MACQUARIE HARBOUR GRABEN
PALAEOZOIC TROUGH
MT FIELD GRAVITY HIGH
(?) COLES BAY GRABEN
10
20
30
40
50
CRUSTAL DEPTH (KMS)
30 KMS STANDARD CRUST
35 KMS STANDARD CRUST
200
300
400
500
600
700
800
DISTANCE (KMS)

FIGURE 4·10

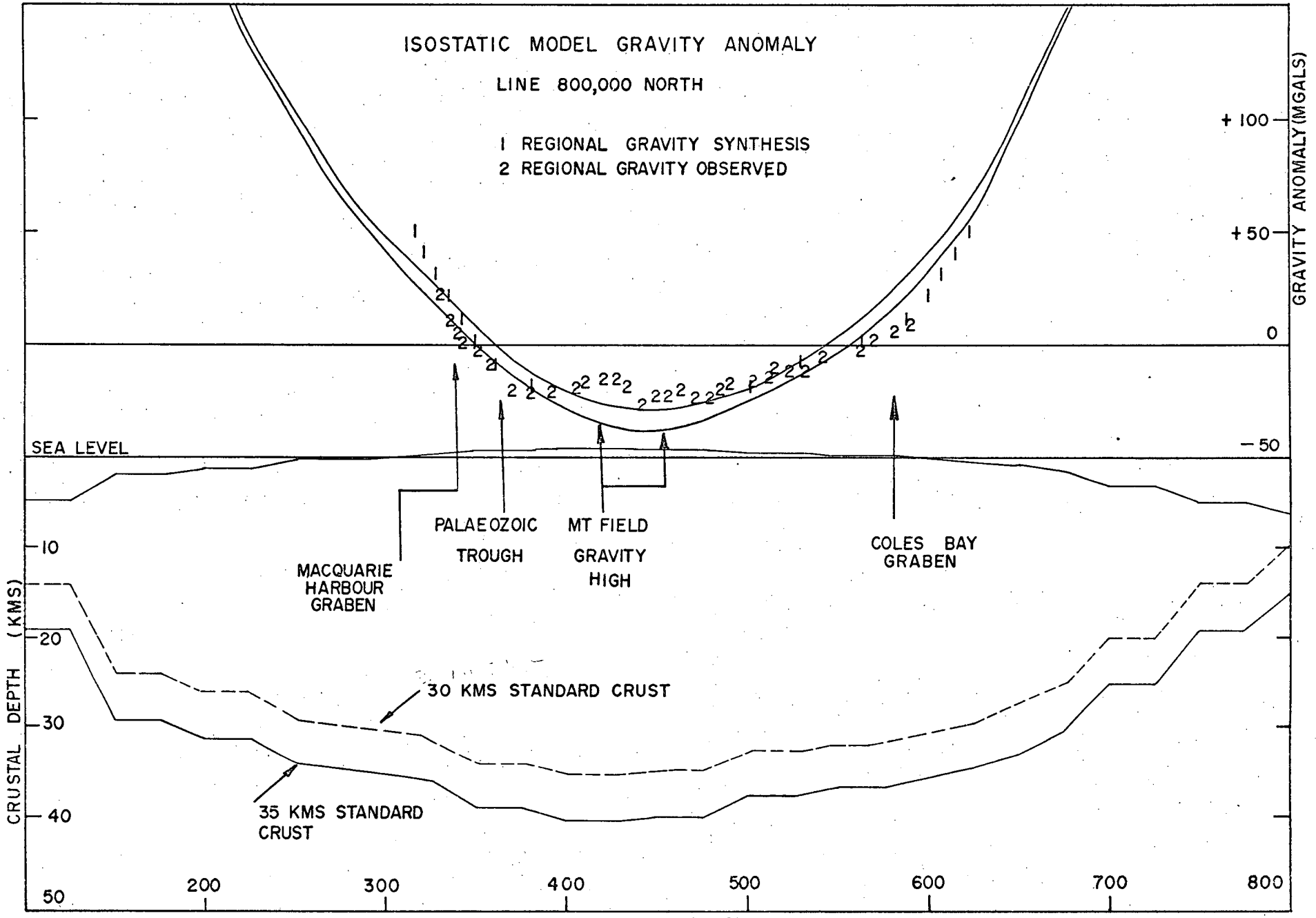
ISOSTATIC MODEL GRAVITY ANOMALY
LINE 800,000 NORTH
1 REGIONAL GRAVITY SYNTHESIS
2 REGIONAL GRAVITY OBSERVED
+100
+50
0
-50
GRAVITY ANOMALY (MGALS)
SEA LEVEL
MACQUARIE HARBOUR GRABEN
PALAEOZOIC TROUGH
MT FIELD GRAVITY HIGH
COLES BAY GRABEN
10
20
30
40
50
CRUSTAL DEPTH (KMS)
30 KMS STANDARD CRUST
35 KMS STANDARD CRUST
200
300
400
500
600
700
800
DISTANCE (KMS)

FIGURE 4·11

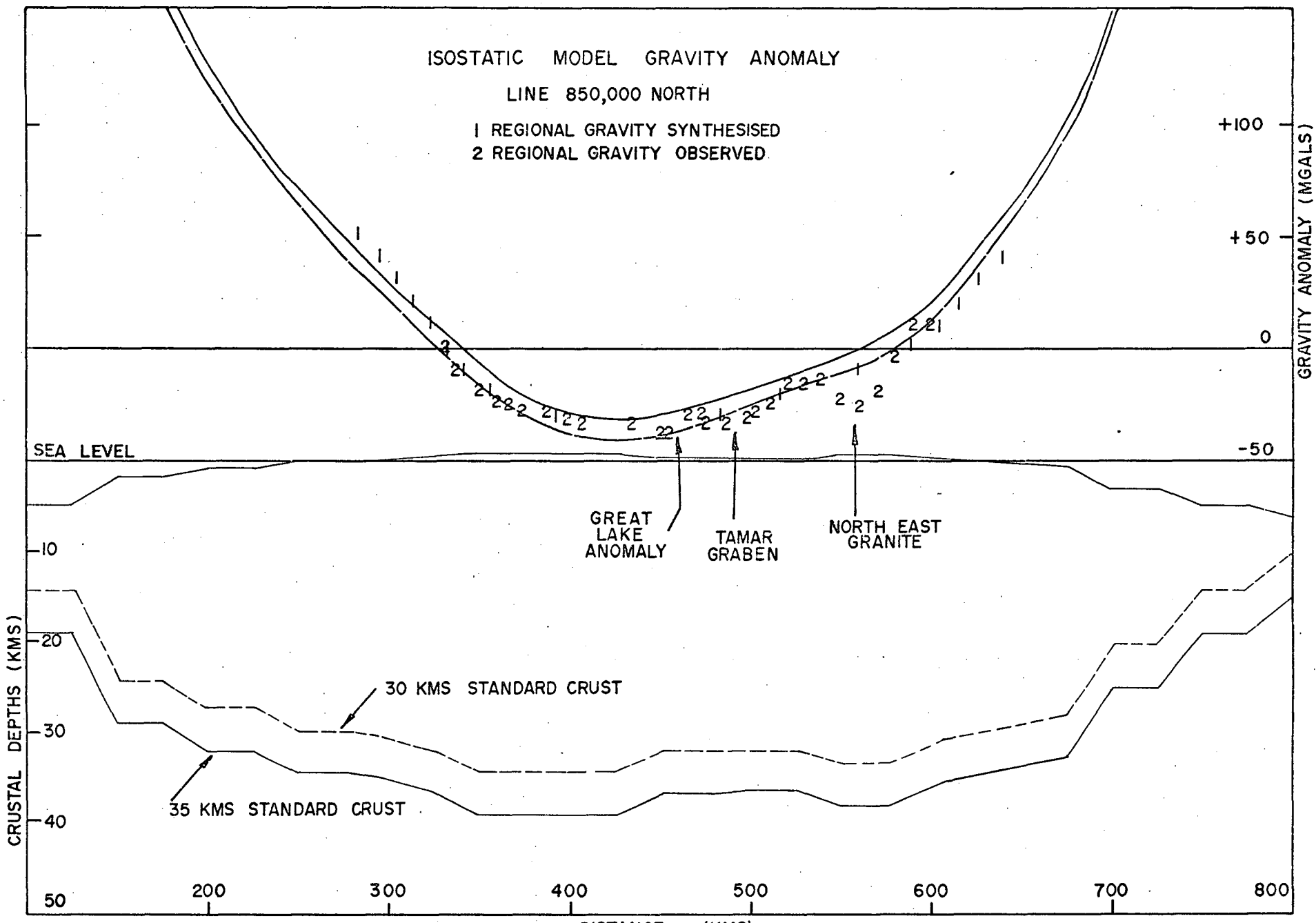
ISOSTATIC MODEL GRAVITY ANOMALY
LINE 850,000 NORTH
1 REGIONAL GRAVITY SYNTHESISED
2 REGIONAL GRAVITY OBSERVED
+100
+50
0
-50
GRAVITY ANOMALY (MGALS)
SEA LEVEL
GREAT LAKE ANOMALY
TAMAR GRABEN
NORTH EAST GRANITE
10
20
30
40
50
CRUSTAL DEPTHS (KMS)
30 KMS STANDARD CRUST
35 KMS STANDARD CRUST
200
300
400
500
600
700
800
DISTANCE (KMS)

FIGURE 4·12

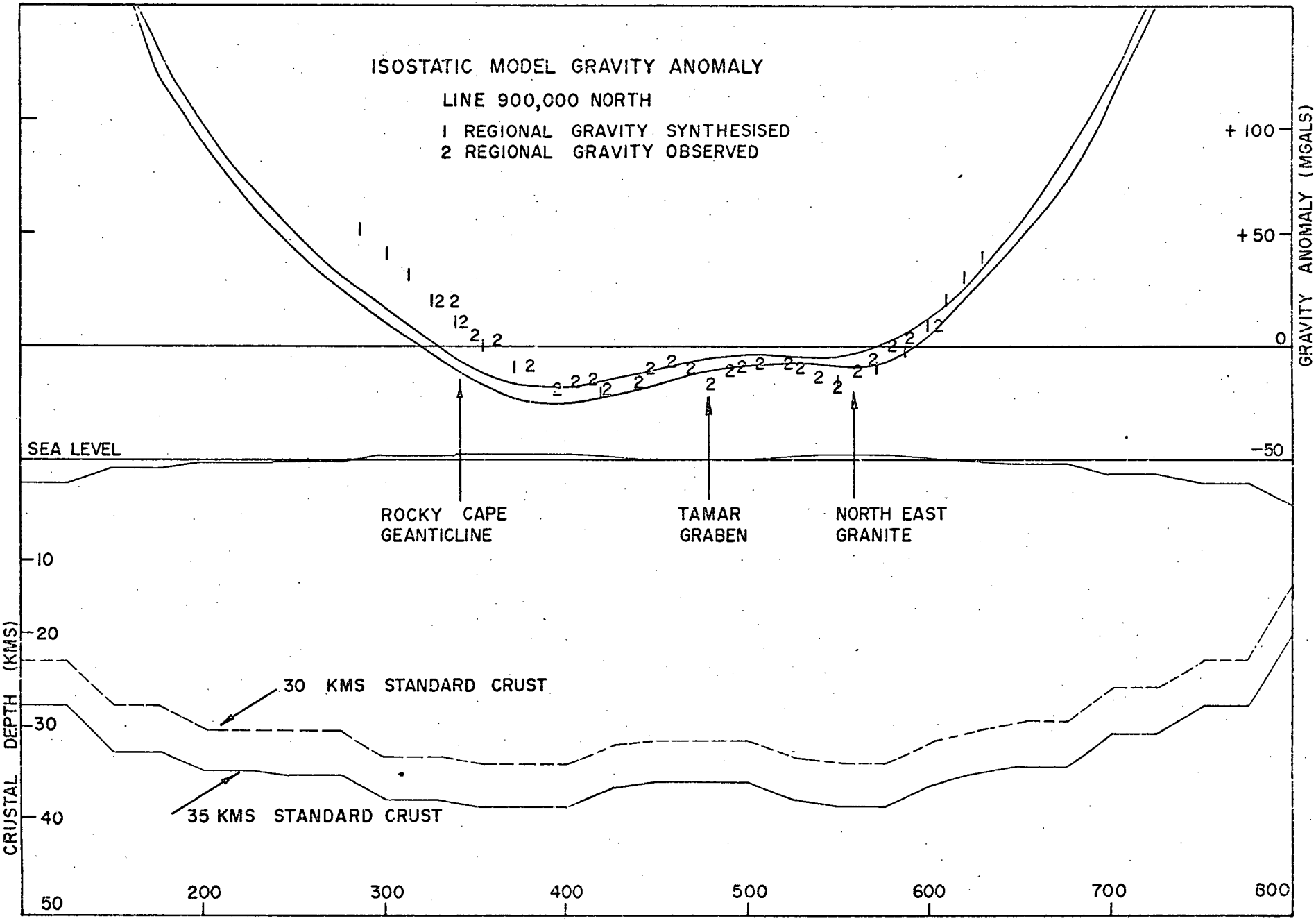
ISOSTATIC MODEL GRAVITY ANOMALY
LINE 900,000 NORTH
1 REGIONAL GRAVITY SYNTHESISED
2 REGIONAL GRAVITY OBSERVED
+100
+50
0
-50
GRAVITY ANOMALY (MGALS)
SEA LEVEL
ROCKY CAPE GEANTICLINE
TAMAR GRABEN
NORTH EAST GRANITE
10
20
30
40
50
CRUSTAL DEPTH (KMS)
30 KMS STANDARD CRUST
35 KMS STANDARD CRUST
200
300
400
500
600
700
800
DISTANCE (KMS)

FIGURE 4·13

from examining the Bouguer anomaly map. Secondly, the model may be inadequate, in the sense that there are rapid topographic variations which are not sufficiently defined by the relatively few blocks. Thirdly, the actual model may be incorrect, in that no account has been made of the apparent spreading of the base of the crust, as in the Vening Meinesz isostatic model (Heiskanan and Vening Meinesz, 1958, p.137).

4.2.3.2 *Line 700000 North (Figure 4.9)*

The next line to the north shows much the same effects as the anomaly calculated for the south coast. A large negative anomaly can be seen in the vicinity of the Arthur Ranges. It is possible that this is related to the South Coast Anomaly and/or a previously unidentified area of unusually low density rocks.

The southernmost portion of the Mt. field gravity high can be identified as part of a broad positive anomaly. To the east the observed Bouguer anomalies have a remarkably low value. The east coast is morphologically unusual in this region with drowned river estuaries close to a very steep continental slope. At the base of the slope there is a swell composed of sediments which are ponded by probably volcanic rocks. This has been termed variously the Derwent Rise or the East Tasmania Rise. This feature may give rise to the low gravity values observed in the Freycinet Peninsula.

4.2.3.3 *Line 750000 North (Figure 4.10)*

This line extends from Pt. Hibbs to Maria Island. In the west there is an observed positive anomaly corresponding to the Cape Sorell ultrabasics. Immediately to the east of these there is a narrow negative anomaly due to the Macquarie Harbour graben. The most negative part of the observed Bouguer anomaly corresponds with an area of relatively light Palaeozoic rocks (K.D. Corbett, pers. comm.). To the east of this is the Mt. Field Gravity High. The easternmost part of the gravity data is rather lower than the model isostatic anomaly and this may correlate with the Coles Bay Graben.

4.2.3.4 *Line 800000 North (Figure 4.11)*

This line is similar to the previous line in that the Palaeozoic Trough, the Mt. Field Gravity High and the Coles Bay Graben anomalies can all be identified. The Mt. Field High is now much more complex may be composed of two or three parallel sections.

4.2.3.5 *Line 850000 North (Figure 4.12)*

This line crosses the centre of the Central Plateau region and corresponds to the position of deepest crust. The northernmost tip of the Great Lake Anomaly High and the Tamar Graben Low can be seen. To the east there is the North East Granite anomaly showing clearly that this granite body is large and that the anomaly is not due to compensation of the high mountainous region in the northeast.

4.2.3.6 *Line 900000 North (Figure 4.13)*

This is the northernmost line considered in this comparison. The western part of the observed data is unavailable and hence the predicted values obtained by the Gram Schmidt analysis should be treated with great caution. However where there is data it appears to be much more positive than would be expected. This may correlate with the Rocky Cape Geanticline, a large structural feature separating the far northwest part of the state from the remainder of the state. The Tamar graben and the Northeast Granite may also be identified on this profile.

4.2.3.7 *General Comments on interpretation of isostatic model profiles*

It appears that the model of the crust used in this isostatic calculation bears a close resemblance to the true nature of the crust.

The disappointing feature of these comparisons is that it is not clear whether 30 kms or 35 kms should be used for the thickness of the standard crust. The exception to this is that Figures 4.10 and 4.11 give positive and negative residual anomalies which correspond better with known geology when using the 35 kms standard crust model.

It is also apparent that the Gram-Schmidt analysis of the gravity data has incorporated some of the near surface geological variations. For example, in the far southwest the

synthesis has been distorted by the granite anomalies. However, in general, the correspondence between the isostatic model anomalies and the regional gravity values is good.

CHAPTER FIVE

ANALYSIS OF BASS STRAIT UPPER MANTLE CRUSTAL REFRACTION EXPERIMENT

5.1 THE BASS STRAIT UPPER MANTLE PROJECT (BUMP)

A seismic refraction study of the crust and upper mantle in the Bass Strait region was undertaken by the Geophysics Group of the Australian Institute of Physics. A detailed report was prepared by C. Kerr Grant entitled "The Bass Strait Upper Mantle Project, Data and First Arrival Interpretation". This report remains unpublished but is on file available through the Australian Institute of Physics. A much briefer account of the project was prepared by R. Underwood, on behalf of the Bass Strait Upper Mantle Project Committee (Underwood, 1969). This paper contains the shot point locations and fixing times, the receiving station locations, the distances between shots and locations and the first arrival times. Figure 1 of this paper is reproduced here as Figure 5.1 showing the location of the shots and stations.

The discussion in the following section is restricted to the analysis that I have carried out on the data. My contribution to the project was to collate and check all the data obtained in Tasmania.

5.2 TIME TERM ANALYSIS OF BUMP DATA

5.2.1 The time term method

The time term analysis method of interpreting crustal refraction data (Scheidegger and Willmore, 1967) has been applied to the analysis of large scale experiments (e.g.

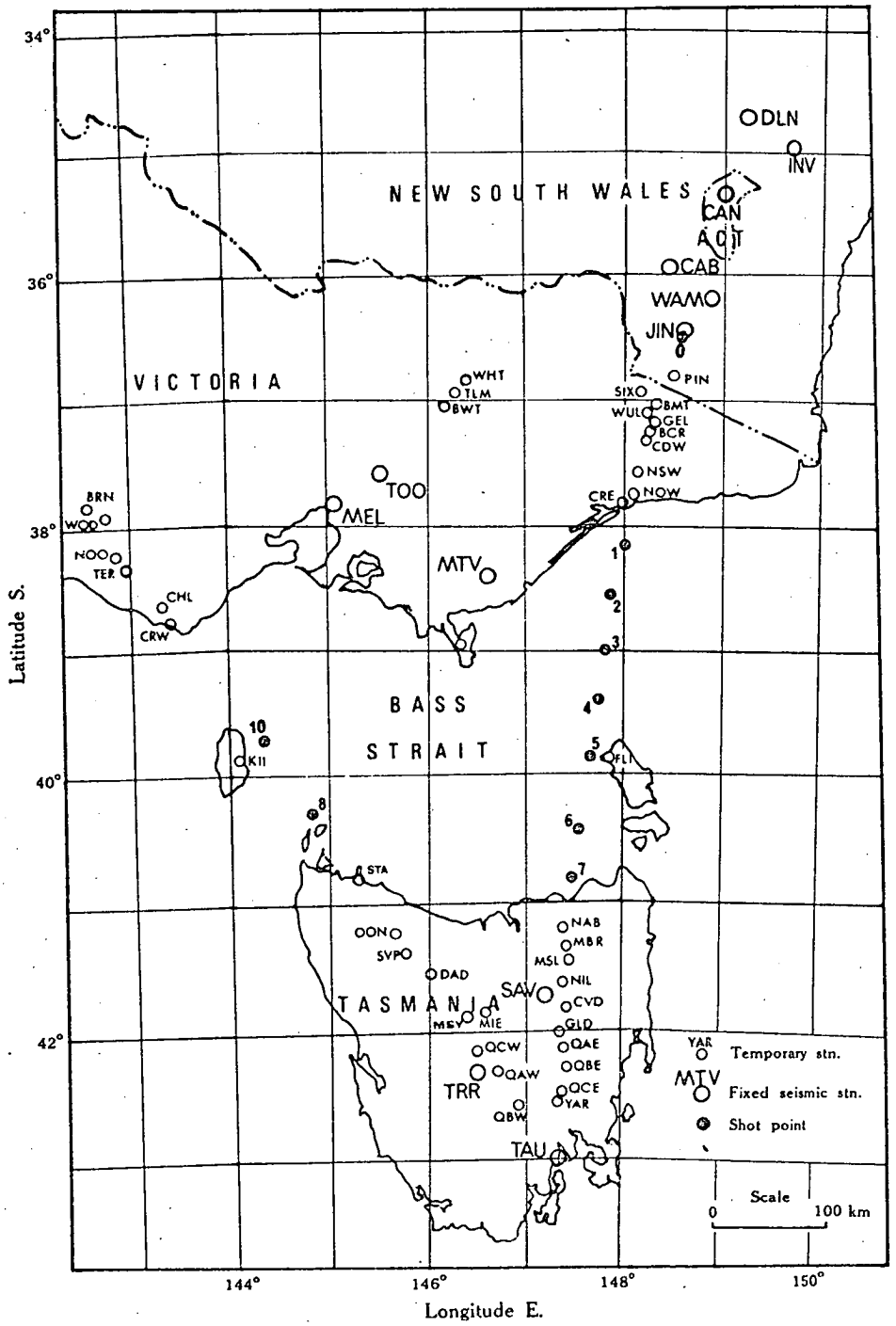

Fig. 5.1—Locations of shots and stations.

the Lake Superior experiment; (Smith, Steinhart and Aldrich, 1966). The same approach has been applied to the analysis of the BUMP data.

The technique is based on the separation of the travel time into three terms, the first two of which are functions of the shot and station and the third of the path between the shot and station. Thus the travel time, T_{ij}, is the sum of the time terms a_i (shot point), a_j (station) and Δ_{ij}/V where Δ_{ij} is the distance between shot i and station j and V is the refractor velocity. This if there are a number of shots and stations then there are a number of equations of the form

$$T_{ij} = a_i + a_j + \Delta_{ij}/V$$

If there are sufficient observations then this results in an overdetermined system. The equations may then be solved by standard least squares techniques.

The full set of equations is linearly dependant and therefore one complete set of observations must be removed before proceeding with the least squares procedure. This is normally overcome by reversing one of the shots, i.e. one of the shot points is replaced by a station after the shot has been fired.

In the case of the BUMP data, there is no exact reversal. The shot at Lake Jindabyne was received at only a few stations and these were not far enough away to receive mantle refractions.

The result of this non-reversal is that the time terms a_i and a_j are not related. An arbitrary constant, α, must be chosen to be added to the a_i's and subtracted from the a_j's or vice versa.

The method of choosing the constant α employed is to adjust the time terms such that the structure is most nearly constant.

5.2.2 Calculation of crustal thickness

In order that the thickness of the crust may be calculated from the time terms the velocity of the intermediate layers must be considered. Following Steinhart and Meyer (1961) the time term for the (n + 1)th layer may be written.

$$a_{n+1} = \sum_{k=i}^{n} h_k \left(\frac{1}{\bar{V}_k^2} - \frac{1}{\bar{V}_{n+1}^2} \right)^{\frac{1}{2}}$$

where h_k and V_k are the thickness and velocity of the kth layer.

Expanding this in terms of a Taylor series (Smith, Steinhart and Aldrich, 1966) the total depth to the n^{th} refracting layer may be obtained by the relation.

$$H_n = \frac{a\bar{V} V_{n+1}}{\left(V_{n+1}^2 - \bar{V}^2 \right)^{\frac{1}{2}}}$$

where $\overline{V}$ is the weighted mean velocity above the refractor.

Hence it can be seen that a formulation for converting time terms into crustal thickness is obtained that is not particularly sensitive to lower crustal velocities. This latter point is particularly important in this region as we have only indications of higher velocities in the lower crust from scattered second arrivals.

5.2.3 Results of the analysis

The time terms obtained from the analysis and adjusted to give a relatively smooth structure are plotted in Figure 5.2. The time terms are plotted against the distance from station YAR which recorded both the eastern and western lines. The time term scales are given on the left end of the graphs while on the right are the crustal depths based on a mantle velocity of 8.0 kms/sec and a mean crustal velocity of 6.0 kms/sec.

The time terms in Bass Strait are very interesting in that they are considerably lower than for Tasmania or Victoria indicating a considerable amount of crustal thinning. The calculated crustal thickness for Bass Strait is 20-25 kms while the thicknesses of Tasmania and Victoria are 30-35 kms. The northern end of the Eastern Line indicates crustal thicknesses of the order of 45 kms, supporting the earlier work in this region (Doyle, Everingham and Hogan, 1959; Doyle, Underwood and Polak, 1966).

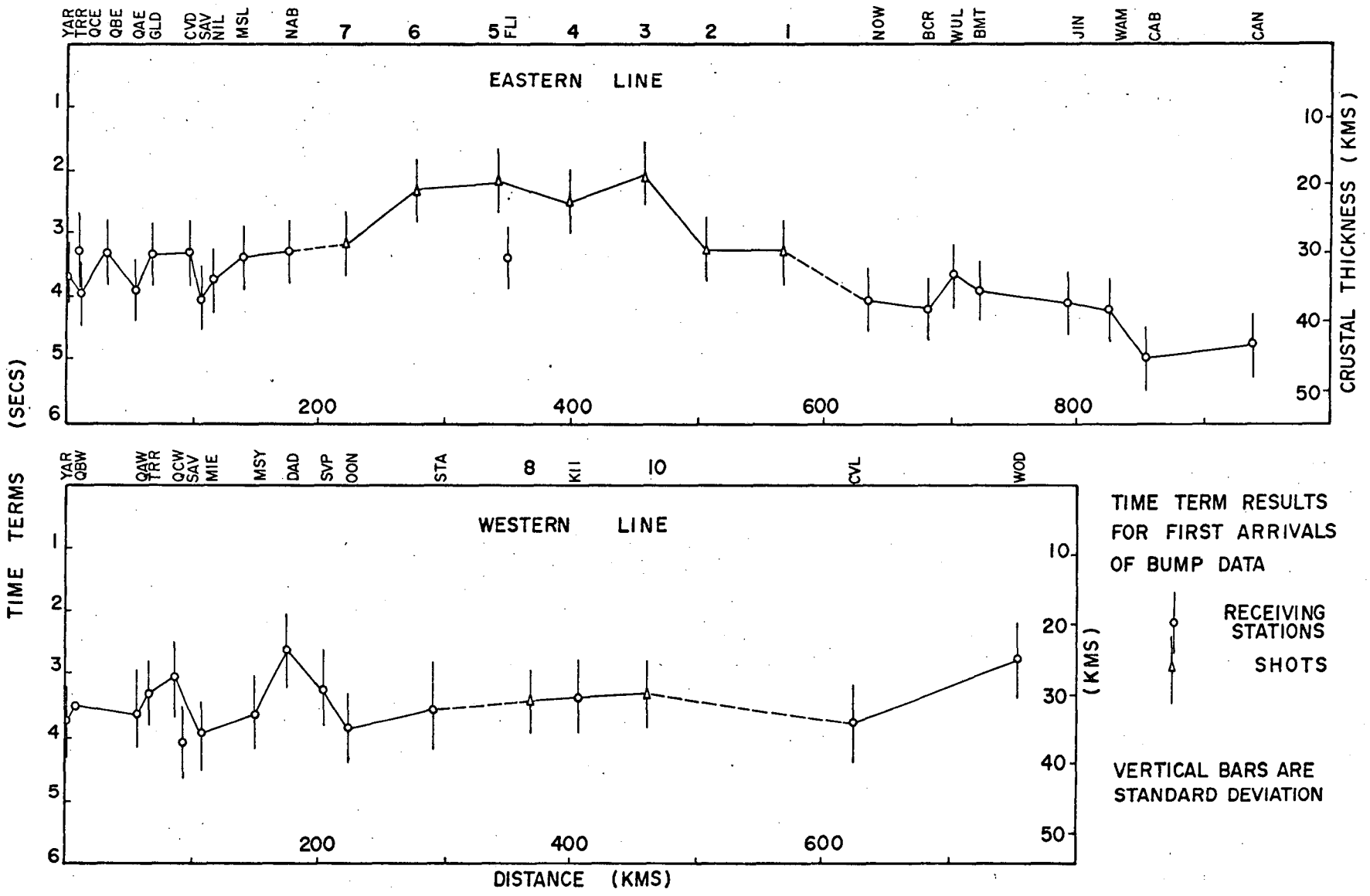
YAR
TRR
QCE
QBE
QAE
GLD
CVD
SAV
NIL
MSL
NAB
7
6
5
FLI
4
3
2
1
NOW
BCR
WUL
BMT
JIN
WAM
CAB
CAN
EASTERN LINE
TIME TERMS (SECS)
CRUSTAL THICKNESS (KMS)
200
400
600
800
YAR
QBW
QAW
TRR
QCW
SAV
MIE
MSY
DAD
SVP
OON
STA
8
KII
10
CVL
WOD
WESTERN LINE
(KMS)
DISTANCE (KMS)
TIME TERM RESULTS
FOR FIRST ARRIVALS
OF BUMP DATA
RECEIVING
STATIONS
SHOTS
VERTICAL BARS ARE
STANDARD DEVIATION

FIGURE 5·2

There remain some problems in this interpretation; for example, on the eastern line the time terms for shot 5 and station FLI are very different, while on the western line the time terms for shot 10 and station KIJ are very similar. One would expect a closer correspondence but the time term solution is necessarily limited to mantle first arrivals.

5.2.4 General comments on the BUMP results

The BUMP results are not good in that there was no complete reversal obtained. The arrivals for the western line are limited by the fact that only two shots were fired before weather terminated the experiment.

It would appear necessary to attempt to repeat the eastern line with an exact reversal. Many of the observation points can be reoccupied and this would enable much needed control on such experiments.

Once such a control line has been established then other experiments can be interpreted. At least one receiving station must be common to both experiments before the two sets of time terms may be related.

CHAPTER SIX

SPECTRAL ANALYSIS OF AEROMAGNETIC PROFILES

6.0 SPECTRAL ANALYSIS OF AEROMAGNETIC PROFILES

This section describes an attempt to obtain information on the structure of the deeper layers of the crust from an examination of the spectral characteristics of aeromagnetic profiles. The work is incomplete at this stage; it has however progressed sufficiently to warrant reporting.

6.1 PREVIOUS WORK

In the last decade there has been a complete revolution in the approach to the analysis of geophysical data. Prior to this period, the development of communications theory applied to geophysical data had been largely restricted to seismic reflection techniques. At the present time, the impact of new methods of data enhancement using filtering techniques can be observed in all geophysical applications. One of the earliest descriptions of geophysical data processing techniques in terms of filter operations is that of Dean (1958).

The earlier work on depth estimation from aeromagnetic profiles was based on statistical techniques (e.g. Serson and Hannaford, 1957; Alldredge, et al, 1963; Horton, et al, 1964; Whitham, 1965). It became evident that anomalies observed in an aeromagnetic survey could be differentiated into short-wave length, near-surface anomalies and long-wave length, deeper anomalies. Bhattacharyya and Morley (1965) were able to apply filter techniques to extract the

deep-source anomalies and thence model these anomalies in terms of vertical prisms (Bhattacharyya, 1966a) whose lower surfaces were terminated by the Curie point geotherm.

The next stage in this development was to determine the spectral characteristics of the prism model (Bhattacharyya, 1966b). It was found that the dimensions and the resultant magnetisation vector of the prism could be determined from the spectrum of the field due to a prism.

The problem of extracting geophysical signals from noise had rapidly become of great importance and the work of Strakhov (1963, and many subsequent papers) on the design of optimum filters has proved to be of utmost importance. Naidu has developed the techniques further (1966) and has also investigated the spectra of randomly distributed sources (Naidu, 1967, 1968).

By this stage, it had become evident that examination of aeromagnetic data in the frequency domain was likely to provide useful information. The work of Spector (1968) which has been partially summarised in Spector and Bhattacharyya (1966) and Spector and Grant (1970), must now be classified among the keystones of recent developments in geophysical interpretation.

Spector was able to examine the general characteristics of the power spectrum due to a finite prism of varying vertical dimensions. He was thus able to derive the

following general equation describing the power spectrum of a finite body:-

$$E(u,v) = K.\ H(h)_{u,v} \cdot RT_{u,v} \cdot RM_{u,v} \cdot S(a,b,\gamma)_{u,v}$$

where K is a constant proportional to square of the magnetisation,

H(h) is a factor dependant upon the depth to the upper surface of the body (h),

RM and RT are factors related to the direction of the Earth's magnetic field and the resultant direction of magnetisation, and

$S(a,b,\gamma)$ is a "form factor" related to the horizontal dimensions (a,b) and the orientation (γ) of the body.

Spector then introduced the concept of an ensemble of prism models to represent the geological situation. There are however definite limitations to the ensemble model chosen, an example of which is given by Gudmundsson (1971).

One major difference between the Spector approach and that described in the next section is that he has been able to assume that the data has been sufficiently sampled in both directions. It has yet to be shown that across flighline aliasing is not important in the type of data that Spector was analysing. In the following analysis the data is treated as separate lines in order to determine the amount of information that can be derived from single profiles. The

work of Spector was not available during the development of the techniques outlined in the next section.

6.2 THE DEPTH DETERMINATION TECHNIQUE

6.2.1 The upward continuation filter

The amplitude spectra of aeromagnetic profiles show a characteristic exponential decrease in amplitude with increasing frequency. This is a direct result of measuring the field at some distance removed from the source. This effect is an upward continuation filter, the distortion of the spectra being a function of the distance of continuation.

The frequency response function, R(s), of upward continuation has long been known (Dean, 1958) and may be written.

$$R(s) = e^{-2\pi.h.|S|}$$

where h is the amount of continuation (upward) and S is the frequency (cycles/unit length)

Also, the frequency may be defined in terms of wavenumber.

$$S = \frac{k}{L}$$

where k is the wavenumber, L is the data length.

By taking logarithms of both sides, of the frequency response function, we obtain

$$\log_{10}R(s) = \left[\frac{-h.2\pi.\log_{10}e}{L}\right] k$$

Hence, by plotting the logarithm of the frequency response function against the wavenumber, we obtain a straight line whose gradient, g, is given by

$$g = -\left(\frac{\log_{10} e.2\pi}{L}\right)h$$

Thus we may obtain a relationship between the distance of continuation, h, and the gradient of the response function when plotted on a semi-logarithmic scale.

$$h = -g\left(\frac{L}{2\pi \log_{10} e}\right)$$

where h is in the same units as L.

Since the upward continuation response function may be thought of as a filter in a linear system, it is possible to predict the spectrum of the field at one height knowing the spectrum of the field at another height and the height difference.

6.2.2 The source spectrum

Up to this stage, we have only been able to say what happens to the spectrum due to the process of continuation. There remains the problem of the spectrum that would be obtained for a geologically reasonable body or group of bodies.

The simplest approach is to assume that the spectrum at the source is "white", i.e. contains all frequences at

the same power. Some justification for this assumption is given by Bhattacharyya (1967), in a review of space and frequency domain properties of potential fields, in which he states from theoretical considerations:

> *"the amplitudes of different frequencies, synthesising a potential field signal, are limited by an upper bound given by a fixed constant multiplied by exp (-hs), where h is the depth to the top of the source, and s, the frequency".*

The model therefore chosen results in this upper bound condition. The work of Spector indicates that this is also the spectrum produced by his ensemble of bottomless prisms of relatively small areal extent.

6.2.3 Limitations of the spectra of profiles

6.2.3.1 *The finite length of the data*

Following the work of Spector, it can be shown that the finite length of the profile imposes a restraint on the calculated amplitude spectrum. The data may be thought of as a sample subset of the complete field. The sample function is such that it has a value of zero outside the data area and unity within the data area (the box-car function).

Thus if we let f(x) be the complete field function along the profile and g(x) the box-car sample function then h(x), the resultant data set is obtained by the following expression.

$$h(x) = f(x) \times g(x)$$

This may also be expressed in terms of the frequency domain, where the multiplication operator becomes a convolution and capitals are used to denote Fourier Transform equivalents.

$$H(s) = F(s) \ast G(s)$$

Since the Fourier Transform of the box-car function is an expression of the form sin kS/kS then it becomes apparent that this is a process of smoothing the spectrum F(s) to obtain H(s). It is common practice to use some other sample function (or data window) the most popular of which is the Hanning window: (Blackman and Tuckey, 1958).

$$g_H(x) = \tfrac{1}{2}\left[1 + \cos\frac{2\pi x}{L}\right] \qquad |x| \leq \frac{L}{2}$$

$$= 0 \qquad |x| > \frac{L}{2}$$

the advantage being that the Fourier Transform is much better behaved.

The result of this spectral smoothing due to the finite length of the data is that the information pertaining to the deepest sources (and thus having very long wavelengths) is not retained. There is thus a practical limit to the deepest source layers that are attributable to characteristics of the spectrum. Spector's estimate of this upper limit is that sources deeper than L/4, where L is the length of the data, cannot be determined; there seems to be no reason for this to be modified.

6.2.3.2 *The sampling interval of the data*

The sampling interval of the data, Δx, should be such that there is no signal at or above the Nyguist frequency $1/2\Delta x$. This can be shown to be the case if the amplitudes of highest frequencies do not decrease with increasing frequency but maintain a more or less constant level. This constant amplitude portion of the spectrum is due to random effects in the data such as digital round-off. If signal energy is present above the Nyguist limit aliasing will occur resulting in general, in a spectrum with a lower rate of decay.

6.2.3.3 *The Geomagnetic Field Variation*

From an analysis of an aeromagnetic profile around the world (Alldredge, et al, 1963) it has been shown that the sources of magnetic anomalies lie in two regions: (a) above the Curie point geotherm and (b) within the core of the earth. Unless the geomagnetic variation (i.e. that part originating in the core) has been accurately removed from the data, then very low wavelength anomalies will still be present in the data. The magnitude of this effect can be calculated from the International Geomagnetic Reference field.

The effect of the incomplete removal of the geomagnetic field will be to add very low frequency components to the spectrum. The extent of the spectral distortion should be ascertained and those frequencies ignored. This may thus

impose a further restriction on the ability to detect deep magnetic sources.

6.2.3.4 *The digitising round-off level*

The accuracy of the data is restricted in several different ways.

1. The accuracy of the measuring device
2. The accuracy of positioning, and
3. The size of the minimum variation, giving a change in value.

The first two effects are unpredictable, but are likely to cause only minor effects, probably restricted to low frequency components. The last effect, commonly termed round-off, has the effect of introducing a random noise component to the data. This in turn superimposes a white spectrum on the signal spectrum.

6.2.3.5 *Estimation of depths from profiles*

The depth estimations made by the method outlined in # 6.2.1 have assumed that the relationship between two dimensional spectra at different elevations is the same as that of one dimensional spectra. This assumption requires examination before proceeding further.

The relationship between the spectrum H_1, at elevation h_1, and the spectrum H_2 at h_2, may be written

$$H_1 = H_2 e^{-2\pi s(h_1 - h_2)} \quad \text{where } s^2 = u^2 + v^2$$

Taking logarithms we obtain

$$\log H_1 = \log H_2 - 2\pi s(h_1 - h_2)$$

The continuation distance $(h_1 - h_2)$ is estimated from the gradient of the spectra. Thus in the two dimensional case we have

$$\frac{d}{ds}(\log H_1) = \frac{d}{ds}(\log H_2) - 2\pi(h_1 - h_2)$$

whereas in the one dimensional case we have

$$\frac{d}{du}(\log H_1) = \frac{d}{du}(\log H_2) - 2\pi(h_1 - h_2)\frac{ds}{du}$$

$$\frac{d}{du}(\log H_2) - 2\pi(h_1 - h_2)\frac{u}{S}$$

Providing that the source spectrum H_2 is white, then the only difference between the above expressions is the factor u/s, which is generally less than 1.

The ratio u/s will only be exactly equal to 1 in the case where the magnetic field is linear in the across profile direction thus giving rise to a spectrum that is confined to the v = 0 axis. This type of magnetic anomaly spectrum is observable in the sea floor spreading anomalies which are essentially the same for large distances parallel to strike. The alternate case where the spectrum is confined to u = 0 is trivial as the profile would then be along strike and resulting in no anomalies.

In the case where the spectrum is uniformly distributed the ratio u/s is of the order of $1/\sqrt{2}$. Depth estimations

will therefore be of the order of 70% of the true depth.

In general, therefore, the depth estimates will be too shallow by a factor ranging from 0.7 to 1.0. An examination of the spectra of two orthogonal profiles, or of the geology where known, can be made to give an estimate of the directional characteristics of the spectrum.

6.2.3.6 *Band limited source spectra*

The work of Spector has clearly indicated that the presence of a small finite number of bodies of finite thickness will tend to band limit the observed spectrum. At the higher frequencies this is due to a sin u/u.sinv/v decay due to the dimensions of single bodies (Bhattacharyya, 1966b). At the lower frequencies the amplitude is also reduced due by the finite thickness of the bodies (Spector and Grant, 1970).

The result of this band limiting is to give an over-estimate of the depth of the shallower magnetic horizons. The estimation of the depths based on the lowest frequencies will also be badly effected. The work of Spector (1968) should be referred to for more detailed considerations.

6.3 THE HIGH LEVEL AEROMAGNETIC SURVEY OF TASMANIA

During early 1966, the Bureau of Mineral Resources, Canberra, carried out a high level aeromagnetic survey of Tasmania (Finney and Shelley, 1967). The purpose of this survey was to collect data in which the anomalies due to deep crustal sources were emphasised with respect to shallow

source anomalies. Tasmania was chosen for this experimental survey, since a reasonably sized area could sample both oceanic and continental regions.

The flight lines were orientated east-west having a total length of the order of 600 kms, about half of which was over land. The flight line separation of 15 kms was based on economic reasons, enabling the whole of the state of Tasmania to be flown within the space of two months. A flight altitude of 3.3 kms above sea level was chosen to significantly reduce the amplitude of the short wavelength anomalies.

Navigation was carried out using a flight path camera (over land) and dead reckoning (over the sea). The estimated errors in positioning were ±3 kms over land to a maximum probable error of ±15 kms over the sea. The survey was flown with a DC3 aircraft fitted with a fluxgate magnetometer with both analogue and digital recording devices.

A map of the total magnetic intensity profiles with linear gradients removed is shown in Figure 6.1

6.4 DATA PREPARATION

6.4.1 Translation of data tapes

Before any spectral work could be carried out on the data the digital output had to be converted into a form suitable for the University of Tasmania's Elliott 503 Computer.

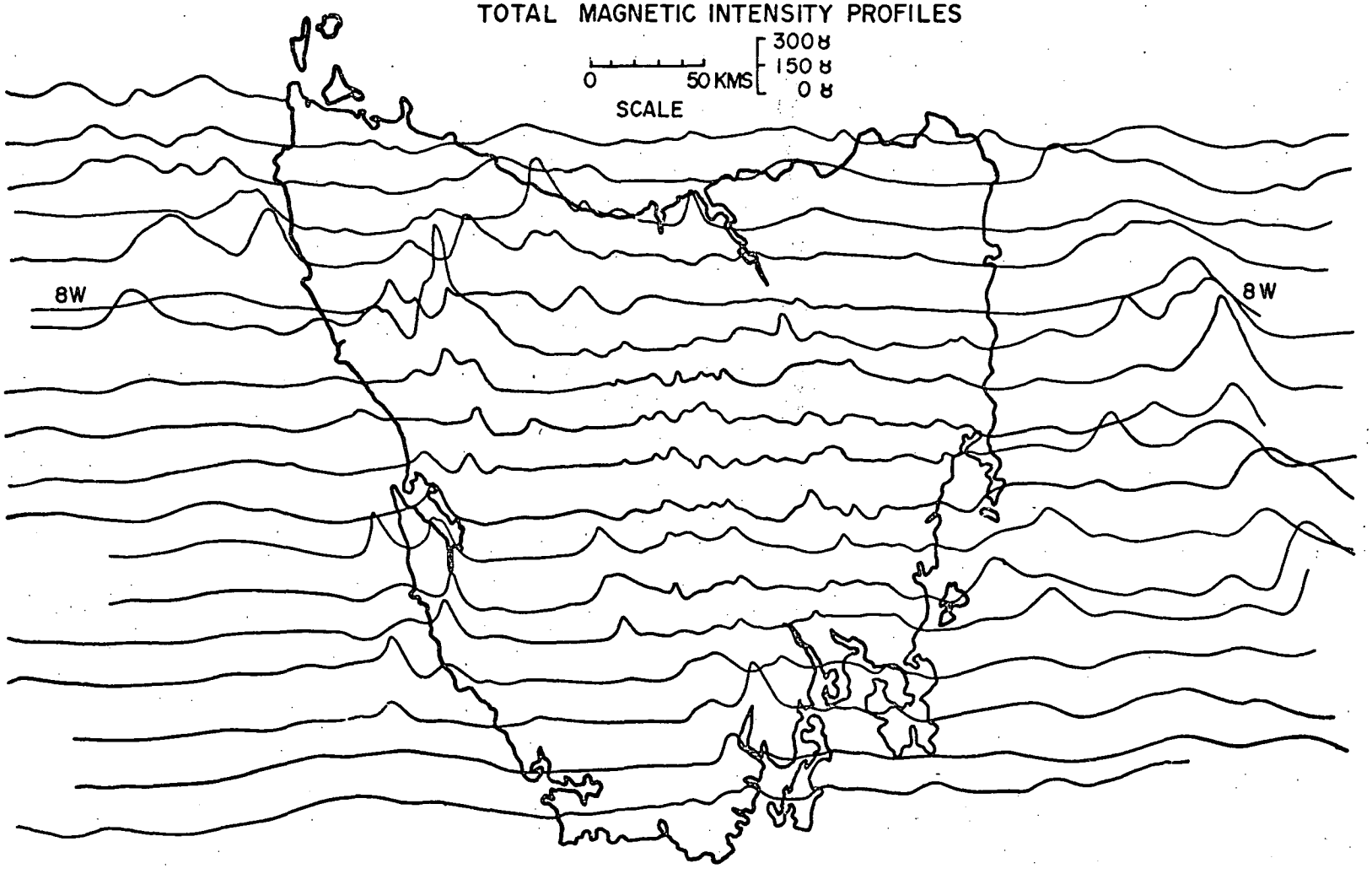
TOTAL MAGNETIC INTENSITY PROFILES
300 γ
150 γ
0 γ
0
50 KMS
SCALE
8W
8W

FIGURE 6·1

The digital code in the magnetometer output device is that of the now-retired Silliac computer (University of Sydney). Five channel paper tape is used, the fifth channel of which is used for fiducial marks.

It was found necessary to test for miss-punching in the tapes. This was carried out by checking the number of characters punched between fiducial marks. An acceptance test was also applied to the values, each reading being tested to see if it lay within prescribed limits of a linear prediction based on the previous two values.

Tapes were finally punched containing the corrected magnetic field value in gammas together with fiducial marks.

6.4.2 Preliminary smoothing of the data

Since the majority of the flight lines were flown in at least two sections, due to weather conditions, the data had to be combined to form continuous profiles.

The overlapping portions of each flight line were plotted and overlain. A point was then chosen to transfer from one section to the next.

In order to band limit the data, and thus to reduce the number of points required, a low-pass convolution filter was designed (Johnson, 1971). A modification of the ideal low-pass filter, the sin x/x function (Bracewell, 1965, p.52), was made in which the Gibbs oscillations, due to the finite length of the filter, were reduced by a process of σ smoothing (Lanczos, 1957, p.267).

The cut off frequency of the filter is defined in terms of the width of the main lobe of the filter. If M is the number of points between the centre of the filter and the first zero, then the frequency cut off is at 1/2M cycles/data interval. If there are N points in the unfiltered data set then only N/M points are required to specify the filtered data. To reduce computation time therefore, the convolution filter is applied at intervals of M data points along the profiles.

6.4.3 Data files

All flight lines of the aeromagnetic survey of Tasmania have been corrected, combined and filtered. Punched paper tapes of the unsmoothed and smoothed data are held in the Geology Department, University of Tasmania.

6.5 DEPTH ANALYSIS OF TASLINE 8W

6.5.1 Spectral Analysis

Only one flight line has so far been analysed by the procedures outlined previously. Tasline 8W was chosen as it was the first complete line to be flown during the survey. It is planned to complete the analysis with the remaining lines now that the techniques have been shown to give interesting results.

The total length of the flight line is 600 kms the centre half of which is entirely over land. To attempt to

obtain some regional significance the flight line was divided into four equal sections; two over land and two over water. The location of the flight line and subdivisions are shown in Figure 6.2

Each of the four sections of Tasline 8W were Fourier transformed using a Fast Fourier Transform programme (originally written by J. Boothroyd of the University of Tasmania Computing Centre), based on the algorithm of Cooley and Tukey (1965). The spectra are characteristically irregular and were thus smoothed using a 3-point Hanning convolution filter applied a number of times.

Plots of the amplitude of the spectrum for the first 80 wavenumbers on a semi-logarithmic scale and normalised by the maximum amplitude, are shown in Figures 6.3 to 6.6.

6.5.2 Section 1 (Figure 6.3)

The spectrum of this westernmost section shows three segments having near linear gradients. The first is up to wavenumber 10 and has a gradient indicating a depth of 66 kms. The second is from wavenumbers 10 to 38 and has a gradient indicating a depth of 10 kms. This segment is more irregular than the previous. The remaining segment, above wavenumber 38 has a near horizontal gradient and is therefore attributable to random noise.

The 66 kms depth line requires explanation since this depth is well below the Curie point geotherm. It may be due

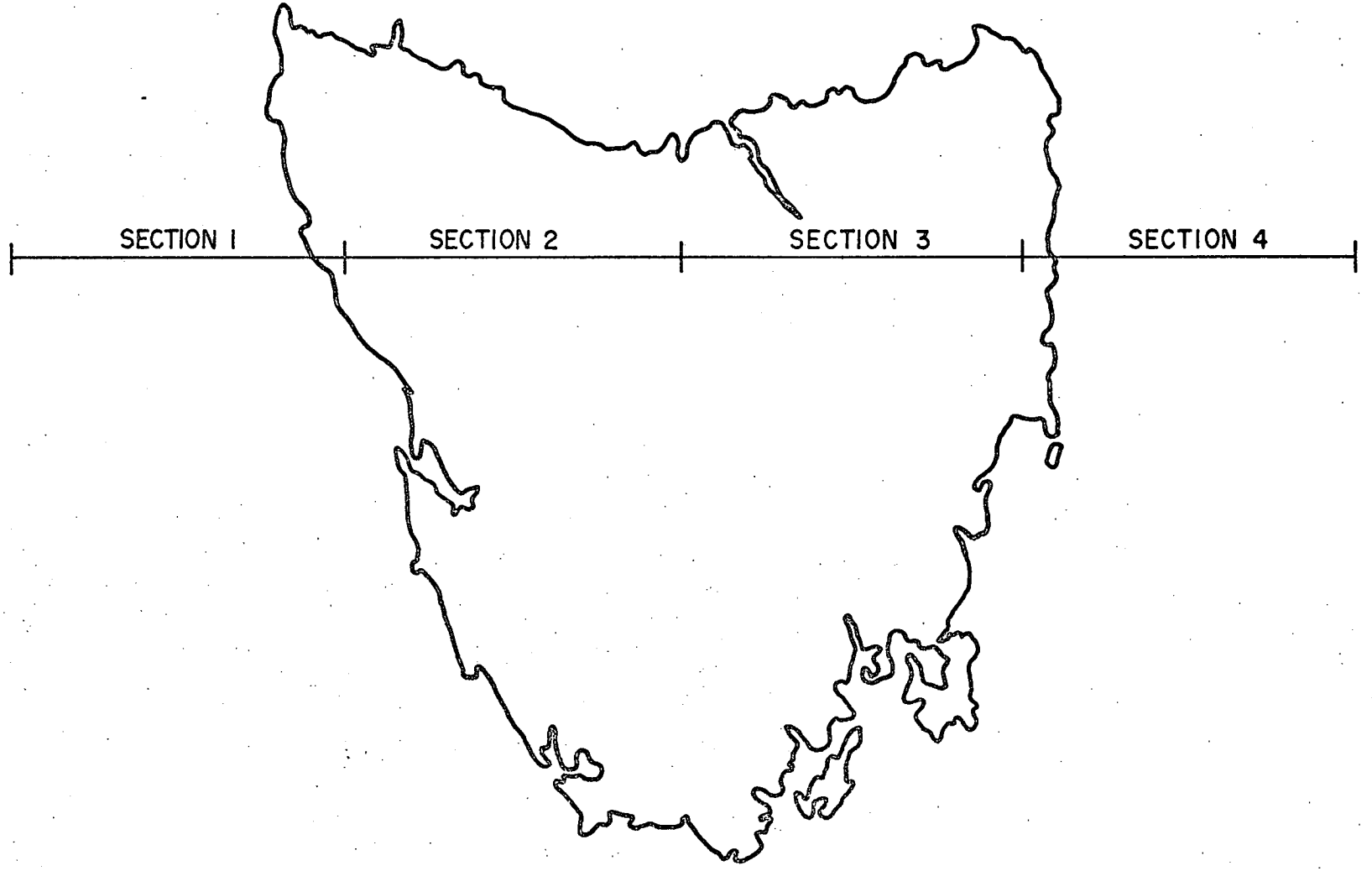

LOCATION OF TASLINE 8W

FIGURE 6·2

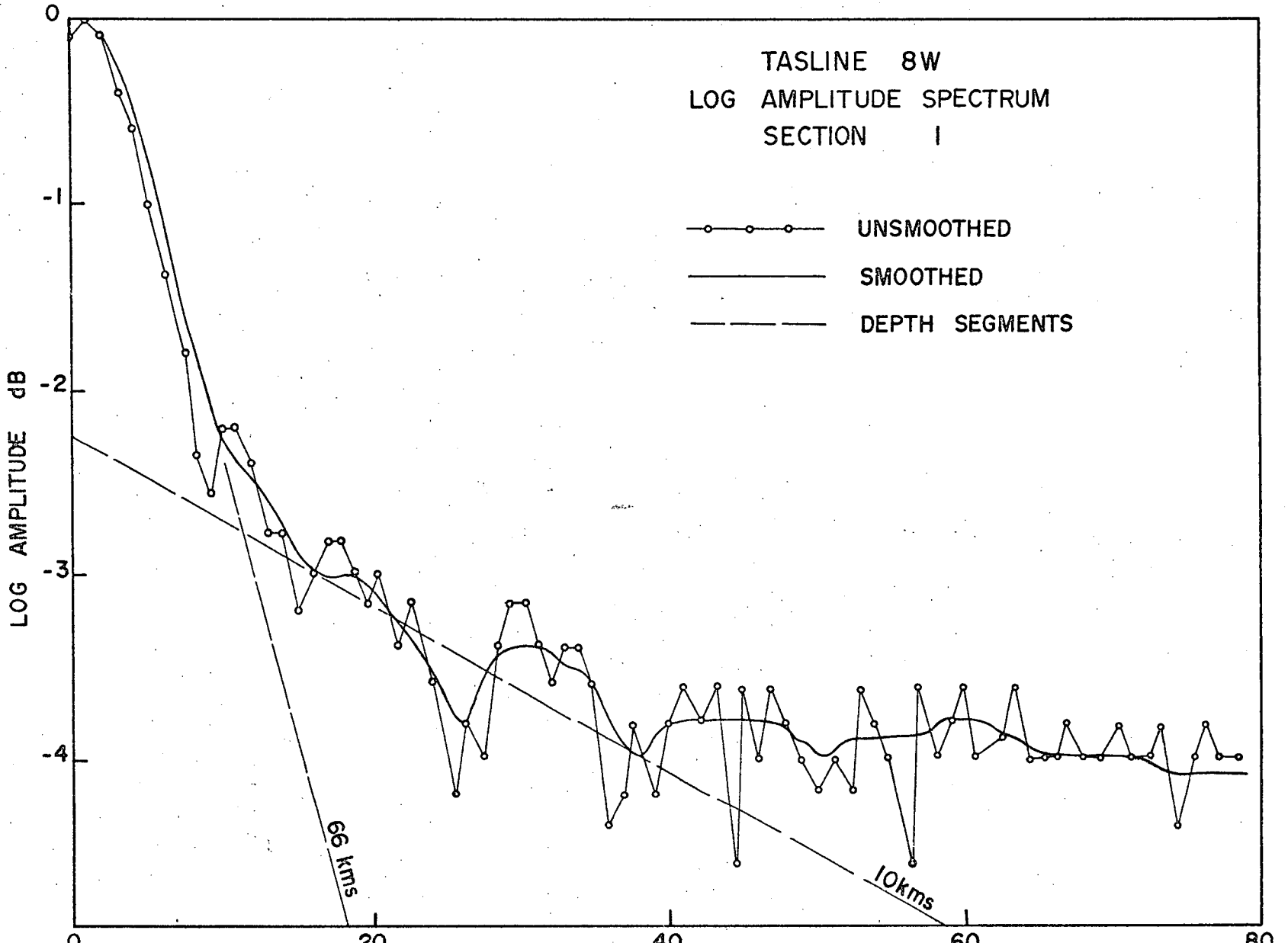
TASLINE 8W
LOG AMPLITUDE SPECTRUM
SECTION 1
UNSMOOTHED
SMOOTHED
DEPTH SEGMENTS
LOG AMPLITUDE dB
0
-1
-2
-3
-4
0
20
40
60
80
k (WAVE NUMBER)
66 kms
10kms

FIGURE 6·3

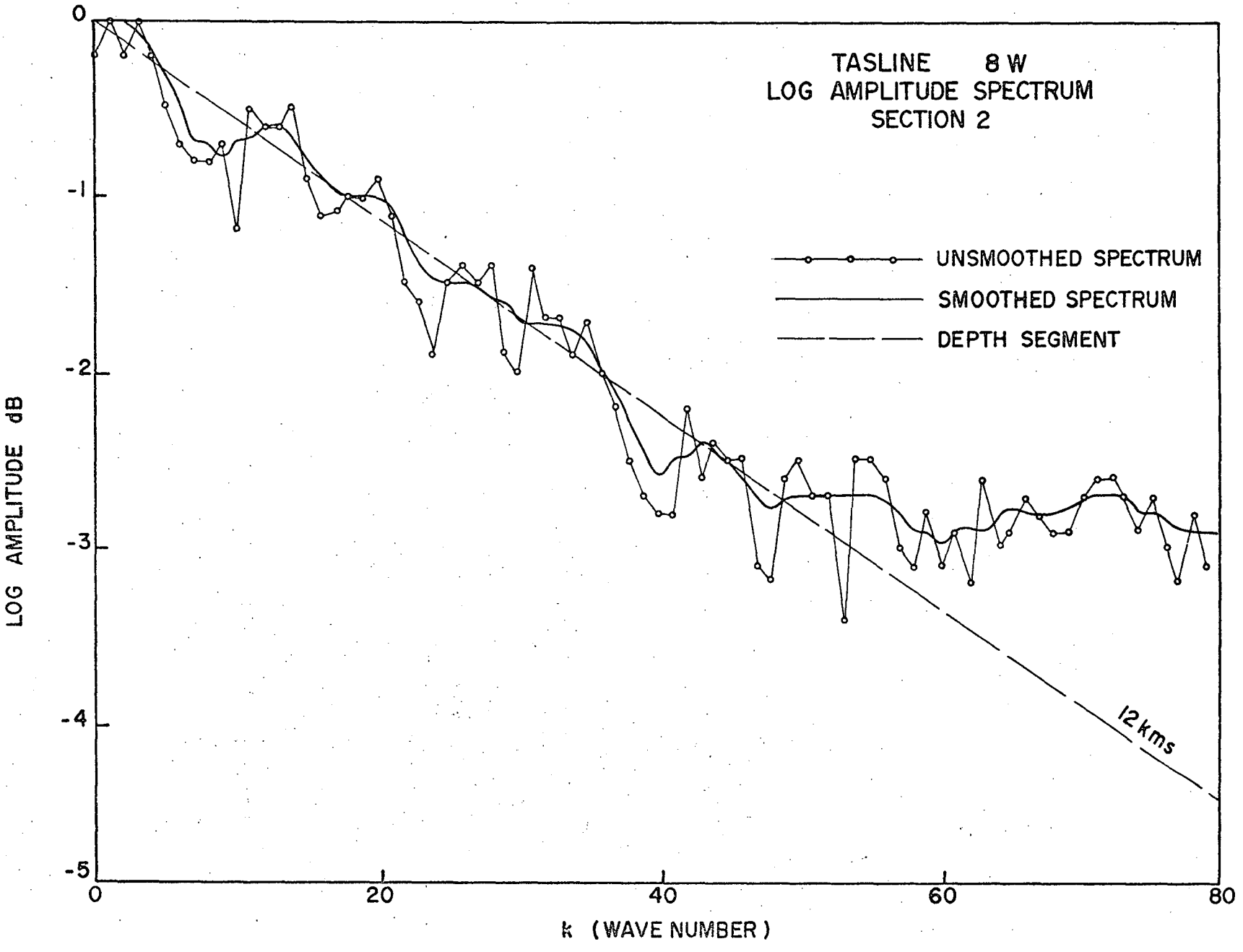
TASLINE 8 W
LOG AMPLITUDE SPECTRUM
SECTION 2
UNSMOOTHED SPECTRUM
SMOOTHED SPECTRUM
DEPTH SEGMENT
12 kms
LOG AMPLITUDE dB
0
-1
-2
-3
-4
-5
0
20
40
60
80
k (WAVE NUMBER)

FIGURE 6·4

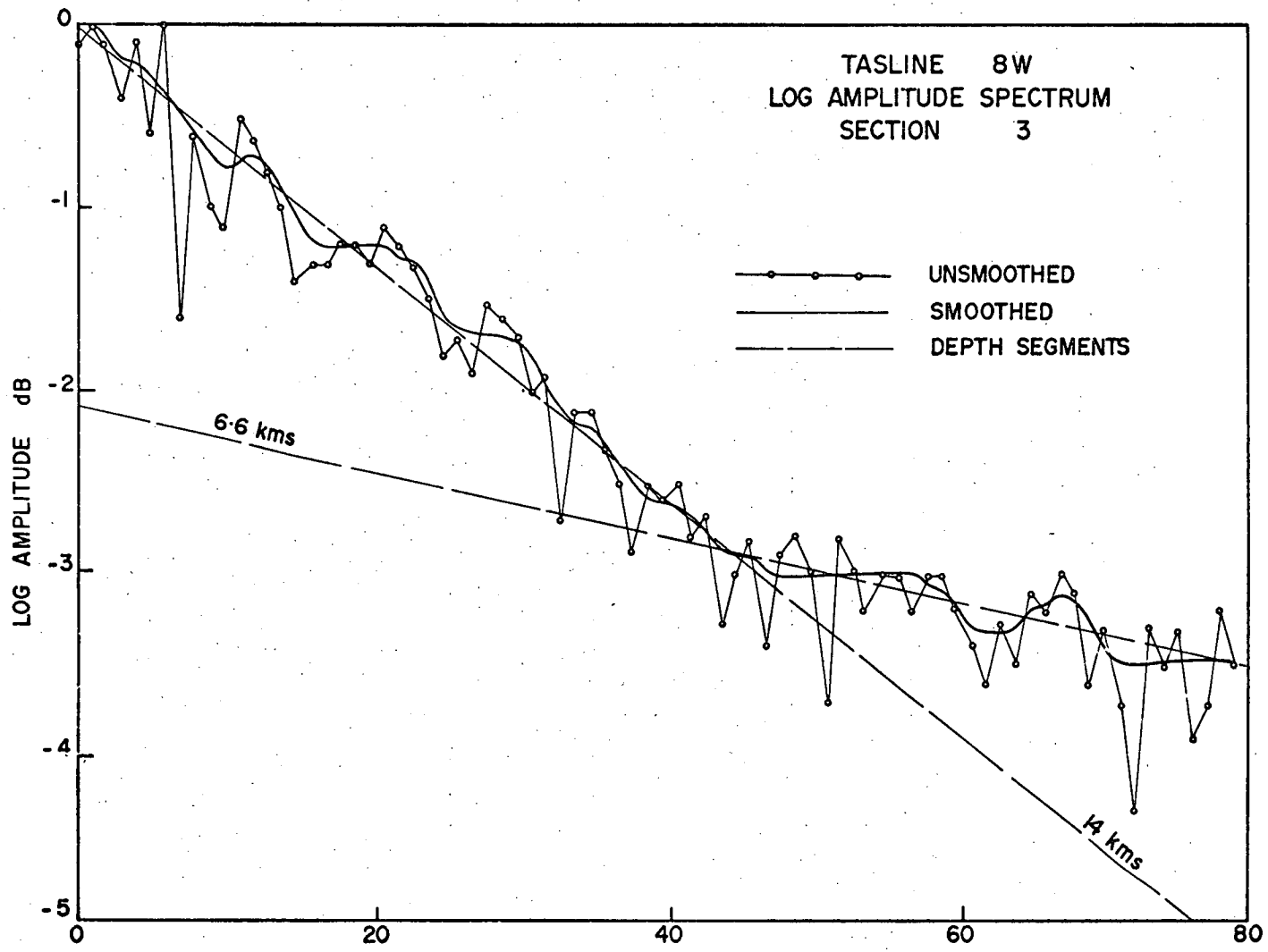
TASLINE 8W
LOG AMPLITUDE SPECTRUM
SECTION 3
UNSMOOTHED
SMOOTHED
DEPTH SEGMENTS
6·6 kms
4 kms
LOG AMPLITUDE dB
0
-1
-2
-3
-4
-5
0
20
40
60
80
k (WAVE NUMBER)

FIGURE 6·5

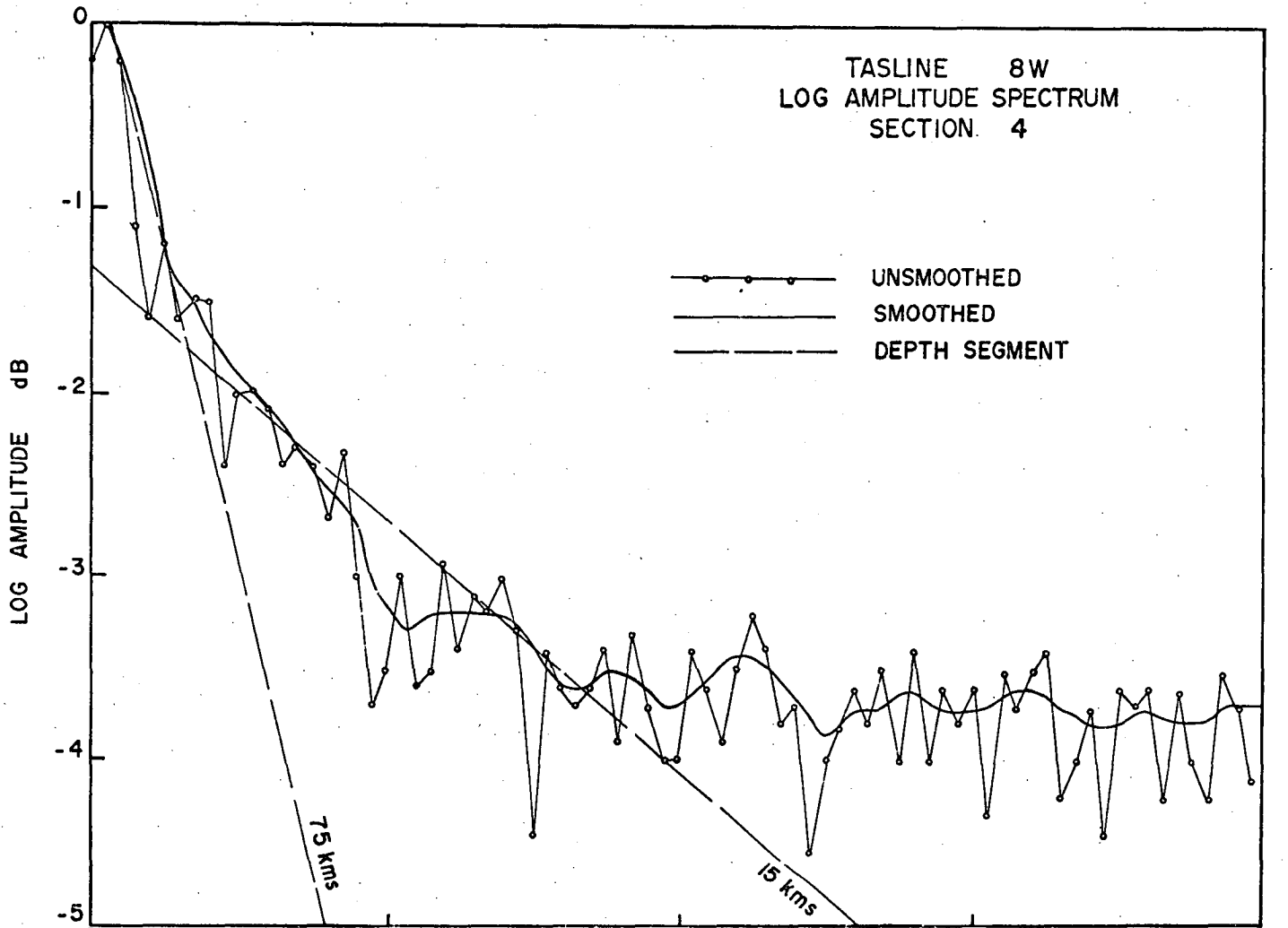
TASLINE 8W
LOG AMPLITUDE SPECTRUM
SECTION 4
UNSMOOTHED
SMOOTHED
DEPTH SEGMENT
75 kms
15 kms
LOG AMPLITUDE dB
0
-1
-2
-3
-4
-5
0
20
40
60
80
k (WAVE NUMBER)

FIGURE 6·6

to inadequate removal of the geomagnetic field as a simple linear approximation was used. Alternatively, the source may be real enough but that the depth is incorrect due to the finite nature of the source. If the source is large with respect to the flight length then the spectrum is artificially steep (and thus giving an over-estimate of the depth).

6.5.3 Section 2 (Figure 6.4)

The spectrum of section 2 has a very different structure to that of the previous section. There are only two linear gradient segments; the first of which is from wavenumber 0 to 45 and corresponding to a depth of 12 kms. The remainder of the spectrum, above wavenumber 45, is near horizontal and is thus due to random noise.

The 12 kms depth segment is in good agreement with the intermediate depth obtained from section 1.

6.5.4 Section 3 (Figure 6.5)

The spectrum of section 3, shows a similar character to that of section 2, except that there also appears to be a shallower source. The first segment, between wavenumbers 0 to 42, has a gradient indicating a depth of 14 kms. The second segment, from wavenumbers 42 to 80, has a gradient indicating a depth of the order of 6.6 kms.

6.5.5 Section 4 (Figure 6.6)

The spectrum for section 4 is very similar to that of section 1 and again has three linear segments. The first segment, from wavenumbers 0 to 7, has a gradient indicating a depth of 75 kms. The second segment, from wavenumbers 7 to 33, has a gradient indicating a depth of 15 kms. The remaining segment has a near horizontal gradient and is therefore attributable to noise.

6.5.6 General comments on the depth interpretation

The depths interpreted from the spectra of the four sections have been plotted from the flight path level (Figure 6.7). For comparison the isostatic crustal model from the analysis of the regional gravity field is included.

The 66 and 75 kms depths for sections 1 and 4 have been omitted as their significance (or true depth) has not been determined.

There is a startling continuity in the intermediate depths plotted from all four sections. The accuracy of the depth calculations is largely controlled by the gradient estimation and is probably in the region of ±1 km. This would give credence to the presence of a dipping magnetic layer whose upper surface has a depth of 6.7 kms (below sea level), at the western end of the line, and a depth of 11.7 kms (below sea level), at the eastern end.

DEPTH INTERPRETATION FOR SPECTRA OF TASLINE 8W COMPARED WITH ISOSTATIC CRUSTAL MODEL

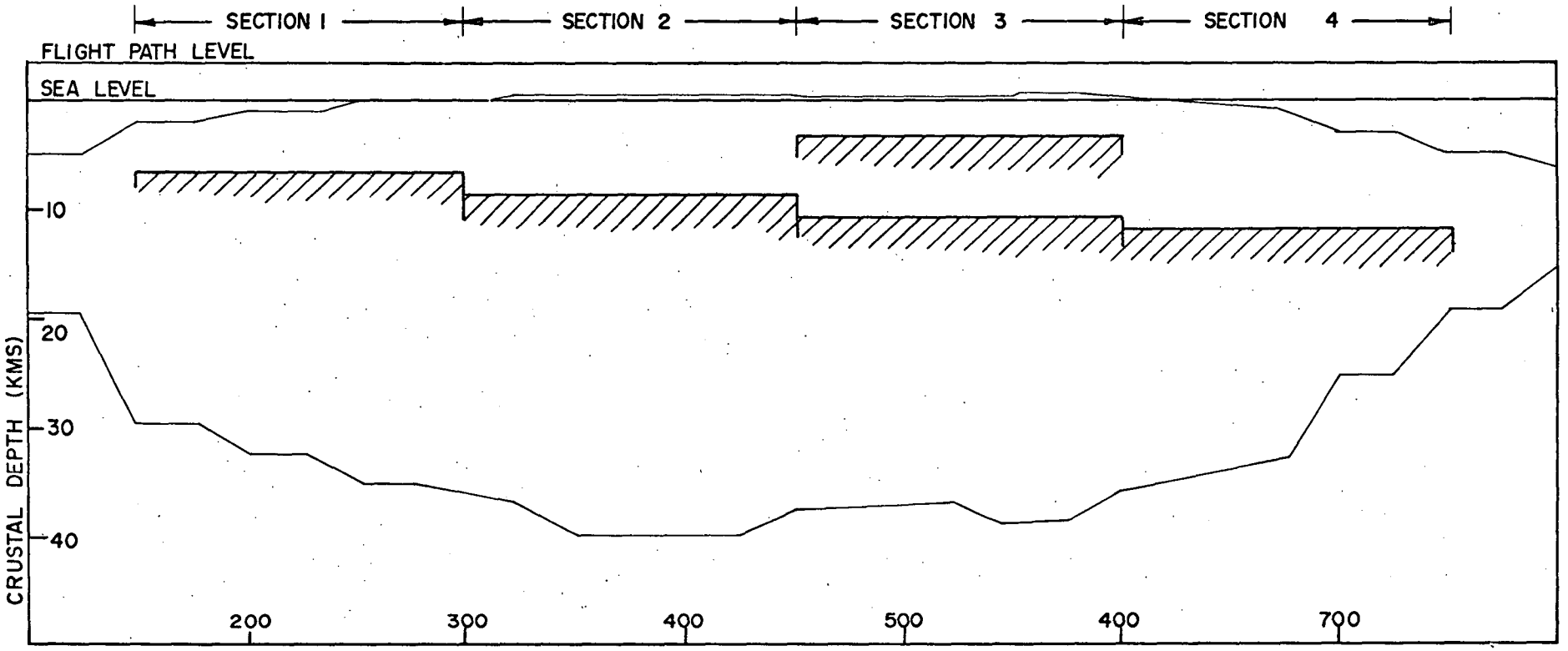

FIGURE 6·7

The geological significance of this magnetic layer is not clear but several possibilities present themselves. The dipping nature of the layer is not surprising in view of the fact that the more recent geological horizons are confined to the eastern part of the state. The depth to the layer is too deep for it to be simply due to the upper surface of the Pre-Cambrian (which outcrops in many parts of the west coast of Tasmania). The most satisfying concept that comes to mind is that we have a representation of the "primordial crust" which is presumably the same feature that some seismologists term the Conrad discontinuity. It will be interesting to see the development of the definition of this layer following the analysis of other lines.

The shallower magnetic surface in section 3 is at a depth of about 3 kms below sea level. This is rather difficult to explain as the main geological structure in this part of Tasmania is the north-east granite. There appear to be two possible solutions; the first being that the depth calculation is effected by the size of the granite body (i.e. Spector's form factor: # 6.1) and secondly that the surface represents magnetic horizons which terminate against the granite. It is interesting to note that the depth to the base of the granite calculated from gravity observations corresponds very closely to the depth of the main magnetic horizon.

The interpretation of the spectra of the aeromagnetic profile analysed is admittedly speculative. The reliability of it will increase (or decrease) depending upon the results of the analyses of the remaining data.

CHAPTER SEVEN

CONCLUSIONS

7.1 CONCLUSIONS

The analysis of the regional gravity data has shown that the crustal thickness under Tasmania is of normal continental thickness (35 kms). The higher topography of the Central Plateau and other mountainous areas appear to be isostatically compensated by a crustal root extending down to over 40 kms. Steep regional gravity gradients have been interpreted in terms of rapid crustal thining towards an oceanic structure around the continental margin.

The representation of the regional component by fitting a series of orthogonalised functions has been shown to be effective. A set of coefficients are presented which enable the regional field to be specified at any location.

Large scale upper crustal structures have been identified from the gravity field. The Mt. Field gravity high is interpreted as a dyke-like structure composed of dolerite having a total length of some 160 kms and having an average width of 8 kms. The feature trends NW-SE for most of its length but appears offset in a N-S direction in places. It may also form a more complex sequence of dykes as it approaches the Central Plateau region.

The North-east granite complex is clearly shown to be a large body of granite possibly extending to some 10 kms in depth. Granitic bodies have been identified in other parts of the state but the granites of the south-west Cape region

appear to be much larger than previously thought. A gravity low in the vicinity of the Arthur Ranges and towards the South Coast has yet to be explained but is most likely to be due to previously undiscovered low density rocks.

The gravity results have been confirmed (to some extent) by the interpretation of the crustal refraction experiment data. The time terms obtained from this data indicate crustal thicknesses of the order of 30-35 kms for Tasmania and 20-25 kms for Bass Strait. The agreement in the crustal thicknesses by both methods may be more apparent than real since knowledge of the densities and velocities of the lower crust is very poor.

Spectral analyses of data obtained during a high level aeromagnetic survey of Tasmania has revealed the presence of a magnetic layer whose upper surface dips down towards the east. The depth to this surface varies from 6 kms (below sea level) at the west to 12 kms in the east. The attitude and depth of this feature is consistent with some horizon within the basement rocks of Tasmania.

7.2 ACKNOWLEDGEMENTS

I wish to acknowledge the assistance of the many persons and organisations who have materially contributed to this work.

In particular, I am grateful to Professor S.W. Carey, who provided facilities and encouragement, and to my

supervisors, Dr. W.D. Parkinson and Associate Professor R. Green, who were able to provide the depth of supervision required for such a thesis. The entire staff of the Geology Department has devoted time to discussions of parts of the work.

The remote nature of much of Tasmania necessitated the co-operation of several organisations, including the Broken Hill Company Pty. Ltd., who through the efforts of R. and M. Hall were able to supply me with many hours of helicopter time. The Hydro-Electric Commission and the Australian Newsprint Mills provided access.

No person has worked in the south-west of Tasmania without meeting Denny King of Malaleuka Inlet who freely gave me his time and assistance.

Much of the contents of this thesis has been modified following conversations with many Ph.D. students, of whom the following are a few: J.A. Brooks, K.D. Corbett, I.K. Crain, D.A. Falvey, D.I. Groves, R. Johnson, D.A. Leaman, M.J. Rubenach, V.P. St. John, J. Shirley, R. Underwood, and J.K. Weissel.

Mr. B.F. Cameron provided a basis for the regional gravity survey and later co-operated to a large degree in the production of the Bouguer Anomaly Map of Tasmania.

The Bureau of Mineral Resources, Canberra, has been generous and helpful in various phases of the work. In

particular, I would like to thank the Director for making available the aeromagnetic data and to B.C. Barlow and I. Briggs for their assistance.

The computing facilities of the University of New South Wales, Macquarie University, Bureau of Mineral Resources and the University of Tasmania were used in various phases of the project. The diagrams and maps in this thesis were prepared by the School of Earth Sciences, Macquarie University.

Most of the research work reported in this thesis was carried out while I held a Post-graduate Commonwealth Scholarship at the University of Tasmania.

REFERENCES

Alldredge, L.R., Van Voorhis, G.D., and Davis, T.M., (1963), A magnetic profile around the world: J. Geophys. Res., 68, 3679-3692.

Anderssen, R.S., (1970), Note on the fitting of non-equispaced two-dimensional data: Geoexploration, 8, 41-48.

Barlow, B.C., (1967), Gravity Meter Calibration ranges in Australia: Bureau of Mineral Resources, Canberra, rep. 122.

Barlow, B.C., (1970), National Report on Gravity in Australia: unpublished Bureau of Mineral Resources, Canberra, record 70/62.

Bhattacharyya, B.K. and Morley, L.W., (1965), The delineation of deep crustal magnetic bodies from total field aeromagnetic anomalies: J. Geomag. and Geoelec., Tokyo, 17, 237-252.

Bhattacharyya, B.K., (1966a), A method for computing the total magnetisation vector and the dimensions of a rectangular block-shaped body from magnetic anomalies: Geophysics, 31, 74-96.

Bhattacharyya, B.K., (1966b), Continuous spectrum of the total magnetic field anomaly due to a rectangular prismatic body: Geophysics, 31, 97-121.

Bhattacharyya, B.K., (1967), Some general properties of potential fields in space and frequency domains: a review: Geoexploration, 5, 127-143.

Blackman, R.B., and Tukey, J.W., (1958), The measurement of power spectra: Dover, New York.

Bracewell, R., (1965), The Fourier Transform and Its Applications: McGraw Hill, New York, 381 pp.

Cameron, B.F., (1967), A regional gravity survey of eastern Tasmania: Univ. Tasmania unpublished Honours thesis.

Cooley, J.W. and Tukey, J.W., (1965), An algorithm for the machine calculation of complex Fourier Series: Math. Comput., 19, 297-301.

Crain, I.K. and Bhattacharyya, B.K., (1967), The treatment of non-equispaced two-dimensional data with a digital computer: Geoexploration, 5, 173-194.

Crain, I.K., (1970), Computer interpolation and contouring of two-dimensional data: a review: Geoexploration 8, 71-86.

Davis, H.F., (1963), Fourier Series and Orthogonal Functions: Allyn and Bacon, Boston, 403 pp.

Davis, J.L., (1959), High level erosion surfaces and Landscape Development in Tasmania: Aust. Geogr. 7, 193-203.

Davis, J.L., (1965), (ed.), The Atlas of Tasmania: Mercury, Hobart.

Davis, P. and Rabinowitz, P., (1954), A multiple purpose orthonormalising code and its uses: Journal of the Association of Computing Machinery, 1, 183-191.

Dean, W.C., (1958), Frequency analysis for gravity and magnetic interpretation: Geophysics, 23, 97-127.

Doyle, H.A., Everingham, I.B. and Hogan, T.K., (1959), Seismic recordings of large explosions in south-eastern Australia: Aust. J. Phys. 12, 222-230.

Doyle, H.A., Underwood, R. and Polak, E.J., (1966), Seismic velocities from explosions off the central coast of New South Wales: J. geol. Soc. Aust. 13, 355-372.

Finney, W.A. and Shelley, E.P., (1967), Tasmania Aeromagnetic Survey, 1966: unpublished Rec. Bur. Min. Res., Canberra, 1967/19.

Fougere, P.F., (1963), Spherical Harmonic Analysis 1. A new method: J. Geophys. Res., 68, 1131-1139.

Fougere, P.F., (1965), Spherical Harmonic Analysis 2. A new model derived from magnetic observatory data for epoch 1960.0: J. Geophys. Res., 70, 2171-2179.

Glasson, K., (1967), Some observations on airborne magnetometer surveys in relation to mineral exploration: Univ. of Tasmania, Symposium on the Geology of Western Tasmania (unpublished).

Griffiths, J.R., (1971), Continental Margin Tectonics and the Evolution of South East Australia: The APEA Journal, 75-79, (1971).

Gudmundsson, G., (1971), Discussion on "Statistical models for interpreting aeromagnetic data", (A. Spector and F.S. Grant): Geophysics, 36, 617-618.

Heiskanen, W.A., and Vening Meinesz, F.A., (1958), The Earth and Its Gravity Field: McGraw Hill, New York.

Hinch, A.J., (1957), A gravity survey of the Cressy Area, Northern Tasmania: Univ. Tasmania, unpublished Honours thesis.

Horton, C.W., Hempkins, W.B. and Hoffman, A.A.J., (1964), A statistical analysis of some aeromagnetic maps from the north-western Canadian shield: Geophysics, 29, 582-601.

Jennings, J.N., (1959), The Coastal Geomorphology of King Island, Bass Strait, in Relation to Changes in the Relative Level of Land and Sea: Rec. Q. Vict. Mus., 11.

Johnson, B.D., (1967), A regional gravity survey of the West Coast of Tasmania: University of Tasmania, Symposium on the Geology of Western Tasmania (unpublished proceedings).

Johnson, B.D., (1972), Convolution filtering at ends of data sets: Bull. Aus. Soc. Expl. Geophysicists, 2, 11-24.

Jones, B.F., (1963), A gravity survey of the Great Lake Area, Tasmania: Univ. Tasmania, unpublished Honours thesis.

Jones, B.F., Haigh, J. and Green, R., (1966), The structure of the Tasmanian Dolerite at Great Lake: J. Geol. Soc. Aust. 13, 527-242.

Jones, W.B. and Gallett, R.M., (1962), The Representation of Diurnal and Geographical Variations of Ionospheric Data by Numerical Methods: Telecommunication J. 5, 3-23.

Lanczos, C., (1957), Applied Analysis: Pitman, London.

Leaman, D.E., (1965), Geophysics of the Cygnet Area: Univ. of Tasmania unpublished Honours thesis.

Leaman, D.E., (1970), Dolerite Intrusion Hobart District Tasmania: Univ. of Tasmania unpublished Ph.D. thesis.

Longman, M.J. and Leaman, D.E., (1967), Geology and Geophysics of the Tertiary Basins of Northern Tasmania: Dep. Min. Tasm. Unpub. Rep.

McDougall, I. and Stott, P.M., (1961), Gravity and Magnetic Observations in the Red Hill Area, Southern Tasmania: Pap. Proc. Roy. Soc. Tasmania 95, 7-15.

Nagy, D., (1966), The gravitational attraction of a right rectangular prism: Geophysics, 31, 362-371.

Naidu, P.S., (1966), Extraction of potential field signal from a background of random noise by Strakhov's method: J. Geophys. Res., 71, 5987-5995.

Naidu, P.S., (1967), Statistical properties of potential fields over a random medium: Geophysics, 32, 88-98.

Naidu, P.S., (1968), Spectrum of the potential due to randomly distributed sources: Geophysics, 33, 337-345.

Parkinson, W.D., (1971), An analysis of the geomagnetic diurnal variation during the International Geophysical Year: Gerlands Beitr. Geophysik. Leipzig, 80, 199-232.

Ringis, J., (1970), Magnetic Lineations in the Tasman (abstract): Geoexploration, 8, 250.

Rubenach, M.J., (1967), The Serpentine Hill Complex: Univ. of Tasmania unpublished Honours thesis.

Scheidegger, A.F. and Willmore, P.L., (1957), The use of a least squares method for the interpretation of data from seismic surveys: Geophysics, 22, 9-22.

Serson, P.H. and Hannaford, W.L.W., (1957), A statistical analysis of magnetic profiles: J. Geophys. Res., 62, 1-18.

Sheehan, M.J., (1969), The gravity field in the Sheffield area: Univ. of Tasmania unpublished Honours thesis.

Shelley, M.J., (1965), Gravity and Magnetic Survey at Sorell: Univ. Tasmania unpublished Honours thesis.

Smith, T.J., Steinhart, J.S. and Aldrich, L.T., (1966), Lake Superior crustal structure: J. Geophys. Res., 71, 1141-1172.

Spector, A. and Bhattacharyya, B.K., (1966), Energy density spectrum and autocorrelation function of anomalies due to simple magnetic models: Geophys. Prosp., 14, 242-272.

Spector, A., (1968), Spectral Analysis of Aeromagnetic Data: Ph.D. Thesis, University of Toronto.

Spector, A. and Grant, F.S., (1970), Statistical models for interpreting aeromagnetic data: Geophysics, 35, 293-302.

Spry, A.H. and Banks, M.R., (1962), (eds.), Geology of Tasmania: J. Geol. Soc. Aust. 9, 107-362.

St. John, V.P., (1967), The Gravity Field in New Guinea: Univ. Tasmania unpublished Ph.D. Thesis.

St. John, V.P. and Green, R., (1967), Topographic and Isostatic Corrections to Gravity Surveys in Mountainous Areas: Geophys. Prosp. 15, 151-162.

Steinhart, J.S. and Meyer, R.P., (1961), Explosion studies of continental structure; Carnegie Inst. Wash. Publ. 622, 409 pp.

Strakhov, V.N., (1963), The derivation of optimum numerical methods for the transformation of potential fields: Bull. Acad. Sci. U.S.S.R., Geophys. Ser. (Eng. Transl.), 1081-1090.

Taylor, C.P., (1966), Geophysical Exploration for Petroleum in Bass Strait: Proc. Aust. Inst. Min. & Met. 217, 39-48.

Underwood, R., (1969), A seismic refraction study of the crust and upper mantle in the vicinity of Bass Strait: Aust. J. Phys., 22, 573-587.

Whitham, K., (1965), On the depth of magnetic sources derived from long aeromagnetic profiles: J. Geomag. and Geoelec., Tokyo, 17, 253-262.

```
GRAM-SCHMIDT ORTHOGONALISATION PROGRAMME;,UCXXX;

begin       integer  N,Kmax,kmax;   switch  ss:=fin;

comment  This programme carries out a Gram-Schmidt orthogonalisation of the Fourier functions which are
         non-orthogonal with respect to the N data points,x(k), having values y(k).
          The number of functions is defined in terms of the maximum wave number, Kmax, of the approximating
         series, thus giving rise to kmax=2*Kmax+1 functions.
          This programme may be generalised to orthogonalise any series of functions by suitable modification
         of the initial statements -- those definig the number of functions and setting up of the functions;


     read N,Kmax;   if N<0 then goto fin;
     kmax:=1+2*Kmax;

          begin array F[2:kmax, 1:N],x,y[1:N],a[1:kmax*(kmax+1) div 2],var,c,d,Fsq[1:kmax];
               real sum,Ysq;   integer kT,jT,iT,i,j,k,l,n,K,kk;   switch  ss:=again;

               for i:=1 step 1 until N do read x[i],y[i];
               for i:=1 step 1 until N do print aligned(4,6),x[i],sameline,y[i];

               comment position and value of data points read in;

               kk:=0;   Fsq[1]:=N;

               for K:=1 step 1 until Kmax do
                    begin k:=2*K;
               again;       kT:=k*(k-1) div 2;
                            for j:=k-1 step -1 until 1 do a[kT+j]:=0.0;

                            for i:= 1 step 1 until N do
                                 begin if kk=0 then F[k,i]:=cos(K*x[i]) else F[k,i]:=sin(K*x[i]);
                                      for j:=k-1 step -1 until 2 do a[kT+j]:=a[kT+j]+F[k,i]*F[j,i];
                                      a[kT+1]:=a[kT+1]+F[k,i]
                                 end;

                            for j:=k-1 step -1 until 1 do a[kT+j]:=a[kT+j]/Fsq[j];   Fsq[k]:=0.0;

                            for i:=1 step 1 until N do
                                 begin sum:=F[k,i]-a[kT+1];
                                      for j:=k-1 step -1 until 2 do sum:=sum-a[kT+j]*F[j,i];
                                      F[k,i]:=sum;   Fsq[k]:=Fsq[k]+sum*sum
                                 end;

                            if k#2*(k+1) then begin kk:=1;   goto again   end else kk:=0;
                    end computation of orthogonal functions F;


               for j:=1 step 1 until kmax do
                    begin sum:=0.0;
                          for i:=1 step 1 until N do sum:= if j=1 then (sum+y[i]) else (sum+y[i]*F[j,i]);
                          c[j]:=sum/Fsq[j]
                    end computation of orthogonal coefficients c;
```

```
                    for i:=1 step 1 until kmax do
                          begin iT:=i*(i-1) div 2;   a[iT+1]:=1;
                                for j:=1 step 1 until i-1 do
                                      begin sum:=0.0;
                                            for n:=j step 1 until i-1 do sum:=sum+a[iT+n]*a[n*(n-1) div 2 + j];
                                            a[iT+j]:=-sum
                                      end
                          end a matrix now contains b matrix;

                    for j:=1 step 1 until kmax do
                          begin sum:=0.0;
                                for i:=j step 1 until kmax do sum:=sum+c[i]*a[i*(i-1) div 2 + j];
                                d[j]:=sum
                          end computation of non-orthogonal coefficients;

                    print ££12s4? y[k] £12??;

                    Ysq:=0.0;
                    for k:=1 step 1 until N do
                          begin sum:=0.0;
                                print aligned(4,6),y[k];   Ysq:=Ysq+y[k]*y[k];
                                for i:=1 step 1 until kmax do
                                      begin sum:= if i=1 then (sum+c[i]) else (sum+c[i]*F[i,k]);
                                            print sameline ,aligned(4,6),sum
                                      end
                          end of calculation of term by term approximation of the data;

                    print ££12?variance£s4??;

                    for i:=1 step 1 until kmax do
                          begin sum:= if i=1 then c[1]*c[1]*N else sum+c[i]*c[i]*Fsq[i];
                                if i<N then var[i]:=(Ysq-sum)/(N-i) else var[i]:=(Ysq-sum);
                                print aligned(4,6),sameline,var[i]
                          end;

                    print ££12s35?d[j]£1s6? c[j]£s10?real£s8?imag£s8?amp£12??;

                    print aligned(4,6),c[1],££s14??,d[1];
                    for j:=2 step 2 until kmax-1 do
                    print aligned(4,6),c[j],sameline,c[j+1],d[j],d[j+1],sqrt(d[j]*d[j]+d[j+1]*d[j+1]);

              end;

        top of form;   restart;
fin: end of programme;
```

This l·ŃJűłŎfŜ has been removed for copyright or proprietary reasons.

Convulution filtering at ends of data sets, B. David Johnson, ASEG Bulletin, vol. 2, no. 4 (October), P11-24, 9 figs.